

Stony Brook University



OFFICIAL COPY

The official electronic file of this thesis or dissertation is maintained by the University Libraries on behalf of The Graduate School at Stony Brook University.

© All Rights Reserved by Author.

Entanglement in low dimensional systems

A Dissertation Presented

by

Raul A. Santos

to

The Graduate School

in Partial Fulfillment of the Requirements

for the Degree of

Doctor of Philosophy

in

Physics

Stony Brook University

July 2013

Stony Brook University

The Graduate School

Raul A. Santos

We, the dissertation committee for the above candidate for the Doctor of Philosophy degree, hereby recommend acceptance of this dissertation.

Vladimir Korepin – Dissertation Advisor
Professor, C. N. Yang Institute for Theoretical Physics,
Department of Physics and Astronomy

Tzu-Chieh Wei – Chairperson of Defense
Assistant Professor, Department of Physics and Astronomy

Eden Figueroa – Committee Member
Assistant Professor, Department of Physics and Astronomy

Alexander Kirillov Jr. – Outside Member
Associate Professor, Department of Mathematics

This dissertation is accepted by the Graduate School.

Charles Taber
Interim Dean of the Graduate School

Abstract of the Dissertation

Entanglement in low dimensional systems

by

Raul A. Santos

Doctor of Philosophy

in

Physics

Stony Brook University

2013

In the ground state of gapped systems, the entanglement entropy of a subsystem A scales with the length of the boundary of A. This observation suggests that the entanglement properties of the subsystem can be described in terms of degrees of freedom living in the boundary of A. We will discuss the connection between entanglement properties and effective boundary descriptions in spin systems in one and two dimensions. In one dimension we present analytic results for the spin $S = 1$, Affleck-Kennedy-Lieb-Tasaki (AKLT) ground state entanglement, characterized by negativity and entanglement spectrum. We also discuss a generalization of the AKLT model, based on the quantum group $U_q(sl(2))$ for general integer spin S . In two dimensions, we study two spin systems whose ground state can be written in terms of tensor product states of bond dimension two, the AKLT model in the hexagonal lattice and the Ising projected entangled pair state (Ising PEPS) in the square lattice. We show how the reduced density matrix of a partition is associated with a thermal state of a one dimensional model along the boundary of that partition. We also present arguments

supporting this correspondence for arbitrary gapped systems. Finally we discuss the behavior of this boundary theory when the original two dimensional model is tuned through a quantum phase transition.

To my family.

“Four essential conditions for happiness.
life in the open air,
the love of a woman,
the indifference to any feeling of ambition
and the creation of a new type of beauty.”

Edgar Allan Poe

Contents

| | |
|--|-------------|
| List of Figures | ix |
| Acknowledgements | xiii |
| 1 Introduction | 1 |
| 2 Entanglement in pure and mixed states | 5 |
| 2.1 Requisites for entanglement measures | 6 |
| 2.2 Entanglement in pure states | 7 |
| 2.2.1 Bipartite systems | 8 |
| 2.2.2 Multipartite states | 13 |
| 2.3 Entanglement in mixed states | 13 |
| 2.3.1 Bipartite states | 13 |
| 2.3.2 Multipartite states | 15 |
| 2.3.3 Geometric entanglement | 15 |
| 3 Tensor Network States | 17 |
| 3.1 Matrix product states | 17 |
| 3.2 Tensor Network states and PEPS | 20 |
| 3.2.1 PEPS | 21 |
| 4 Negativity in AKLT ground state | 22 |
| 4.1 The AKLT model and the VBS state | 23 |
| 4.2 Density matrix pure state | 24 |
| 4.3 Density matrix for the mixed system of 2 disjoint blocks | 27 |
| 4.3.1 Open boundary conditions | 27 |
| 4.3.2 Periodic Boundary Conditions | 32 |
| 4.4 Mutual Entropy | 35 |
| 4.5 Conclusions | 36 |

| | | |
|----------|--|------------|
| 5 | Generalization of AKLT: AKLT_q | 39 |
| 5.1 | Reduced density matrix of MPS. | 41 |
| 5.2 | AKLT_q model. | 43 |
| 5.2.1 | General Spin S , Quantum algebra | 47 |
| 5.2.2 | Matrix product representation | 48 |
| 5.2.3 | Transfer matrix | 50 |
| 5.2.4 | Reduced Density Matrix | 52 |
| 5.3 | Double scaling limit | 53 |
| 5.3.1 | Eigenvalues of reduced density matrix | 53 |
| 5.3.2 | Entanglement spectrum and entropy | 54 |
| 5.4 | Finite-size corrections | 56 |
| 5.4.1 | Isotropic case | 56 |
| 5.4.2 | Anisotropic case | 59 |
| 5.5 | KSZ model | 60 |
| 5.6 | Conclusions | 61 |
| 6 | Bulk-Edge Correspondence of Entanglement Spectrum | 63 |
| 6.1 | Spin S VBS ground state on a two dimensional torus | 64 |
| 6.2 | Partial density matrix and Schwinger boson representation of VBS ground state | 65 |
| 6.3 | Quantum to Classical mapping | 68 |
| 6.4 | Graph expansion of the density matrix | 70 |
| 6.5 | Continuous limit and Entanglement Hamiltonian | 74 |
| 6.6 | Ising PEPS quantum model | 77 |
| 6.7 | Density matrix of a subsystem | 78 |
| 6.8 | Expansion of ρ_A | 82 |
| 6.9 | Small and High β expansion | 83 |
| 6.9.1 | $\beta \rightarrow \infty$ limit | 83 |
| 6.9.2 | $\beta \rightarrow 0$ limit | 85 |
| 6.10 | Entanglement Hamiltonian | 85 |
| 6.11 | Discussion | 87 |
| 7 | Conclusion | 90 |
| | Bibliography | 92 |
| A | Distance between states, Purification and Fidelity | 102 |
| A.0.1 | Hilbert-Schmidt inner product | 102 |
| A.0.2 | Purifications | 102 |
| A.0.3 | Fidelity | 103 |

| | | |
|----------|--|------------|
| B | More results on Negativity | 104 |
| | B.0.4 Classical Variable representation | 104 |
| | B.0.5 Identities | 106 |
| | B.0.6 General Results | 108 |
| C | Representation theory of $SU_q(2)$ | 111 |
| | C.1 Identities for q-CG coefficients | 111 |
| | C.2 q-deformed F-matrix and 6j symbols | 111 |

List of Figures

| | | |
|-----|---|----|
| 2.1 | a) Subsystems A (red) and B (green) of a one dimensional system $0 \leq x \leq L$. Euclidean time τ is periodic with period β . b) The density matrix elements are obtained integrating the euclidean action over the fields, subject to specific boundary conditions. c) The partial density operator ρ_A is obtained tracing over degrees of freedom in B | 10 |
| 2.2 | (a) We start with a base manifold $\mathcal{M}_{\text{base}}$ which in this case is a torus (periodic system in space $0 \leq x \leq L$ and periodic in Euclidean time due to the introduction of temperature). We define our subsystem to be a region of the interval $0 \leq x_A \leq L_A$ with $L_A < L$. (b) To compute the Reyni entropy, we have to glue α copies of ρ_A along the subsystem A | 11 |
| 3.1 | (a) Pictorial representation of the operator A_n . Right and left lines correspond to the matrix indices of A (auxiliary), while the upper line corresponds to the quantum state. (b) Construction of the state by joining auxiliary indices. | 18 |
| 3.2 | (a) Transfer matrix (see text). (b) Computation of correlation functions with MPS state. The matrix $T_{\mathcal{O}_i}$ is obtained by inserting the operator \mathcal{O}_i between matrices A | 19 |
| 3.3 | (a) Linear map from the black bonds (auxiliary space) to the red bond (physical index) useful for two dimensional lattices. (b) Tensor network states are constructed by joining neighbor tensors and tracing out auxiliary degrees of freedom. Doing this we are left with just physical indices, characterizing the quantum state. | 20 |
| 3.4 | a) Maximally entangled state. Each circle coincide with one part of the state. b) Local PEPS. Given a coordination number z at site i , z maximally entangled states are brought to site i , where a projection onto the physical subsystem (red circle) is applied as in the figure. | 21 |

| | | |
|-----|---|----|
| 4.1 | Graphic representation of the 1D VBS state. | 23 |
| 4.2 | Partition of the 1D chain in three subsystems A, B_1, B_2 . Subsystem A , consisting of L sites. Subsystem $B = B_1 \cup B_2$ is the complement of A | 24 |
| 4.3 | We made a partition of the VBS state in 5 sectors, labeled A, B, C, D and E as shown in the figure. To obtain the density matrix for the blocks A and B , we trace away the spin variables at the sites inside C, D and E | 28 |
| 4.4 | We trace blocks C and D , leaving a reduced density matrix in terms of the states of the A and B blocks. | 33 |
| 5.1 | (a) In the double scaling limit the reduced density matrix of $ \text{VBS}_q\rangle$ has four degenerate eigenvalues at the isotropic $q = 1$ point. The two middle eigenvalues are always degenerate (bold line). In the classical limit $q \rightarrow 0$ the ground state is a product state and the only nonzero eigenvalue is unity. (b) The Rényi entropy S_R vanishes as $q \rightarrow 0$. It saturates to the maximally entangled value $S_R = \log 4$ at the AKLT point $q = 1$. The von Neumann entropy (bold line) is obtained at $\lim_{\alpha \rightarrow 1} S_R(\alpha)$. . . | 44 |
| 5.2 | The von Neumann entropy decreases away from the isotropic AKLT points $q = 1$ for $ \text{VBS}_q\rangle$ (a) and $a = 2$ for $ \text{KSZ}_a\rangle$ (b). At the isotropic point finite-size corrections are largest for $ \text{VBS}_q\rangle$ and smallest for $ \text{KSZ}_a\rangle$ | 47 |
| 5.3 | Diagrammatic representations of matrices used in the MPS description of the $\text{VBS}_q(S)$ state (upper row). The q -deformed Clebsch-Gordan coefficients (lower left) are important in the diagonalization of the transfer matrix. The matrix $\tilde{\rho}_l$ (lower right) is related to the reduced density matrix ρ_l of l sequential spins in a chain of L sites by $\rho_l = \tilde{\rho}_l / \text{tr} \mathbf{G}^L$ | 49 |
| 5.4 | Diagrams representing the contraction of the transfer matrix \mathbf{G} with a q -deformed Clebsch-Gordan coefficient. The q -deformed F -matrix is defined according to the upper diagram in which the leg labeled by b' is shifted. The lower diagram represents the eigenvalue equation (5.45). In these diagrams internal lowercase indices are summed over. | 51 |
| 5.5 | The Rényi entropy $S_R(\alpha)$ of a q -deformed spin- S VBS state vanishes in the limit $q \rightarrow 0^+$. At the isotropic point $q = 1$, large blocks are maximally entangled $S_R(\alpha) = 2 \ln(S + 1)$. The von Neumann entropy is obtained in the limit $\alpha \rightarrow 1$ (bold line). . | 54 |

| | | |
|-----|---|----|
| 5.6 | The eigenvalues of the reduced density matrix of a block of ℓ spins in a spin-2 VBS $_q$ state (solid and dashed blue lines) are compared to the perturbation result (red dotted lines). Solid blue lines denote nondegenerate eigenvalues while dashed blue lines denote doubly degenerate ones. The dominant eigenvalue approaches unity as $q \rightarrow 0$. For $\ell = 1$ four eigenvalues are zero for all q | 59 |
| 6.1 | a) Original planar graph \mathcal{G} , vertices represented with black dots. b) VBS state on \mathcal{G}' , circles (vertices of \mathcal{G}') represent symmetrization of constituents spin 1/2 (black dots) particles, while bonds represent anti-symmetrization of neighboring spins. Note that any loop in \mathcal{G} would make the associated VBS state vanish, as it would correspond to the antisymmetrization of a state with itself. | 65 |
| 6.2 | (color online) a.- The VBS ground state in its tensor product representation can be viewed as a two dimensional lattice build up from contractions of virtual indices (black lines in the plane). The physical indices stick out of the plane. After making the partition, virtual indices at the boundary are free. b.- The overlap matrix $M_{\alpha\beta}^{[A]} = \langle A_\alpha A_\beta \rangle$ can be obtained by stacking two of this systems and contracting their physical index. This creates a two layer stack. c.- Graphical representation of the partial density matrix ρ_A , for a particular partition. For periodic boundary conditions, the overlap matrix corresponds to a section of the torus with two different, inner and outer, layers. To compute $(\rho_A)_{\alpha\beta}$, we glue the inner layers of the overlap matrices $M^{[A]}$ and $M^{[B]}$ (contracting the virtual indices), obtaining a two layer torus with a cut in the outer sheet along the boundary of the partition. The cut here is represented by the dashed line. | 68 |
| 6.3 | First terms in the graph expansion of the RDM ρ_A . For a generic lattice, the number of bonds arriving to a boundary vertex (big circles) can be any even integer, here we show for simplicity the case corresponding to an hexagonal lattice where the number of bonds arriving to a vertex is exactly 2. Dashed lines show the remaining bonds after taking the trace over the whole lattice, except for the boundary vertices joined by wiggly lines. | 73 |

| | | |
|-----|---|----|
| 6.4 | (color online) a. Loop contribution to A_1 in the hexagonal lattice. Big circles represent boundary sites, along the partition (dashed line). b. Dashed line represent a partition in the square lattice. The contributions to A_1 consist now of configurations of overlapping loops. | 74 |
| 6.5 | (color online) Graphical notation for the interaction terms of the Hamiltonian. Sites who interact are connected by bonds. a) Vertex and nearest neighbors in the square lattice. b) Two body interactions. c) Four body interactions. Different colors represent different interaction strengths (for $K_h = K_v$). | 79 |
| 6.6 | (color online) J_1, J_2 and J_3 couplings as function of K_h . The black dots corresponds to the value of the couplings at the critical $(K_h)_{crit} = \frac{\ln(1+\sqrt{2})}{4}$, where the correlations in the groundstate become long range. In the large K_h limit, the entanglement Hamiltonian is well approximated by the an Ising type Hamiltonian. | 87 |

Acknowledgements

I thank my advisor Vladimir Korepin for introduce me to this completely novel line of research for me and also for his always illuminating comments. Also I am grateful of all the support from my collaborators, specially prof. Andreas Klümper for including me, along with prof Korepin, in two fun projects regarding deformations of Lie Algebras. Without prof. Klümper's ideas those projects would have never seen the light. I want to thank also Francis Paraan, with whom we spent several afternoons talking about interesting projects and ideas related (and not so much sometimes) to our work. I am also indebted to prof. Tzu-Chieh Wei, who was been very supportive and has always had some time to listen to my new ideas. Special thanks to prof. Robert Schrock, for all his comments of support and interest in my future academic well being. I further thank Prof. Eden Figueroa and Prof. Alexander Kirillov, Jr. for their critical reading of this manuscript as committee members of my defense.

On a personal note, I want to thank all the good friends that I make during this four years in grad school. Now I feel that I have a lot of places to visit all over the world. Special regards to Anibal Medina and Marcos Crichigno, for being always open to share with me their new findings, and to teach me some fun stuff too. I am beholden to Pedro Liendo and Pilar Staig for their countless help in setting up practical matters.

I want also to express my deepest gratitude to Fernanda Duarte, for being with whom I feel at home, away from home. Finally I just want to thank my family, specially my parents, because without them, without their effort, sacrifice, and love nothing of this would be possible.

Chapter 1

Introduction

Quantum entanglement, the spooky action at a distance that has been attributed as *the* characteristic of quantum mechanics [1], has received renewed attention recently, especially with the growth of quantum information science [2], and as a new tool to study properties of many-body systems [3, 4].

In quantum mechanics, entanglement arises from interactions between two (or more) quantum systems. These interactions create novel correlations that persist even when the constituent quantum systems are taken far apart. The idea of objects been entangled over arbitrary distances (non-locality) is clearly a puzzling one. It was first challenged in the classic article of Einstein, Podolsky and Rosen *Can Quantum-Mechanical Description of Physical Reality Be Considered Complete?* [5], where the idea of non-locality is contrasted with the postulates of special relativity, which impose a maximum speed to any physical signal. This contradiction, they argued, indicates an incomplete description of the physical world by quantum mechanics. They proposed the existence of local hidden variables, not accounted in the original formulation of quantum mechanics, as a solution of the problem. Despite of the apparent paradox between locality and quantum mechanics, in 1965, John Bell [6] proved that the principle of locality - the principle establishing that objects can be influenced directly by their immediate surroundings - is incompatible with the assumption of local hidden variables. Furthermore, he demonstrated that any theory based in local realism should obey some inequalities, known nowadays as Bell's inequalities, that bound the amount of correlations between systems described by those theories. He also showed that quantum mechanics predicts a violation in those inequalities. Such violations have been confirmed experimentally (see [7] for a review).

Nowadays, there is great consensus in the community that quantum mechanics is the more accurate theory of the microscopic world currently at our disposal. An inevitable consequence of quantum mechanics of many (more

than one) particles is entanglement.

Instead of fighting back the apparent weird consequences of entanglement, physicists have taken the approach of studying it as a real physical phenomenon. This point of view has been increasingly fruitful, as many applications based on entangled states have been developed in quantum information science. In this context, the purely quantum correlations that appear in entangled states are a resource that can be used for communication tasks otherwise impossible between distant parties. This ideas have been confirmed experimentally and used for example in teleportation [8], dense coding [9] or quantum cryptography [10].

In quantum information science, entanglement is regarded as a resource, like energy for example, that can be used to achieve some purpose. It can be distilled from a highly entangled state or can be diluted from a high entangled state to a less entangled one (see Chapter 2).

Entanglement properties are crucially dependent of which type of partition we are able to perform. So far we have talked about spatial separation, but the system can also be separated in momentum, number of species, even time. A system can be entangled respect to one partition, while being disentangled respect to other. Moreover, for a particular type of partition, let's say a partition in space, different number of subsystems can be entangled in different ways, and the situation becomes even more complicated if we start with a mixed system. These difficulties complot against a full characterization of entanglement in quantum systems. In order to quantify the presence of entanglement, it is necessary to introduce different measures. These measures can be separated in two categories, measures for pure systems and measures for mixed systems. Within each category we can study entanglement in bipartite and multipartite states. An account for the different measures used in both categories is given in Chapter 2. Among all these measures we concentrate in this text in the measures for bipartite systems, either for pure or mixed states.

Entanglement generates correlations in quantum systems which are not properly described by the usual theory of order parameters. Using some bipartite measures like entanglement entropy or negativity, properly introduced in chapter 2, we explore in the subsequent chapters the characterization of entanglement in many body systems.

The main focus of this thesis is to identify the presence of entanglement in quantum systes using some of its ubiquitous measures, namely entanglement entropy and entanglement spectrum for pure systems, and negativity for mixed systems.

Among states appearing in many body systems, the ground state - the state of the system with the lowest energy- is of special interest regarding

entanglement. A unique ground state has zero entropy, but if entanglement is present, the entropy between two subsystems of this ground state is nonzero, reflecting the purely quantum nature of entanglement. In a classical system, if the entropy of the whole system is zero, the entropy of all the subsystems is strictly zero. It is for this reason that the entanglement entropy is a good measure of the entanglement properties between regions of a quantum system only if the whole system is in its ground state, because it is here where we know that the state does not have residual thermal, or von Neumann entropy.

The von Neumann entropy has the same mathematical definition as the entanglement entropy, so if we compute the von Neumann entropy for an arbitrary quantum system, this entropy should scale with the volume of the system, because it is an extensive quantity. Contrary to this idea, it has been found that the entanglement entropy in ground states of gapped systems scales with the length of the boundary of the partition (see [4] for a review), a fact that it is now known as area law of entanglement entropy. Using this as an input, a novel way to approximate (in some cases even describe exactly) ground states has been devised. This construction is given in terms of so called matrix product states and its generalizations called generically tensor network states (TNS) and projected entangled pair states (PEPS). The states obtained from this objects follow an area law for entanglement entropy by construction. We review the construction of ground states in terms of these local matrices (or tensors) in Chapter 3. This method of obtaining ground states is efficient (scales just polynomially with the number of constituents keeping bounded errors) for gapped systems.

Having defined how to construct ground states of gapped systems in general, we review a simple example, originally introduced for a completely different purpose, the Affleck-Lieb-Kennedy-Tasaki (AKLT) model [11], which is a model of a spin one chain with nearest neighbors interactions. The AKLT model plays an important role in the understanding of condensed matter systems, specially in one dimension, being the first rigorous example of an isotropic spin chain which agrees with the Haldane conjecture, i.e. Haldane's suggestion that an anti-ferromagnetic Hamiltonian describing half-integer spins is gapless, while for integer spins it has a gap [12]. The ground state of this model has a simple description in terms of matrix product states. This state is known as Valence-Bond Solid (VBS).

The VBS state is relevant for quantum information processing, as it has been proved [13] that in two dimensions it can support all necessary quantum gates (a generalization of binary logic gates in classical computation) needed to process information encoded in qubits. This possibility makes the VBS state a good candidate where universal quantum computation could be realized.

In Chapter 4 we introduce the AKLT model in one dimension and study its entanglement properties, using entanglement entropy for a bipartition of the pure ground state, and negativity for the case of mixed systems. Different boundary conditions are considered and an area law for entanglement entropy is rederived.

The AKLT model is based on the $SU(2)$ symmetry of the system. This symmetry can be enlarged to a more general symmetry called *quantum group*. This quantum group is a natural deformation of the Lie algebra, in terms of a parameter q . In Chapter 5 we investigate the entanglement properties for this type of models. Not only the entanglement entropy is derived, but also a boundary description in terms of a local Hamiltonian at the boundary of the partition, the so called Entanglement Hamiltonian. The eigenvalues of this entanglement Hamiltonian, the entanglement spectrum (ES) [14], provide a complete description of the entanglement properties of bipartite pure state $|\Psi\rangle$ composed of subsystems A and B . It has been shown that the entanglement Hamiltonian describes excitations living at the edge of partitions of the ground state of fractional quantum Hall states [14].

Lou *et al* [15] and Cirac *et al.*[16], using Montecarlo simulations and projected he entangled pair states (PEPS) [17] in finite size systems, showed that the ES of a partition in the ground state of the AKLT model is related with the conformal XXX Heisenberg model on the boundary of the partition. In Chapter 6 we show that the ES of a partition of a whole class of ground states defined in translational invariant lattices, can be approximated by the spectrum of a series of local Hamiltonians along the boundary. Evidence for the structure of the entanglement Hamiltonian is given in Section 6.5 based on the analysis in the continuous limit.

This Bulk-Edge correspondence between the entanglement properties in the bulk of gapped systems and the emergence of a boundary description is explored further in Section 6.6. Here we analyze the Ising PEPS model which is a model whose ground state wavefunction is given by the partition function of the classical Ising model in two dimensions with zero external field. This model allows us to explore the change in boundary description for a model under a quantum phase transition at zero temperature. The temperature parameter in the classical model is mapped to a parameter in the local two dimensional Hamiltonian that interpolates between two different phases for the many body ground state. At the critical value corresponding to the critical temperature in the classical partition function, occurs a quantum phase transition in the quantum model. This is also reflected in the boundary/entanglement Hamiltonian.

In the last chapter we present an unified overview of the results obtained

in this work and discuss some interesting open questions.

Chapter 2

Entanglement in pure and mixed states

Entanglement is a phenomena where two (or more) quantum systems are linked together and their description cannot be done separately, disregarding their spatial separation. Mathematically, we say that two systems are entangled if the state vector of the whole system cannot be written as a product of states living in each system separately. Since the early days of Quantum Mechanics (QM), entanglement posed an important challenge in the understanding of the microscopic world. Counterintuitive ideas already appear in 1935 Schrodinger's paper [18] where the known thought experiment of Schrodinger's cat was proposed. In this article also the word *Entanglement* (*Verschränkung* in german) was introduced for the first time.

Einstein, Podolsky and Rosen (EPR) in their 1935 paper [5] showed, using reasonable assumptions on locality and reality, that the description of the physical world using QM was incomplete. In particular they showed how the appearance of entanglement conflicted with the usual notion of signals propagating with a maximum speed (speed of light). EPR proposed the existence of hidden local variables, carrying information about the state of the system. Since this hidden variables are not accounted for in QM, they claimed that the description of the physical world in terms of QM was incomplete. John Bell, in his 1964 paper [6] indicated that such description using local hidden variables should satisfy some specific inequalities (today known as Bell's inequalities). Bell showed that local hidden variables cannot reproduce the predictions dictated by quantum mechanics. Several experimental test on the inequalities introduced by Bell, using entangled states have been performed so far (see [7] for a review), indicating that quantum mechanics is indeed the correct description of the microscopic world.

Before proceeding, let's recall the basic definition of entanglement for bi-

partite systems Given an state of the system $|\phi_{A\cup B}\rangle$ as a vector in the Hilbert space $\mathcal{H}_A \otimes \mathcal{H}_B$, we call the system separable if

$$|\phi_{A\cup B}\rangle = |\phi_A\rangle \otimes |\phi_B\rangle, \quad (2.1)$$

for some pair of vectors $|\phi_A\rangle \in \mathcal{H}_A$, $|\phi_B\rangle \in \mathcal{H}_B$. If the state cannot be written as (2.1), then the subsystems A and B are entangled.

As entanglement appears as the main characteristic of quantum mechanics, it is important then to typify the different amounts of entanglement present in a quantum system, and hence how “quantum” a system really is.

In order to study and characterize entanglement and its role in the dynamics of quantum systems, is necessary to define some type of measure of entanglement. Different measures are useful for different settings.

In this chapter we will present some measures of entanglement, both for bipartite and multipartite systems. In the first section we discuss the general requisites for a given entanglement measure. In the second section we introduce some useful measures for bipartitions in pure states. Entanglement in mixed states will be defined in the last section of this chapter.

2.1 Requisites for entanglement measures

Let’s consider a quantum state \mathcal{Q} shared by several parties A, B, \dots . We will take an operational standpoint, where we have different laboratories (parties) separated spatially, that can share a quantum system (let’s say a photon) initially prepared elsewhere. We assume that each party can perform local arbitrary quantum operations on its subsystem (this means, any operation allowed by QM, but otherwise arbitrary). We also assume that parties can communicate classically (using a classical channel, e.g sending an email, etc.) so they can correlate their actions on \mathcal{Q} . Protocols that can be decomposed in this local operations (LO) and classical communication (CC) are denoted by LOCC’s. A typical example of this type of protocol in quantum communication is teleportation [19]. It is natural to assume that the action of LOCC on \mathcal{Q} can increase *classical* correlations, but **cannot** increase quantum correlations. This idea generates the first requisite for a measure of entanglement,

Requisite 1: Monotonicity Any entanglement measure should be non increasing under LOCC’s.

Although from the point of view of measuring true quantum correlations, the requisite discussed above is enough, it generates infinite measures of entanglement, even for pure bipartite systems (which is the simplest scenario).

It is useful then to introduce further requisites that, at least in the case of pure bipartite systems, make all the entanglement measures equivalent to one [20, 21]. These requisites are

Requisite 2: Additivity

For two copies of the same system, described by a density matrix ρ_1, ρ_2 , we would like to have a measure E which is additive, so that it is extensive (in principle) on the number of particles

$$E(\rho_1, \rho_2) = E(\rho_1) + E(\rho_2). \tag{2.2}$$

Although this condition seems natural, sometimes it is too restrictive. Some widely used measures, like the distillable entanglement seems to not fulfill this requisite.

Requisite 3: Continuity Entanglement Measures should be continuous.

Continuity allows us to study properties related with entanglement using perturbation theory or other powerful methods. It is reasonable to expect that small changes in the parameters of the system (coupling constants, external magnetic fields, population densities, etc) produce small changes in the entanglement properties of the quantum systems. If on the other hand, using an entanglement measure which is continuous, we spot a point where continuity breaks down, this should signal an abrupt change in the entanglement properties, for a small change in the parameter. This could be used to characterize phase transitions. An entanglement measure E which is sufficiently continuous is equivalent, for pure states, to entanglement entropy $S(\rho)$, defined in the next section.

2.2 Entanglement in pure states

For pure states, all measures of entanglement (entanglement monotones [20]) are equivalent. A class of measures is related to the eigenvalue spectrum of the reduced density operator of a partition in the pure state (2.2.1). Another class of measures is geometric in nature. It is related to the maximum overlap (fidelity) between the given pure state and all possible separable states with zero entanglement (2.3.3).

2.2.1 Bipartite systems

Reduced density matrix

Consider a normalized state vector $|\Psi\rangle$ in a Hilbert space \mathcal{H} that represents a pure state. Let us partition the Hilbert space according to $\mathcal{H} = \mathcal{H}_A \otimes \mathcal{H}_B$. This partitioning may be done in coordinate space, wavenumber space, particle label space, etc. Different schemes reveal different physical aspects of the resulting entanglement. Given the pure state $|\Psi\rangle$ there exists a Schmidt decomposition [22–24]

$$|\Psi\rangle = \sum_{i=1}^d a_i |i_A\rangle \otimes |i_B\rangle, \quad (2.3)$$

where $\{|i_U\rangle\}$ is an orthonormal basis in \mathcal{H}_U . This decomposition can always be done, due to the existence of a singular value decomposition of matrices. The set of Schmidt coefficients a_i are unique up to constant phase factors. They satisfy $\sum_i |a_i|^2 = 1$. We may choose all a_i to be real and positive and label them in order of descending magnitude $a_1 \geq a_2 \geq \dots \geq a_d$.

To see how entangled region A is with region B , we distinguish region A by taking the full density operator $\rho = |\Psi\rangle\langle\Psi|$ and taking the partial trace of the degrees of freedom in B . The result is the reduced density operator

$$\rho_A = \text{tr}_B |\Psi\rangle\langle\Psi| = \sum_i |a_i|^2 |i_A\rangle\langle i_A|. \quad (2.4)$$

This operator acts on the subspace spanned by the block state vectors $\{|i_A\rangle\}$. The set of eigenvalues $p_i = |a_i|^2$ of the reduced density operator is used to quantify the entanglement between regions A and B .

Entanglement spectrum

Instead of using just the entanglement entropy as a measure of entanglement in bipartite systems, Li and Haldane proposed [25] that the full eigenvalue spectrum of the partial density matrix could be used as a measure of entanglement. The reduced density operator is thus interpreted as a mixture (Gibbs ensemble) of quantum states governed by an effective Hamiltonian called Entanglement Hamiltonian, at temperature T which depends on the particular characteristics of the model.

$$\rho_A = \sum_i e^{-\beta E_i} |i_A\rangle\langle i_A| = \frac{\exp(-\beta H_{ent})}{\text{tr} \exp(-\beta H_{ent})} \quad (2.5)$$

For some models, this effective Hamiltonian is proportional to a physical

subsystem Hamiltonian [26–28]. This connection will be developed in detail in Chapter 6. It has been shown that ES can distinguish non-local order in topological insulators [29, 30], quantum Hall states [31], and spin systems [32]. Also, the closing of Schmidt gap (difference between two largest eigenvalues of entanglement spectrum) can be used to identify quantum critical points [33]. For example, degeneracies in the entanglement spectrum of blocks of sites in the extended Bose-Hubbard model were analyzed to construct the quantum phase diagram in the ground state [34]. Additionally, the scaling of the Schmidt gap near the boundaries of the Haldane phases in anisotropic spin-1 chains were studied [35].

Entanglement entropy

The entanglement entropy (EE) is a scalar function of the eigenvalue spectrum $\{p_i\}$ of the reduced density operator. It was proposed as an entanglement measure for pure states [36–39]. It is an entanglement monotone for pure states. The von Neumann entropy is defined as

$$S_A = -\text{tr} \rho_A \ln \rho_A = - \sum_i p_i \ln p_i. \quad (2.6)$$

From the Schmidt decomposition is trivial to see that $S_A = S_B$, so the entanglement entropy does not depend on a the particular subsystem. A generalization of S which is easier to compute in some context because involve powers of ρ_A is the Rényi entropy, defined as

$$S(\alpha) = \frac{\ln \text{tr} \rho_A^\alpha}{1 - \alpha} = \frac{1}{1 - \alpha} \ln \sum_i p_i^\alpha. \quad (2.7)$$

The Rényi entropy reduces to the von Neumann entropy as $\alpha \rightarrow 1$. Instead of being an extensive quantity (as usual for thermal states) that scales with the volume of the region considered, the EE for typical ground states scales linearly with the boundary size, following an area law, or an area law with a small (often logarithmic) correction [4].

From (2.7), we can compute the Reyni entropy in continuous models, using the replica trick as follows. We compute $\text{tr} \rho_A^\alpha$ for an integer α . If we succeed, then taking the limit $\alpha \rightarrow 1$ (through analytical continuation) we obtain the desired von Neumann entropy. Having S_α for generic α allow us to recover the eigenvalues of ρ_A , the entanglement spectrum [40, 41].

To obtain the reduced density matrix of a subsystem, $\rho_A = \text{tr}_B \rho$, we define a bipartition of the space degrees of freedom into two disjoint sets A and B and we sew the degrees of freedom in one of the sets (let's take for definiteness

to be the set B). The sewing corresponds to taking the partial trace over the degrees of freedom in B , which means integrating over all the fields in the path integral with support in B (see Fig. 2.1).

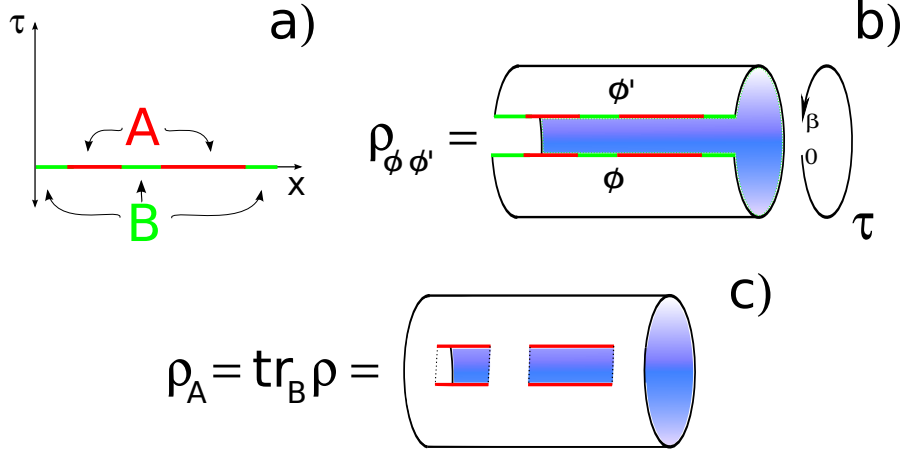


Figure 2.1: a) Subsystems A (red) and B (green) of a one dimensional system $0 \leq x \leq L$. Euclidean time τ is periodic with period β . b) The density matrix elements are obtained integrating the euclidean action over the fields, subject to specific boundary conditions. c) The partial density operator ρ_A is obtained tracing over degrees of freedom in B

Let's introduce some notation. The theory under consideration is described by a Hamiltonian H , and its density operator is in turn $\rho \sim e^{-\beta H}$. A set of mutually commuting operators in this theory is $\hat{\phi}(x, t)$, where we take the base manifold $\mathcal{M}_{\text{base}}$ of the theory to be a line in space $0 \leq x \leq L$ and continuous time $t \geq 0$. The density operator in the basis of eigenstates of $\hat{\phi}(x, t)$, $|\phi(x, t)\rangle$ is then

$$\rho_A(\{\phi\}, \{\phi'\}) = \frac{\langle \phi(x, t) | e^{-\beta H} | \phi'(x, t) \rangle}{Z(\beta)}. \quad (2.8)$$

This expression can be rewritten as an Euclidean partition function,

$$\begin{aligned} \rho(\{\phi\}, \{\phi'\}) &= \frac{1}{Z(\beta)} \int \mathcal{D}\phi e^{-\int_0^\beta d\tau \int dx \mathcal{L}_E} \delta(\phi(x, 0) - \phi(y)) \delta(\phi(x, \beta) - \phi'(y)). \\ \rho_A(\{\phi\}, \{\phi'\}) &= \int \mathcal{D}\phi_{y \in B} \rho(\{\phi\}, \{\phi'\}) \end{aligned} \quad (2.9)$$

To compute $\text{tr} \rho_A^\alpha$, we glue α copies of ρ_A , along the cuts,

$$\mathrm{tr} \rho_A^\alpha = \frac{1}{Z(\beta)^\alpha} \int \mathcal{D}\phi_1 \dots \mathcal{D}\phi_\alpha \rho_A(\phi_1, \phi_2) \rho_A(\phi_2, \phi_3) \dots \rho_A(\phi_{\alpha-1}, \phi_\alpha) \rho_A(\phi_\alpha, \phi_1), \quad (2.10)$$

with this procedure, the computation of the Reyni entropy becomes the computation of the Euclidean action (as opposed to the action in Minkowsky space) of the theory on the Riemann surface \mathcal{M}_α , obtained by gluing together α copies of the manifold $\mathcal{M}_{\text{base}}$ along the cuts corresponding to the subsystem A (see Fig 2.2).

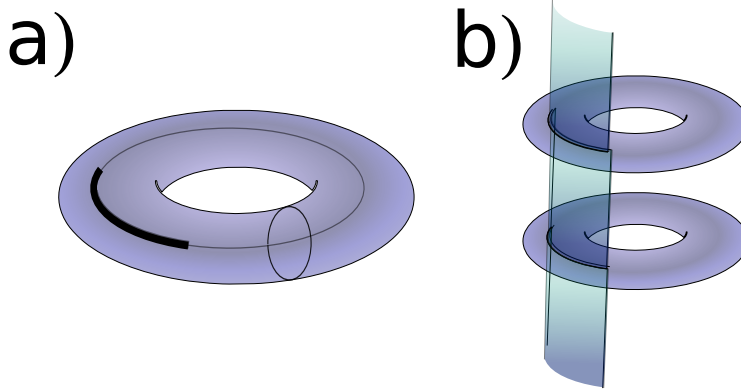


Figure 2.2: (a) We start with a base manifold $\mathcal{M}_{\text{base}}$ which in this case is a torus (periodic system in space $0 \leq x \leq L$ and periodic in Euclidean time due to the introduction of temperature). We define our subsystem to be a region of the interval $0 \leq x_A \leq L_A$ with $L_A < L$. (b) To compute the Reyni entropy, we have to glue α copies of ρ_A along the subsystem A

The trace of ρ_A^α will have the generic form

$$\mathrm{tr} \rho_A^\alpha = \sum_k g_k \lambda_k^\alpha, \quad (2.11)$$

where g_k is the degeneracy of the eigenvalue λ_k . We can recover the distribution of eigenvalues of ρ_A from (2.11) using

$$\sum_{k=0}^{\infty} \mathrm{tr} \rho_A^k z^{-k} = \frac{1}{\pi} \int dy \frac{zP(y)}{z-y} = zP(z), \quad (2.12)$$

where $P(z) = \sum_i \delta(z - \lambda_i)$ is the distribution of eigenvalues of ρ_A .

Topological entanglement entropy

In topological systems, the entanglement entropy has an expansion of the form

$$S(A) = a_1 L - \gamma + O(L^{-b}) \quad b > 0, \quad (2.13)$$

where L is the length of the boundary of A . The first term in (2.13) is the usual area term, and γ is called *topological entanglement entropy* [42]. A non vanishing topological entropy is an indicator of long range entanglement in the quantum state. It corresponds to the logarithm of the total quantum dimension of the excitations (quasiparticles) in the many-body state.

Entanglement of formation and and dilution

From an operational point of view, we can ask: Given n q-bits (two level quantum system) which are little entangled (in a sense defined below), It is possible to distill from these n qbits, m highly entangled q-bits?. To answer this question it is necessary to introduce the concept of entanglement distillation and dilution.

We take the minimal entangled state to be a Bell state

$$|\phi\rangle = \frac{|01\rangle + |10\rangle}{\sqrt{2}}, \quad (2.14)$$

if from n copies of $|\phi\rangle$ we are able to create $m(n)$ high fidelity (see A.0.3) copies of a desired state $|\psi\rangle$ using LOCCs, we can define the entanglement of formation of $|\psi\rangle$ as

$$E_f(\psi) = \lim_{n \rightarrow \infty} \frac{m(n)}{n}, \quad (2.15)$$

this conversion process is also called *entanglement dilution* as takes n copies of maximally entangled states $|\phi\rangle$ and converts them into m less entangled states $|\psi\rangle$.

Similarly, we can define the distillable entanglement of $|\psi\rangle$ as the inverse process. Starting with m copies of $|\psi\rangle$, we ask ourselves, how many Bell pairs can we obtain?. We define then the distillable entanglement of $|\psi\rangle$ to be the asymptotic limit of obtaining $n(m)$ Bell states, starting from m copies of $|\psi\rangle$,

$$E_d(\psi) = \lim_{m \rightarrow \infty} \frac{m}{n(m)}. \quad (2.16)$$

it turns out that $E_f(\psi) = E_d(\psi)$ [2].

2.2.2 Multipartite states

Entanglement in multipartite systems is more difficult to treat as there is not known convertibility process to take one state into other, by means of dilution or distillation. Another problem is related to the existence of entanglement between different subsystems of a multipartite state. For example, in a tripartite state, we can have no entanglement whatsoever, like in the state $|\varphi_A\rangle \otimes |\varphi_B\rangle \otimes |\varphi_C\rangle$, or we can have entanglement between just two subsystems like in $|\varphi_{AB}\rangle \otimes |\varphi_C\rangle$ or we can have entanglement between all the subsystems. In this last case, it is difficult to establish a measure that can discriminate uniquely between two states. For example we can take the N -partite states

$$|W\rangle = \frac{|100\dots 00\rangle + |010\dots 00\rangle + \dots + |00\dots 01\rangle}{\sqrt{N}}, \quad (2.17)$$

$$|GHZ\rangle = \frac{|111\dots 1\rangle + |0000\dots 0\rangle}{\sqrt{2}}, \quad (2.18)$$

which are entangled between all the subsystems. In quantum information applications, their entanglement properties become useful depending on the context.

2.3 Entanglement in mixed states

2.3.1 Bipartite states

In mixed states, to characterize the entanglement between subsystems is more subtle due to the presence of quantum *and* classical (statistical) correlations. In this scenario, the spectrum of the reduced density matrix is no longer useful and it is necessary to rely on different measures.

Concurrence

Concurrence is an entanglement monotone defined for a mixed state ρ of two qbits as $C(\rho) = \max(0, \lambda_1 - \lambda_2 - \lambda_3 - \lambda_4)$ with $\lambda_1 \geq \lambda_2 \geq \lambda_3 \geq \lambda_4$ the eigenvalues of the operator $\mathbb{O} = \sqrt{\sqrt{\rho} M \rho M \sqrt{\rho}}$ with $M = \sigma_y \otimes \sigma_y$ the tensor product of two σ_y Pauli matrices [43, 44].

Using concurrence, we can establish one of the main characteristics of entanglement:

Monogamy of entanglement: If two qbits A and B are maximally (quantum) correlated they cannot be correlated at all with a third qbit C . This can be formally stated using the Coffman-Kundu-Wootters (CKW) inequality [45]

$$C_{AB}^2 + C_{AC}^2 \leq C_{A(BC)}^2, \quad (2.19)$$

where $C_{\alpha\beta}$ is the concurrence between systems α and β . This inequality can be extended to the case of n qbits.

Mutual information

Concurrence is a good measure of entanglement in mixed systems composed of two qbits, but for bigger quantum systems we need another measure. From information theory we know that the mutual information $I(x, y)$ between two random variables X and Y measures the amount of correlation between them. It can be defined in terms of the entanglement entropy as

$$I(A, B) = S(A) + S(B) - S(A \cup B), \quad (2.20)$$

where $S(A)$ is the entropy of region A . This measure does not distinguish between quantum and classical correlations [46]. It is not a proper measure of entanglement but still it is useful in characterize properties of the quantum systems. It is also useful when considering multipartite correlations [47].

Negativity

An important measure of entanglement is negativity, introduced in [48]. Negativity is a useful quantity to characterize quantum effects in mixed systems, where the standard mutual information entropy fails to provide a clear separation between classical and quantum correlations. Negativity is also useful in the context of quantum information because it does not change under local manipulations of the system [49].

Consider a mixed state ρ , with two subsystems, A and B . Negativity is the sum of negative eigenvalues of the operator ρ^{T_A} which is associated with ρ by the linear map \mathcal{M} which transpose elements of subspace A . In terms of the matrix elements of ρ $\langle l_A, m_B | \rho | i_A, j_B \rangle$, the partial transpose matrix ρ^{T_A} has elements $\langle i_A, m_B | \rho | l_A, j_B \rangle$ [48, 49],

$$\mathcal{N}(\rho) = \frac{\|\rho^{T_A}\| - 1}{2}, \quad (2.21)$$

where $\|V\| = \text{tr}\sqrt{V^\dagger V}$ is the trace norm of V .

Also, based on \mathcal{N} we can define the logarithmic negativity as

$$E_{\mathcal{N}} = \log(2\mathcal{N} + 1). \quad (2.22)$$

Some of the properties mentioned at the beginning of this chapter are **not** properties of $E_{\mathcal{N}}$.

- can be zero even if the state is entangled (if the state is PPT entangled).
- is additive on tensor products: $E_{\mathcal{N}}(\rho \otimes \sigma) = E_{\mathcal{N}}(\rho) + E_{\mathcal{N}}(\sigma)$.
- is not asymptotically continuous.
- is an upper bound to the distillable entanglement.

2.3.2 Multipartite states

The characterization of mixed multipartite entangled states is far from being completely understood. One (incomplete) method is to define all the different partition of the original subsystems and to see if we can write the state as a product of states belonging just to each partition. Let's take a multipartite system, composed of subsystems A, B and C . The whole system which is mixed is described by a density matrix ρ_{ABC} . We can take all the possible partitions, namely

$$\mathcal{P} = \{(A, BC); (AB, C); (AC, B); (A, B, C)\}. \quad (2.23)$$

We now determine if the state in the partition $p = (\alpha, \beta) \in \mathcal{P}$ can be written as

$$|\psi_{ABC}\rangle = |\phi_{\alpha}\rangle \otimes |\varphi_{\beta}\rangle, \quad (2.24)$$

where $|\phi_{\alpha}\rangle$ is a state of the α subsystem.

After doing this we will obtain a table stating all the entangled partitions. This table will be in most of the cases redundant as for example if $\psi_{ABC} = |\phi_A\rangle \otimes |\varphi_B\rangle \otimes |\chi_C\rangle$, then the state will be unentangled in all the other possible partitions.

2.3.3 Geometric entanglement

Geometric entanglement is a measure of entanglement based on the geometry of the Hilbert space. Given an entangled state $|\psi\rangle$ it is defined through the Hilbert-Schmidt metric (see A.0.1) as $G(\psi) = \min_{\phi} \|\psi - \phi\|$ where $|\phi\rangle$ is a separable state. Although this measure is easy to define, the minimization over all the separable states is usually complicated to perform. Additional symmetries of the states, like translation invariance in many body systems simplify this task [50].

This geometric measure of entanglement was introduced for bipartite pure states in [51] and extended to multipartite pure states in [52]. Geometric measures for mixed states were discussed in [50, 53]. Universality of geometric

entanglement near quantum critical point was discussed in [54]. Geometric entanglement in one-dimensional models described by matrix product states is explored in [55].

Chapter 3

Tensor Network States

The exact description of a quantum many body systems with N constituents becomes increasingly complicated as N grows as the number of parameters needed to represent the quantum system grows exponentially with the number of sites, due to the enlarged Hilbert space. For a spin $\frac{1}{2}$ chain with m sites, the Hilbert space of the system is \mathbb{C}^{2^m} and the ground state is described in principle by 2^m parameters. In this chapter we will introduce the concept of matrix product states (MPS) and its generalization as Tensor Network States (TNS) and projected entangled pair states (PEPS). Using TNS, the description of ground states scales just polynomially with the number of sites, providing an useful scheme for analysis of quantum many body systems and their ground state entanglement properties. This formalism is particularly efficient for the description of quantum states with an energy gap [56, 57].

In the first section we motivate the introduction of MPS in one dimensional chains and discuss some of the implications for entanglement given this description. In the second section we generalize the MPS description for arbitrary dimensions using TNS. Finally we discuss the connection between PEPS and area laws in many body ground states.

3.1 Matrix product states

Let's take a one dimensional system on the lattice, consisting of N sites and finite local Hilbert space dimension n_i ($i = 1..N$) at site i . A matrix product state is defined as [58–60]

$$|\Psi\rangle = \sum_{\{n_i\}} \text{tr}(A_{n_1}[1]A_{n_2}[2] \cdots A_{n_N}[N])|n_1, n_2, \cdots, n_N\rangle \quad (3.1)$$

where the matrices A_{n_i} are matrices of dimensions D_i . The size of the matrix

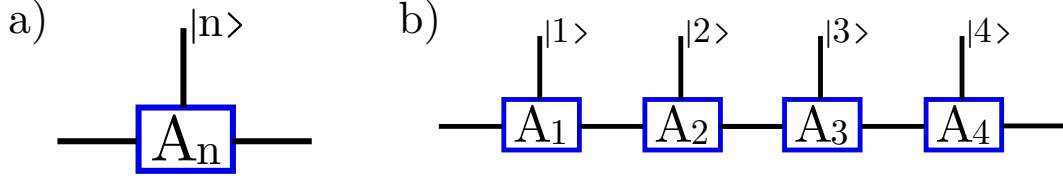


Figure 3.1: (a) Pictorial representation of the operator A_n . Right and left lines correspond to the matrix indices of A (auxiliary), while the upper line corresponds to the quantum state. (b) Construction of the state by joining auxiliary indices.

is called local bond dimension. These matrices are usually represented as three legged objects, where two legs correspond to matrix indices and the third leg corresponds to the so called physical index, which denotes the quantum state of the system, for a given value of the matrix indices (see Fig 3.1)

For translational invariant systems, the matrices A do not depend on the site i . Computation of correlation functions in this formalism is very simple. The object

$$\langle \Psi | \mathcal{O}_i \mathcal{O}_j | \Psi \rangle = \sum_{\{n_i\}} \sum_{\{m_j\}} \text{tr}(A_{n_1} A_{n_2} \cdots) \text{tr}(A_{m_1} A_{m_2} \cdots) \langle n_i, n_j | \mathcal{O}_i m_i, \mathcal{O}_j m_j \rangle, \quad (3.2)$$

is the Ψ -state correlation function of operators \mathcal{O} at different sites (we assume a translational invariant state), and can be computed from local operations by contracting two matrices A at the same site along their physical index, to form a four legged tensor, which is called the transfer matrix. This transfer matrix T is now contracted as in Fig. (3.2) with the matrices at sites i and j $T_{\mathcal{O}_i}, T_{\mathcal{O}_j}$.

The ground states of many spin chains can be represented as a product of $D \times D$ vector valued matrices. Reduced density operators of blocks of spins have at most D^2 nonzero eigenvalues. Entanglement entropy is therefore bounded $S \leq \log D^2$. Due to this transfer matrix structure, the correlation functions decay exponentially. This indicates that the MPS formalism is more appropriate for the description of short range ordered systems, or gapped systems.

The whole discussion presented here is valid for spin systems. Systems with infinite dimensional local Hilbert spaces (e.g bosons) can also be included with the proper modifications.

The matrix A establish a linear map between different spaces, the space

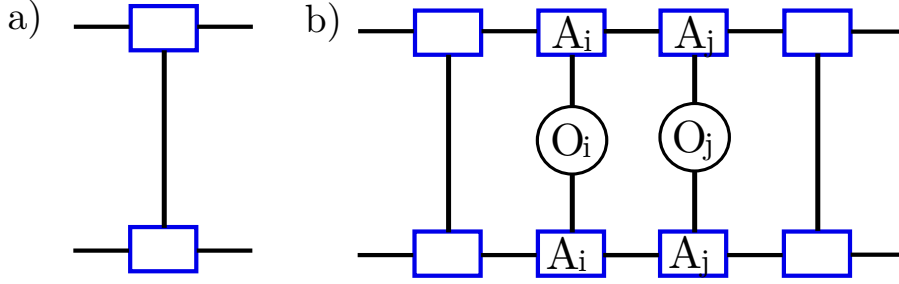


Figure 3.2: (a) Transfer matrix (see text). (b) Computation of correlation functions with MPS state. The matrix $T_{\mathcal{O}_i}$ is obtained by inserting the operator \mathcal{O}_i between matrices A .

where the matrix indices act and the Hilbert space where the quantum states live. This map can be generalized to act between different number of spaces, as we will define next in order to define matrix product states in higher dimensions.

AKLT as an example of MPS

The Affleck Kennedy Lieb and Tasaki (AKLT) model ([61]) is a simple example where the ideas of MPS can be applied quite easily. We will discuss this model in detail in the following chapters, so here we will give just the necessary ingredients to illustrate the power of MPSs.

The AKLT model (in its simpler version) is defined on the lattice, with spin 1 particles at each site, and a local Hamiltonian density acting on neighboring sites, which is a projector Π_{ij} onto total spin 2. We can construct the ground state of this model simply by thinking of each spin 1 particle as a composite of two spin 1/2 particles and antisymmetrizing one of this two spin 1/2 particles with one of the immediate neighbor, in order to produce a singlet. This singlet will prohibit the existence of a spin 2 particle between neighboring sites, then annihilating the Hamiltonian Π_{ij} . The mapping from this two spin 1/2 particles to the spin 1 space is done by the operator

$$P = |1\rangle\langle ++| + |-1\rangle\langle --| + |0\rangle\frac{(\langle + - | + \langle - + |)}{\sqrt{2}} = \sum_{\alpha, \beta, a} A_{\alpha\beta}^a |a\rangle\langle \alpha\beta| \quad (3.3)$$

which implements the map to the symmetric subspace of $\frac{1}{2} \otimes \frac{1}{2}$. The ground state is then

$$|GS_{AKLT}\rangle = \bigotimes_{i=1}^N \varepsilon_{\beta_{i-1}\alpha_i} A_{\alpha_i\beta_i}^a |a_i\rangle \quad (3.4)$$

3.2 Tensor Network states and PEPS

Is it possible to define tensor network states as in (3.1), but the notation gets a little cumbersome, so we prefer to define TNS pictorially,

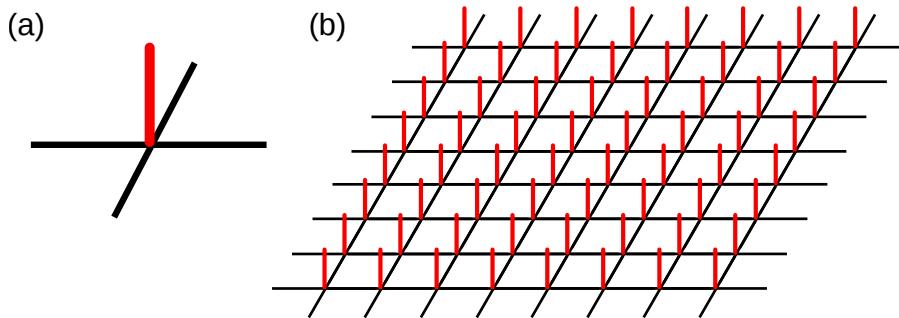


Figure 3.3: (a) Linear map from the black bonds (auxiliary space) to the red bond (physical index) useful for two dimensional lattices. (b) Tensor network states are constructed by joining neighbor tensors and tracing out auxiliary degrees of freedom. Doing this we are left with just physical indices, characterizing the quantum state.

The local tensor (analogous of A in the previous section), can be thought as a linear map from the auxiliary space to the physical Hilbert space. This map can be implemented through the inclusion of tensors (repeated indices are summed)

$$\mathbb{T}(i) = T_{\alpha_1\alpha_2\cdots\alpha_z}^a [i] |a\rangle \langle \alpha_1, \alpha_2, \cdots, \alpha_z|, \quad (3.5)$$

$$\bar{\mathbb{T}}(i) = (T_{\alpha_1\alpha_2\cdots\alpha_z}^a)^* [i] \langle \alpha_1, \alpha_2, \cdots, \alpha_z| \langle a|, \quad (3.6)$$

for a lattice with coordination number z . The constructions presented above for the computation of observables is still valid in more dimensions, where now the local union of $\mathbb{T} \otimes \bar{\mathbb{T}}$ is a $2z$ legged tensor.

Based on the construction used for the AKLT model presented above, we can generalize it for arbitrary dimensions and using more general maximally entangled states. This generalization leads directly to the construction of projected entangled pair states [62].

3.2.1 PEPS

Projected entangled pair states are a natural generalization of MPS, useful in more than one dimension. It can be created by postselection using a quantum circuit. We put with a maximally entangled state

$$|\Phi\rangle = \sum_{n=1}^D |n, n\rangle, \quad (3.7)$$

between two neighboring sites in a lattice. At each site, we will have z halves of the maximally entangled states, which we project onto a physical state using a projector P (in the AKLT case this was just the projector onto the symmetric subspace). This projector defines the PEPS (See Fig 3.4). For a lattice with in d dimensions, with N sites and coordination number z , the number of parameters required to specify the state is NdD^z .

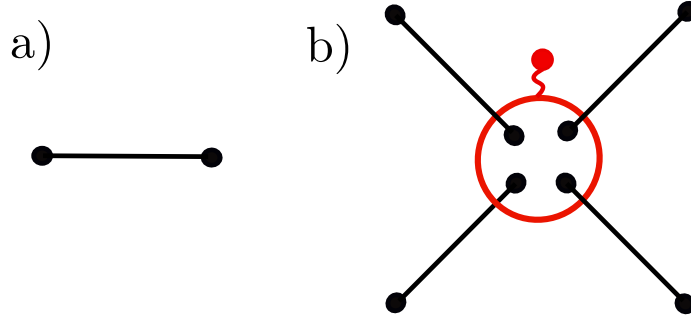


Figure 3.4: a) Maximally entangled state. Each circle coincide with one part of the state. b) Local PEPS. Given a coordination number z at site i , z maximally entangled states are brought to site i , where a projection onto the physical subsystem (red circle) is applied as in the figure.

This construction is fairly flexible, and allows for a efficient approximation of quantum states. Usually for a generic state the value of D to get a good approximation may be very high and may increase with N , but as this types of states follow an area law $S \leq N \log D$, the scaling of D with N is just polynomial. Using this idea, it has been proved [63] that PEPS are an efficient description of a Gibbs state as long as the interactions are local.

PEPS satisfy an area law by construction, due to the presence of maximally entangled states, which cross from one subsystem to the other. For a system with a boundary of length L ,

$$S_{PEPS} \leq L \log(D). \quad (3.8)$$

Chapter 4

Negativity in AKLT ground state

After reviewing the basic concepts regarding entanglement in the previous chapters, we now make explicit use of the some concepts presented in Chapter 2, specially the entanglement measures for bipartite systems, studying a particular model in one dimension, the AKLT model, briefly introduced before.

In the first section we quickly review the formulation of the AKLT model and its valence bond solid (VBS) ground state with its extension to make it unique. We also obtain the density matrix associated with the VBS ground state. In the second section we take a bipartition of the pure ground state. We re-derive the spectrum of the partial density matrix $\rho_A = \text{tr}_B \rho$ using our simpler approach obtaining the results already shown in [64]. We also computed the transposed density matrix ρ^{TA} to illustrate our method. For this case we compute the full spectrum, along with eigenvectors of ρ^{TA} . We also give a value for the negativity in this case, which decays to a constant value twice as fast as expected from correlation functions. In the third section we define two blocks A and B , separated by L sites. We compute the density matrix of the mixed system $A \cup B$ $\rho(A, B)$, evaluated by tracing out environmental degrees of freedom. We obtain the spectrum of $\rho(A, B)$ and the entanglement spectrum as function of the separation L between blocks and the size of A and B . The purity of this system corresponds to the one encountered for maximally mixed states (up to second order corrections). In this section we find that negativity for this system vanish for non adjacent blocks. We also study the case of periodic boundary conditions. In the fourth section we obtain the mutual entropy of the system, in the limit of infinite blocks A and B .

4.1 The AKLT model and the VBS state

The one dimensional AKLT model that we will consider consists of a chain of N spin-1s in the bulk, and two spin-1/2's on the boundary. The location where the spins sit are called sites. We shall denote by \mathbf{S}_k the vector of spin-1 operators and by \mathbf{s}_b spin-1/2 operators, where $b = 0, N+1$. The Hamiltonian is $H = H_{\text{Bulk}} + \Pi_{0,1} + \Pi_{N,N+1}$, where the Hamiltonian corresponding to the bulk is given by

$$H_{\text{Bulk}} = \sum_{i=1}^{N-1} \frac{1}{6} (3\mathbf{S}_i \cdot \mathbf{S}_{i+1} + (\mathbf{S}_i \cdot \mathbf{S}_{i+1})^2 + 2), \quad (4.1)$$

and the sum runs over the lattice sites. The boundary terms Π describe interaction of a spin 1/2 and spin 1. Each term is a projector on a state with spin 3/2:

$$\Pi_{0,1} = \frac{2}{3}(1 + \mathbf{s}_0 \cdot \mathbf{S}_1), \quad \Pi_{N,N+1} = \frac{2}{3}(1 + \mathbf{S}_N \cdot \mathbf{s}_{N+1}). \quad (4.2)$$

In order to construct the ground state $|VBS\rangle$ of H we can associate two spin 1/2 variables at each lattice site and create the spin 1 state symmetrizing them. To prevent the formation of spin 2, we antisymmetrize states between different neighbor lattice sites. Doing this we are sure that this configuration is actually an eigenstate of the Hamiltonian, with eigenvalue 0 (i.e. the projection of $|VBS\rangle$ on the subspace of spin 2-states is zero). Noting that the Hamiltonian H is positive definite, then we know that this is the ground state.

We can associate a graph to this state, defining dots as spins 1/2, links as anti-symmetrization, and circles as symmetrization. The graph representation of the VBS ground state is then given by Fig. 4.1.

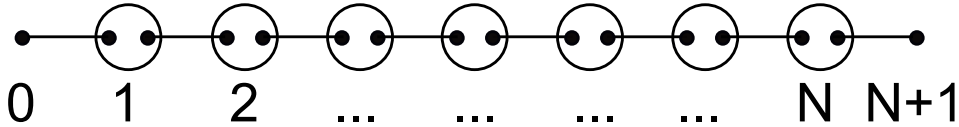


Figure 4.1: Graphic representation of the 1D VBS state.

It is possible to write down a compact expression for this VBS state using bosonic variables. Following [65], we make use of the Schwinger boson representation for $SU(2)$ algebra at each site j , namely $S_j^+ = a_j^\dagger b_j$, $S_j^- =$

$a_j b_j^\dagger$, $S_j^z = \frac{1}{2}(a_j^\dagger a_j - b_j^\dagger b_j)$, with $[S_i^z, S_j^\pm] = \pm S_i^\pm \delta_{ij}$, $[S_i^+, S_j^-] = +2S_i^z \delta_{ij}$, where a and b are two sets of bosonic creation operators, with the usual commutation relations $[a_i, a_j^\dagger] = [b_i, b_j^\dagger] = \delta_{ij}$, $[a_i, a_j] = [b_i, b_j] = 0$ and correspondingly for a^\dagger and b^\dagger . These two sets commute in each and every lattice site, i.e. $[a_i, b_j] = [a_i^\dagger, b_j] = 0$. To have a finite dimensional representation of $SU(2)$, it is necessary to impose one more condition on a and b , given by $\frac{1}{2}(a_j^\dagger a_j + b_j^\dagger b_j) = S_j$, with S_j the value of the spin at site j (in this chapter we have $S_j = 1$ for $j = 1..N$ and $1/2$ at $j = 0, N + 1$). In this language the VBS ground state is given by [65]

$$|\text{VBS}\rangle = \prod_{i=0}^N (a_i^\dagger b_{i+1}^\dagger - a_{i+1}^\dagger b_i^\dagger) |0\rangle. \quad (4.3)$$

where $|0\rangle = \bigotimes_{\text{sites}} |0_a, j\rangle \otimes |0_b, j\rangle$. The state $|0_a, j\rangle$ is defined by $a_j |0_a, j\rangle = 0$, and it's called the vacuum state for the set of operators a . $|0_b, j\rangle$ is defined similarly for the set b . In [66] the authors prove that this ground state is unique for the Hamiltonian H , then we can construct the density matrix of the (pure) ground state $\rho = \frac{|\text{VBS}\rangle\langle\text{VBS}|}{\langle\text{VBS}|\text{VBS}\rangle}$. This is a one dimensional projector on the $|\text{VBS}\rangle$ ground state of the Hamiltonian.

4.2 Density matrix pure state

In order to compute the partial transposed density matrix of the VBS system, we define three subsystems A , B_1 and B_2 , where A is a block of L spins 1 and $B = B_1 \cup B_2$ is it's complement (see Fig. 4.2)

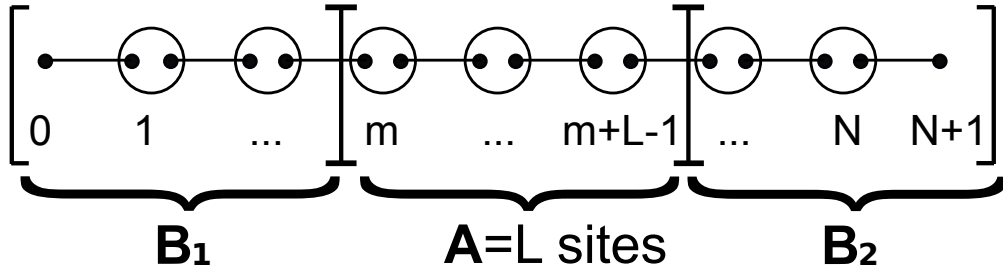


Figure 4.2: Partition of the 1D chain in three subsystems A , B_1 , B_2 . Subsystem A , consisting of L sites. Subsystem $B = B_1 \cup B_2$ is the complement of A .

For the partition defined by (with $1 \leq L, m \leq N$) $B_1 = \{\text{sites } i, 0 \leq i \leq$

$m-1\}$, $A = \{\text{sites } i, m \leq i \leq m+L-1\}$, $B_2 = \{\text{sites } i, m+L \leq i \leq N+1\}$ we can split the expression (4.3) in the corresponding states of the subsystems

$$|\text{VBS}\rangle = (a_{m-1}^\dagger b_m^\dagger - a_m^\dagger b_{m-1}^\dagger)(a_K^\dagger b_{K+1}^\dagger - a_{K+1}^\dagger b_K^\dagger)|A, B\rangle. \quad (4.4)$$

where $K = m+L-1$. $|A\rangle$ and $|B\rangle$ are the VBS states of the A and B subsystems, defined by $|A\rangle \equiv |m^K\rangle$, $|B\rangle \equiv |0^{m-1}\rangle|_{K+1}^{N+1}\rangle$, where the states of the form $|I^J\rangle$ are defined as

$$|I^J\rangle \equiv \prod_{l=I}^{J-1} (a_l^\dagger b_{l+1}^\dagger - a_{l+1}^\dagger b_l^\dagger)|0\rangle, \quad (4.5)$$

respectively. This state describes spin 1 in the bulk (i.e at $l \neq I, J$) and spin 1/2 in the boundary. To recover the spin 1 at those boundaries sites, we introduce the following notation $(\psi_k^1)^\dagger = a_k^\dagger$, and $(\psi_k^2)^\dagger = b_k^\dagger$, to have

$$|{}^c A^d \equiv (\psi_m^c)^\dagger (\psi_K^d)^\dagger |A\rangle, \quad |{}^c B^d \equiv (\psi_{m-1}^c)^\dagger (\psi_{K+1}^d)^\dagger |B\rangle \quad (c, d = 1, 2),$$

then eq. (4.4) becomes

$$|\text{VBS}\rangle = |{}^2 A^1, {}^1 B^2\rangle - |{}^1 A^1, {}^2 B^2\rangle - |{}^2 A^2, {}^1 B^1\rangle + |{}^1 A^2, {}^2 B^1\rangle. \quad (4.6)$$

The four states $|{}^\sigma A^\eta\rangle$ belong to the Hilbert space of the block A of length L . They span the kernel of $H_{\text{Bulk}}(A)$ [11], but they are not orthogonal to each other. We make use of the classical variable method, introduced in [65] (see appendix B.0.4), to prove

$$\begin{aligned} \|{}^\sigma A^\nu\|^2 &= \frac{1}{4} \left(1 - (-1)^{\sigma+\nu} \left(-\frac{1}{3} \right)^L \right), \quad \text{and} \\ \langle {}^\sigma A^\nu | {}^\nu A^\sigma \rangle &= -\frac{1}{2} \left(-\frac{1}{3} \right)^L \quad \text{for } \sigma \neq \nu, \end{aligned} \quad (4.7)$$

valid for $L \geq 1$ ($L \in \mathbb{N}$). The norm $\|u\|^2$ is defined as usual $\|u\|^2 = \langle u|u\rangle$. All other combinations vanish. We can perform a rotation of this basis in order to make the overlap (4.7) vanish. The new basis is defined by

$$\begin{aligned}
|A_0\rangle &\equiv \frac{i}{\sqrt{2}}(|^1A^1\rangle + |^2A^2\rangle), & |A_1\rangle &\equiv \frac{1}{\sqrt{2}}(|^1A^2\rangle + |^2A^1\rangle), \\
|A_2\rangle &\equiv \frac{-i}{\sqrt{2}}(|^1A^2\rangle - |^2A^1\rangle), & |A_3\rangle &\equiv \frac{1}{\sqrt{2}}(|^1A^1\rangle - |^2A^2\rangle),
\end{aligned}$$

In this basis (here $\mu, \nu = 0..3$) the norm is given by

$$\langle A_\mu | A_\nu \rangle = \frac{1}{4} \left(1 - s_\mu \left(-\frac{1}{3} \right)^L \right) \delta_{\mu\nu}, \quad (4.8)$$

where $s_\mu = (-1, -1, 3, -1)$. These four different eigenstates of the bulk Hamiltonian corresponding to the block A , can be labeled by the Bell pair that is formed between the spins $1/2$'s at the boundary. The states of the environment B form an orthonormal basis $\langle B_\mu | B_\nu \rangle = \delta_{\mu\nu}$. The boundary operators a, b which act on the subspace B , also organize themselves in irreducible representations, with the only condition that adjacent boundary operators acting on A and B cannot create a state of spin 2, as required by the VBS ground state symmetry. We define the following operators for further simplicity (here, sum over dummy variables $c = 1, 2$ and $d = 1, 2$ is assumed)

$$T_\mu^\dagger(i, j) = \psi_i^{c\dagger} (\sigma_\mu)_{cd} \psi_j^{d\dagger}, \quad (\mu = 0..3), \quad (4.9)$$

with $\sigma_\mu = (i\mathbb{I}, \sigma_1, \sigma_2, \sigma_3)$ being \mathbb{I} the 2×2 identity matrix and σ_i are the Pauli matrices.

The operators T_μ keep explicit the symmetry between the operators a and b , remaining unchanged (up to phase factors) when we interchange the operators a^\dagger and b^\dagger . This operation corresponds to take the transpose of σ_μ , so $(\sigma_\mu)^T = \sigma_\mu$, for $\mu = 0, 1, 3$ and $(\sigma_2)^T = -\sigma_2$. As the set of operators T_μ acting on the outer edges of a state is just a linear combination of the states defined in (4.8), the states of the form $T_\mu(i, j)^\dagger |i^j\rangle$ are a basis for the four dimensional space of degenerate ground states of the bulk Hamiltonian (4.1).

With the introduction of these operators, we can write the identity (see B.0.5) (sum convention, with $\mu = 0..3$)

$$T_2^\dagger(i, i+1) T_2^\dagger(j, j+1) = -\frac{1}{2} T_\mu^\dagger(i+1, j) T_\mu^\dagger(i, j+1), \quad (4.10)$$

Using this identity in eq. (4.4), we find that the VBS state has the decomposition $(T_\nu^\dagger(m, K) |A\rangle = |A_\nu\rangle)$

$$|\text{VBS}\rangle = -\frac{1}{2}T_\mu^\dagger(m-1, K+1)|A_\mu, B\rangle.$$

Now we can write the density matrix for the VBS state $\rho = \frac{|\text{VBS}\rangle\langle\text{VBS}|}{\langle\text{VBS}|\text{VBS}\rangle}$

$$\rho = T_\mu^\dagger(m-1, K+1)|A_\mu, B\rangle\langle A_\mu, B|T_\mu(m-1, K+1). \quad (4.11)$$

We can define the state $|s\rangle = T_\mu^\dagger(m-1, K+1)|A_\mu, B\rangle$. In terms of this state, the density matrix (4.11) takes the form $\rho = |s\rangle\langle s|$, and the eigenvector is clearly $|s\rangle$ with eigenvalue 1. This is natural because so far we have just taken another basis to represent ρ , which was already a projector onto the VBS ground state.

It's important to note that if we trace the B block in expression (4.11), we get the partial density matrix respect to the A subsystem $\rho_A = |A_\mu\rangle\langle A_\mu|$. This expression was already found in [64]. The von Neumann or entanglement entropy is given by $S_A = -\text{Tr}(\rho_A \ln \rho_A) = -\frac{1}{4}(1+3(-3)^{-L}) \ln \frac{1+3(-3)^{-L}}{4} - \frac{3}{4}(1 - (-3)^{-L}) \ln \frac{1-(-3)^{-L}}{4}$ and scales with the length of the boundary as expected. The entanglement spectrum for $\rho_A = |A_\mu\rangle\langle A_\mu|$ is $\xi_1 = \ln\left(\frac{4}{1+3(-3)^{-L}}\right)$ no degeneracy and $\xi_2 = \ln\left(\frac{4}{1-(-3)^{-L}}\right)$ with triple degeneracy ($L \neq 0$) [64].

4.3 Density matrix for the mixed system of 2 disjoint blocks

4.3.1 Open boundary conditions

So far we have studied the density matrix for the pure VBS system. In this section we want to extend our results to the case of mixed systems. We will study the mixed system composed of two blocks A and B of length L_A and L_B , obtained by tracing away the lattice sites which do not belong to these blocks in the VBS ground state. This situation is described in Fig 4.3.

To define the blocks, we partition the $N+2$ sites of the chain into five different subsets, A, B, C, D and E , of different length.

Given I, J, K, M, N five positive integers ordered as $0 < I < J < K < M < N+1$, we define:

- Block C = {sites i , $0 \leq i \leq I-1$ }, with length $L_C = I$,
- Block A = {sites i , $I \leq i \leq J-1$ }, with length $L_A = J - I$,
- Block D = {sites i , $J \leq i \leq K-1$ }, with length $L = K - J$,

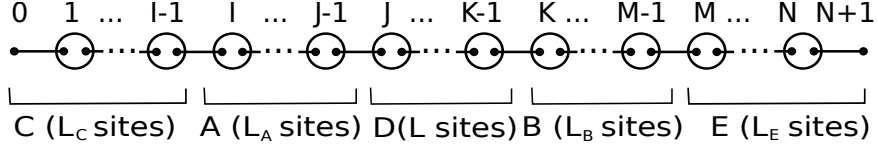


Figure 4.3: We made a partition of the VBS state in 5 sectors, labeled A, B, C, D and E as shown in the figure. To obtain the density matrix for the blocks A and B , we trace away the spin variables at the sites inside C, D and E .

- Block $B = \{\text{sites } i, K \leq i \leq M - 1\}$ with length $L_B = M - K$ and
- Block $E = \{\text{sites } i, M \leq i \leq N + 1\}$ with length $L_E = N + 2 - M$.

We are interested in the density matrix for the mixed system of two different blocks. In order to compute the density matrix we have to trace away the sites outside the corresponding blocks. To do that we use the following results for the bulk states

$$\langle D_\mu | D_\nu \rangle = \delta_{\mu\nu} \lambda_\mu(L) \quad \text{with } \lambda_\mu = \frac{1}{4}(1 + z(L)s_\mu), \quad (4.12)$$

$$z(L) = \left(-\frac{1}{3}\right)^L; \quad s_\mu = (-1, -1, 3, -1),$$

$$\langle C, E | T_\mu(I - 1, M) T_\nu^\dagger(I - 1, M) | C, E \rangle = \delta_{\mu\nu}, \quad (4.13)$$

note that the states $T_\nu^\dagger(I - 1, M) | C, E \rangle$ belong to the environment, so they contain the boundary $1/2$ spins, and consequently are orthogonal.

Density matrix of the blocks C & E

The simplest case occur when we trace away the A, D and B blocks. The density matrix for the C and E blocks is

$$\begin{aligned} \rho_{CE} &= \text{Tr}_{ABD} \left\{ \frac{|\text{VBS}\rangle\langle\text{VBS}|}{\langle\text{VBS}|\text{VBS}\rangle} \right\}, \\ &= \lambda_\mu T_\mu^\dagger(I - 1, M) | C, E \rangle \langle C, E | T_\mu(I - 1, M), \\ &\equiv \lambda_\mu |[C, E]_\mu\rangle \langle [C, E]_\mu|. \end{aligned} \quad (4.14)$$

using identities (4.9) and (B.12) the partial transposed density matrix respect to the E system is

$$\rho_{CE}^{TE} = (\lambda_\mu - (-1)^\mu \frac{\lambda_2 - \lambda_1}{2}) |[C, E]_\mu\rangle \langle [C, E]_\mu|. \quad (4.15)$$

This is a sum of projector operators (a consequence of (4.12)). The negativity is non vanishing just for $L_A + L_B + L = 0$, i.e. when C and E together are in a pure state. In this case we have $\mathcal{N} = 1/2$.

Density Matrix of the blocks A & B, case $L \geq 1$.

In this case we compute the density matrix for blocks A and B . We obtain this density matrix by tracing away the states on the C, D and E subspaces.

$$\rho_{AB} = \text{Tr}_{CDE} \left\{ \frac{|\text{VBS}\rangle \langle \text{VBS}|}{\langle \text{VBS} | \text{VBS} \rangle} \right\}. \quad (4.16)$$

Using the identity (B.15) (See B.0.5), we can write the VBS state as a linear combination of products between the different four fold degenerate ground states of the bulk Hamiltonian (4.1) in the form:

$$\begin{aligned} |\text{VBS}\rangle &= M_{\mu\nu\rho\sigma} T_\sigma^\dagger(I-1, M) |C, A_\mu, D_\nu, B_\rho, E\rangle, \quad \text{with} \\ M_{\mu\nu\rho\sigma} &= (-1)^\nu (g^{\mu\nu} \delta_{\rho\sigma} + g^{\nu\rho} \delta_{\mu\sigma} - g^{\nu\sigma} \delta_{\mu\rho} + g^{\nu\alpha} \epsilon_{\mu\alpha\rho\sigma}). \end{aligned} \quad (4.17)$$

here we have introduced three types of tensors, the Kronecker delta symbol in 4 dimensions $\delta_{\alpha\beta}$, the diagonal tensor $g^{\mu\nu} = (-1, +1, +1, +1)$ and the Levi Civita symbol in four dimensions $\epsilon_{\mu\nu\rho\sigma}$, which is a totally antisymmetric tensor, with $\epsilon_{\mu\nu\rho\sigma} = \text{sign of permutation } (\mu, \nu, \rho, \sigma)$ if (μ, ν, ρ, σ) is a permutation of $(0, 1, 2, 3)$, and zero otherwise.

Using this representation of the VBS state, it's easy to write down the density matrix (4.16) using the orthogonality of the bulk ground states (4.12). We find that the density matrix ρ_{AB} is

$$\rho_{AB} = M_{\mu\nu\rho\sigma} M_{\alpha\nu\beta\sigma} |A_\mu, B_\rho\rangle \langle A_\alpha, B_\beta|, \quad (4.18)$$

with the tensor $M_{\mu\nu\rho\sigma} M_{\alpha\nu\beta\sigma}$ given explicitly by (summation over dummy variables ν and σ is assumed)

$$M_{\mu\nu\rho\sigma} M_{\alpha\nu\beta\sigma} = \delta_{\mu\alpha} \delta_{\rho\beta} - z(L) [\delta_{\mu\rho} \delta_{\alpha\beta} - \delta_{\rho\alpha} \delta_{\mu\beta}] S_{\mu\alpha} + z(L) \epsilon_{\alpha\beta\mu\rho} V_{\rho\beta\mu\alpha}, \quad (4.19)$$

with $S_{\mu\alpha} = (s_\mu + s_\alpha)/2$ and $V_{\rho\beta\mu\alpha} = \frac{S_{\rho\beta} - S_{\mu\alpha}}{2}$. We can identify two parts in (4.18), the first term which does not depend on z and the rest which is linear in z . The first term is a projector on the ground states of the bulk of A and B , namely

$$\rho_0(A, B) = \delta_{\mu\alpha}\delta_{\rho\beta}|A_\mu, B_\rho\rangle\langle A_\alpha, B_\beta|, \quad (4.20)$$

while all the other terms, proportional to $z(L)$, have vanishing trace. From this expression, we can compute the entanglement spectrum associated with $\rho(A, B)$, in the limit $L, L_A, L_B \gg 1$. This density matrix has rank 16, and is exponentially close to a maximally mixed state. The eigenvalues are (using $x_A = (-3)^{-L_A}$, $x_B = (-3)^{-L_B}$ and $z = (-3)^{-L}$)

$$\begin{aligned} \{\lambda_i\}_{i=1}^{11} &= \frac{1 - x_A - x_B - z}{16}, & \{\lambda_i\}_{i=12}^{14} &= \frac{1 + 3x_A + 3x_B + 3z}{16}, \\ \lambda_{15,16} &= \frac{1 + x_A + x_B + z}{16} \pm \frac{1}{8}\sqrt{z^2 + (x_A + x_B)(x_A + x_B - z)}. \end{aligned} \quad (4.21)$$

The entanglement spectrum of $\rho(A, B)$ is $\xi_i = -\ln \lambda_i$. Explicitly we have

$$\begin{aligned} \{\xi_i\}_{i=1}^{11} &= 4 \ln 2 + x_A + x_B + z, & \{\xi_i\}_{i=12}^{14} &= 4 \ln 2 - 3x_A - 3x_B - 3z, \\ \xi_{15,16} &= 4 \ln 2 - x_A - x_B - z \mp \sqrt{z^2 + (x_A + x_B)(x_A + x_B - z)}. \end{aligned} \quad (4.22)$$

The purity, defined as $\gamma = \text{Tr}(\rho^2)$ corresponds in this limit to the purity of a maximally mixed state, up to terms of second order in x_A, x_B and z . We have $\gamma = \frac{1}{16} + \mathcal{O}(2)$. The general results for arbitrary L, L_A, L_B are given in appendix B.0.6.

If we call $\rho_1(A, B)$ to all the linear terms in $z(L)$ on (4.18), we can write for brevity

$$\rho_{AB} = \rho_0(A, B) + z(L)\rho_1(A, B). \quad (4.23)$$

From the expressions (4.18) and (4.19) we can obtain the partial transposed density matrix with respect to the A subsystem.

$$\rho_{AB}^{T_A} = \left[\delta_{\mu\alpha}\delta_{\rho\beta} - z(L) ([\delta_{\alpha\rho}\delta_{\mu\beta} - \delta_{\rho\mu}\delta_{\alpha\beta}]S_{\mu\alpha} - \epsilon_{\mu\beta\alpha\rho}V_{\rho\beta\mu\alpha}) \right] |A_\mu, B_\rho\rangle\langle A_\alpha, B_\beta|. \quad (4.24)$$

from where, comparing with equations (4.18) and (4.19), we learn that

$$\rho_{AB}^{T_A}(z) = \rho_{AB}(-z). \quad (4.25)$$

Given this result, and the fact that $\rho_{AB}(-z)$ is also a density matrix (proved in the following theorem), the negativity vanishes for $L > 0$.

Theorem 1. *The negativity of the transposed density matrix $\rho_{AB}^{T_A}(z(L))$ is strictly zero for two blocks separated by $L > 0$.*

Proof. Consider the family of density matrices

$$\rho_{AB}(z) = \rho_0(A, B) + z(L)\rho_1(A, B), \quad (4.26)$$

defined in eq. (4.23). Recalling that the space of density matrices is convex [2], meaning that for two density matrices ρ_1, ρ_2 , the operator $\tilde{\rho} = \lambda\rho_1 + (1 - \lambda)\rho_2$ is also a density matrix for $\lambda \in [0, 1]$, we proceed as follows. We take the first two members of the family $\rho_{AB}(z)$, namely $\rho_{AB}(z_1)$ and $\rho_{AB}(z_2)$ for fixed $z_1 = 1, z_2 = -1/3$ (We can take any pair different z_1 and z_2 , but the greater z is achieved for $z_1 = 1, z_2 = -1/3$ (or vice versa)). By the convexity of the space of density matrices, $\bar{\rho} = \lambda\rho_{AB}(z_1) + (1 - \lambda)\rho_{AB}(z_2)$ is also a density matrix. Using (4.23), we write explicitly $\bar{\rho} = \rho_0(A, B) + (\lambda z_1 + (1 - \lambda)z_2)\rho_1(A, B)$. We can choose $\lambda = \frac{1}{4}(1 - 3(-\frac{1}{3})^L) \in [0, 1]$ for $L \geq 1$. Using this λ , we find

$$\bar{\rho} = \rho_0(A, B) - z(L)\rho_1(A, B). \quad (4.27)$$

Then $\bar{\rho} = \rho_{AB}(-z)$ is also a density matrix, for $L \geq 1$. Now, by (4.25), $\rho_{AB}^{T_A}(z)$ is also density matrix for $z < 1$ ($L > 0$). Then the negativity (sum of negative eigenvalues) of $\rho_{AB}^{T_A}(z)$ vanishes. \square

Special case $L = 0$.

As in the previous section, we analyze separately the case $L = 0$. In this case the block D is not present and we cannot take a trace over it.

We can study this scenario using the following identity (see B.0.5)

$$\begin{aligned} T_2^\dagger(i, i+1)T_2^\dagger(j, j+1)T_2^\dagger(k, k+1) = \\ (-1)^\nu m_{\mu\nu\lambda} T_\mu^\dagger(i+1, j)T_\nu^\dagger(j+1, k)T_\lambda^\dagger(i, k+1) \end{aligned} \quad (4.28)$$

$$\text{where } m_{\mu\nu\lambda} = \frac{-1}{4}(g_{\mu\nu}\delta_{2\lambda} + g^{2\nu}\delta_{\mu\lambda} - g_{\lambda\nu}\delta_{2\mu} + g^{\nu\alpha}\epsilon_{\mu\alpha 2\lambda}) \quad (4.29)$$

The VBS state splits into

$$|\text{VBS}\rangle = T_2^\dagger(i, i+1)T_2^\dagger(j, j+1)T_2^\dagger(k, k+1)|C, A, B, E\rangle. \quad (4.30)$$

with $i = L_C - 1$, $j = L_A + L_C - 1$ and $k = L_C + L_A + L_B - 1$ and L_C being the number of sites in C , L_A the number of sites in A , L_B the number of sites in B . Here the states $|C\rangle, |A\rangle, |B\rangle, |E\rangle$ are defined as in the previous section taking $m - 1 = K$ ($L = 0$).

Using the identity (4.28), the equation (4.30) becomes

$$|\text{VBS}\rangle = (g_{\mu\nu}\delta_{2\lambda} + g^{2\nu}\delta_{\mu\lambda} - g_{\lambda\nu}\delta_{2\mu} + g^{\nu\alpha}\epsilon_{\mu\alpha 2\lambda})T_\lambda^\dagger(i, k+1)|C, A_\mu, B_\nu, D\rangle$$

Now, given that (see appendix B.0.4)

$$\langle C, D|T_\lambda(i, k+1)T_{\lambda'}^\dagger(i, k+1)|C, E\rangle = \delta_{\lambda\lambda'}, \quad (4.31)$$

we can write the normalized density matrix $\text{Tr}_{C,E}\rho \equiv \rho_{AB}$ as

$$\rho_{AB} = \left(\delta_{\mu\alpha}\delta_{\rho\beta} - [\delta_{\mu\rho}\delta_{\alpha\beta} - \delta_{\rho\alpha}\delta_{\mu\beta}]S_{\mu\alpha} + \epsilon_{\alpha\beta\mu\rho} \left(\frac{S_{\rho\beta} - S_{\mu\alpha}}{2} \right) \right) |A_\mu, B_\nu\rangle\langle A_\alpha, B_\beta|$$

This expression is analogous to the (4.18), with $z(L) = 1$ ($L = 0$). From this result, the transposed density matrix respect to A is now given by

$$\rho_{AB}^{T_a} = \left(\delta_{\mu\alpha}\delta_{\rho\beta} + [\delta_{\mu\rho}\delta_{\alpha\beta} - \delta_{\rho\alpha}\delta_{\mu\beta}]S_{\mu\alpha} - \epsilon_{\alpha\beta\mu\rho}V_{\rho\beta\mu\alpha} \right) |A_\mu, B_\nu\rangle\langle A_\alpha, B_\beta|, \quad (4.32)$$

(with $V_{\rho\beta\mu\alpha} = \frac{S_{\rho\beta} - S_{\mu\alpha}}{2}$). Using this expression it is possible to compute the eigenvalues of the transposed density matrix and the negativity. For the results at finite size of the block A (L_A) and block B (L_B) see appendix (section B.0.6). The negativity in the asymptotic limit $L_A \rightarrow \infty, L_B \rightarrow \infty$ is given by

$$\mathcal{N}_{L_A, L_B \rightarrow \infty} = \frac{1}{2} - \frac{3}{4} \left(\left(-\frac{1}{3} \right)^{2L_A} + \left(-\frac{1}{3} \right)^{2L_B} \right). \quad (4.33)$$

4.3.2 Periodic Boundary Conditions

Using the same technology developed previously, we can also analyze the case of periodic boundary conditions. This state is unique, given that the coordination number for each spin is two [66].

In this state, we make a partition in four sectors, labeled by their length as L_A, L_B, L_C, L_D , with $L_A + L_B + L_C + L_D = L$ the total length of the system. We trace away states from sectors that do not belong to $A \cup B$ (See Fig. 4.4).

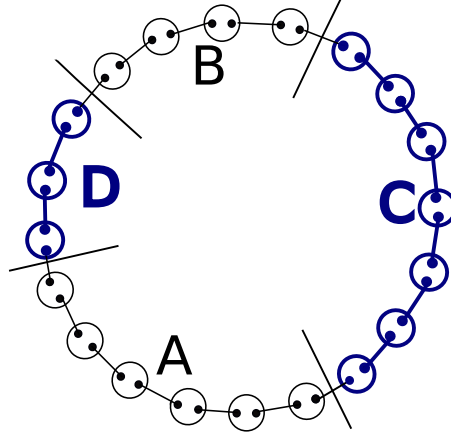


Figure 4.4: We trace blocks C and D, leaving a reduced density matrix in terms of the states of the A and B blocks.

We split the $|\text{VBS}\rangle$ as in the previous section, but now the difference is that the norm of both states that we trace out, namely the block C and D, is nontrivial, each one contributing with a factor $\langle C_\alpha | C'_\beta \rangle = \lambda_\alpha(L_C) \delta_{\alpha\beta}$ and $\langle D_\alpha | D_\beta \rangle = \lambda_\alpha(L_D) \delta_{\alpha\beta}$.

The VBS state can be rewritten as $|\text{VBS}\rangle = M_{\mu\nu\rho\sigma} |C_\sigma, A_\mu, D_\nu, B_\rho\rangle$, with $M_{\mu\nu\rho\sigma} = (-1)^\nu (g^{\mu\nu} \delta_{\rho\sigma} + g^{\nu\rho} \delta_{\mu\sigma} - g^{\nu\sigma} \delta_{\mu\rho} + g^{\nu\alpha} \epsilon_{\mu\alpha\rho\sigma})$. The reduced density matrix in this case is

$$\rho_{AB} = M_{\mu\nu\rho\sigma} M_{\alpha\nu\beta\sigma} \lambda_\nu(L_D) \lambda_\sigma(L_C) |A_\mu, B_\rho\rangle \langle A_\alpha, B_\beta|. \quad (4.34)$$

The tensor $W_{\mu\rho\alpha\beta} = M_{\mu\nu\rho\sigma} M_{\alpha\nu\beta\sigma} \lambda_\nu(L_D) \lambda_\sigma(L_C)$ is given explicitly by

$$W_{\mu\rho\alpha\beta} = \delta_{\mu\alpha} \delta_{\rho\beta} \Lambda_{\alpha\beta}(z_d, z_c) - \delta_{\alpha\rho} \delta_{\mu\beta} \Gamma_{\alpha\mu}(z_d, z_c) + \epsilon_{\alpha\beta\mu\rho} R_{\rho\mu\beta\alpha}(z_d, z_c) - \delta_{\mu\rho} \delta_{\alpha\beta} \Gamma_{\mu\alpha}(-z_d, -z_c), \quad (4.35)$$

where $z_c = z(L_C)$ and $z_d = z(L_D)$. The tensors $\Lambda_{\alpha\beta}(x, y)$, $\Gamma_{\alpha\alpha'}(x, y)$ and $R_{\alpha\beta\alpha'\beta'}(x, y)$ are respectively given by

$$\Lambda_{\alpha\beta}(x, y) = \frac{1 + (s_\alpha s_\beta + s_\alpha + s_\beta)xy}{1 + 3z(L)}, \quad \Gamma_{\alpha\alpha'}(x, y) = \frac{s_\alpha + s_{\alpha'}}{1 + 3z(L)} \left(xy - \frac{x + y}{2} \right)$$

and $R_{\alpha\beta\alpha'\beta'}(x, y) = \frac{s_\alpha - s_\beta + s_{\alpha'} - s_{\beta'}}{4 + 12z(L)}(x - y).$ (4.36)

As with the case studied in section 4.3, the partial transposed operator ρ_{AB}^{TA} is exactly $\rho_{AB}(-z_d, -z_c)$. With this result, a vanishing negativity of the system is analogous to prove that $\rho_{AB}(-z_d, -z_c)$ is a density matrix. We have

Theorem 2. *The negativity of the transposed density matrix for the system with periodic boundary conditions $\rho_{AB}^{TA}(z_d, z_c)$ is strictly zero for L_C and $L_D \neq 0$.*

Proof. Again we proceed as before. The density matrix ρ_{AB} defines a family of operators $\rho_{AB}(z_d, z_c) = \rho_0 + z_d\rho_1 + z_c\rho_2 + z_d z_c\rho_3$, with

$$\begin{aligned} \rho_0 &= \frac{\delta_{\mu\alpha}\delta_{\rho\beta}}{1+3z(L)} |A_\mu, B_\rho\rangle\langle A_\alpha, B_\beta|, \\ \rho_1 &= \left[\frac{s_\alpha + s_\mu}{2+6z(L)} (\delta_{\alpha\rho}\delta_{\mu\beta} - \delta_{\mu\rho}\delta_{\alpha\beta}) + \frac{(s_\alpha - s_\beta + s_\mu - s_\rho)}{4+12z(L)} \epsilon_{\alpha\beta\mu\rho} \right] |A_\mu, B_\rho\rangle\langle A_\alpha, B_\beta|, \\ \rho_2 &= \left[\frac{s_\alpha + s_\mu}{2+6z(L)} (\delta_{\alpha\rho}\delta_{\mu\beta} - \delta_{\mu\rho}\delta_{\alpha\beta}) - \frac{(s_\alpha - s_\beta + s_\mu - s_\rho)}{4+12z(L)} \epsilon_{\alpha\beta\mu\rho} \right] |A_\mu, B_\rho\rangle\langle A_\alpha, B_\beta|, \\ \rho_3 &= \left[\frac{s_\alpha s_\beta + s_\alpha + s_\beta}{1+3z(L)} \delta_{\mu\alpha}\delta_{\rho\beta} - \frac{(s_\alpha + s_\mu)}{1+3z(L)} (\delta_{\alpha\rho}\delta_{\mu\beta} + \delta_{\mu\rho}\delta_{\alpha\beta}) \right] |A_\mu, B_\rho\rangle\langle A_\alpha, B_\beta|. \end{aligned}$$

We choose four different members of this family, $\rho_a = \rho_{AB}(1, 1)$, $\rho_b = \rho_{AB}(-\frac{1}{3}, 1)$, $\rho_c = \rho_{AB}(1, -\frac{1}{3})$ and $\rho_d = \rho_{AB}(-\frac{1}{3}, -\frac{1}{3})$. Recalling that the space of density matrices is convex [2], we have that $\tilde{\rho} = \alpha\rho_a + \beta\rho_b + \gamma\rho_c + (1 - \alpha - \beta - \gamma)\rho_d$ is also a density matrix for $0 \leq \alpha, \beta, \gamma \leq 1$. Choosing $\alpha = \frac{5}{32} + \frac{9}{32}(z_c z_d - z_c - z_d)$, $\beta = \frac{3}{32} + \frac{1}{32}(9z_d - 15z_c + 9z_c z_d)$ and $\gamma = \frac{3}{32} + \frac{1}{32}(9z_c - 15z_d - 9z_c z_d)$, we have

$$\tilde{\rho} = \rho_0 - z_d\rho_1 - z_c\rho_2 + z_d z_c\rho_3 = \rho_{AB}(-z_c, -z_d), \quad (4.37)$$

is also a density matrix for $0 \leq \alpha, \beta, \gamma \leq 1$. This condition breaks down when z_c or z_d are equal to 1. □

4.4 Mutual Entropy

Having the explicit expression for the density matrix of two blocks and the proof of vanishing negativity for any separation of the blocks greater than zero, a natural question to ask is, Does the mutual entropy vanish in this case, too?. We found surprisingly that the answer is negative, i.e. there is non zero mutual entropy even when the separation L is greater than zero. The mutual entropy decays exponentially, as expected from the spin-spin correlations.

From (4.18), we can in principle compute the eigenvalues and eigenvectors of ρ_{AB} , where ρ_{AB} can be written as a 16×16 matrix. This dimension is fixed by the dimension of the ground state space for each block. Being V the Hilbert space spanned by the vector $|A_\mu, B_\nu\rangle$ we have

$$\text{Dim}(V) = \text{Dim}(\text{Ker}A) \times \text{Dim}(\text{Ker}B) = 16 \quad (4.38)$$

where $\text{Ker}A$ is the Kernel of the bulk Hamiltonian defined on the Hilbert space of the block A , and similarly for $\text{Ker}B$. As we have shown, this spaces are spanned by the states $|A_\mu\rangle, |B_\nu\rangle$ $\mu, \nu = 0..3$, states which are orthogonal but not normalized in our convention. In the thermodynamical limit, when the length of each block goes to infinity $L_A \rightarrow \infty, L_B \rightarrow \infty$, the states $|A_\mu\rangle$ become orthonormal

$$\langle A_\nu | A_\mu \rangle = \delta_{\mu\nu}^{\nu}, \quad \langle B_\mu | B_\nu \rangle = \delta_{\mu\nu}^{\nu}. \quad (4.39)$$

In this limit, the matrix elements of ρ_{AB} are

$$\begin{aligned} & \langle A_\mu, B_\nu | \rho_{AB} | A_\alpha, B_\beta \rangle \\ &= \delta_{\mu\alpha} \delta_{\nu\beta} + z(L) [\delta_{\mu\nu} \delta_{\alpha\beta} - \delta_{\nu\alpha} \delta_{\mu\beta}] S_{\mu\alpha} + z(L) \epsilon_{\mu\nu\alpha\beta} (S_{\nu\beta} - S_{\mu\alpha}), \end{aligned} \quad (4.40)$$

The eigenvalues of this matrix are

$$\lambda_I(z) = \frac{1}{16}(1 + 3z), \quad \text{4-fold degeneracy} \quad (4.41)$$

$$\lambda_{II}(z) = \frac{1}{16}(1 - z), \quad \text{12-fold degeneracy.} \quad (4.42)$$

Using the spectral theorem, we find that the entropy of the system described by ρ_{AB} , i.e., the entropy of two blocks of infinite length separated by L sites is

$$\begin{aligned}
S[A, B] &= -\text{Tr}(\rho_{AB} \ln(\rho_{AB})) \\
&= 2 \ln 2 - \frac{3}{4}(1-z) \ln\left(\frac{1-z}{4}\right) - \frac{1}{4}(1+3z) \ln\left(\frac{1+3z}{4}\right)
\end{aligned}
\tag{4.43}$$

The mutual entropy/information is defined as usual

$$I(A, B) = S[A] + S[B] - S[A, B], \tag{4.44}$$

the entropy of a block of length L in the AKLT model was calculated in [64], and also can be obtained trivially from our results of section 4.2. In the limit of infinite length, we have

$$S[A] = S[B] = 2 \ln 2. \tag{4.45}$$

The mutual information is finally

$$I(A, B) = \frac{3}{4}(1-z) \ln(1-z) + \frac{1}{4}(1+3z) \ln(1+3z), \tag{4.46}$$

where z was defined before as $z = z(L) = \left(-\frac{1}{3}\right)^L$.

4.5 Conclusions

In this chapter we have derived the entanglement spectrum of the density matrix of two blocks belonging to the 1D VBS state, corresponding to the ground state of the spin 1 AKLT Hamiltonian. The eigenvalues of the density matrix decay exponentially with the length of the blocks and their separation to the eigenvalues of a completely mixed state. This decay was expected from the behavior of the correlation functions $\langle S_0^i S_L^j \rangle = \frac{4}{3} \left(-\frac{1}{3}\right)^L \delta_{ij}$. The novel result is that in the thermodynamic limit, the density matrix $\rho(A, B)$ eq. (4.18) is maximally mixed, with all the eigenvalues $\lambda_i = \frac{1}{16}$ for $i = 1..16$. The density matrix (4.18) in this limit is a projector on the different ground states obtained as a tensor products of the four ground states of A and B blocks $|A_\mu\rangle|B_\nu\rangle$.

The density matrix for this system (4.18) is clearly non separable. This can be rigorously proved, using that an state is separable iff the quantity $\text{Tr}(O\rho_{AB}) \geq 0$ for any Hermitian operator O satisfying $\text{Tr}(OP \otimes Q) \geq 0$, where P and Q are projections acting on the Hilbert spaces associated to subsystems A (\mathcal{H}_A) and B (\mathcal{H}_B). If we choose for example $O = r(|A_0, B_0\rangle\langle A_1, B_1| + |A_1, B_1\rangle\langle A_0, B_0|)$, it is easy to see that $\text{Tr}(OP \otimes Q) = 0$, while $\text{Tr}(O\rho) \propto r$,

then choosing r properly we can make $\text{Tr}(O\rho) \leq 0$, proving that the state is not separable.

The fact that the operator $\rho(A, B)$ describe a state which is non separable, together with the result that the negativity vanishes for any separation of the blocks A and B tell us that this state is a bound entangled state [67]. In [67] the authors show that this kind of states can not be distilled by local action to create an useful entanglement for quantum communication tasks such as teleportation. However, bound entanglement is still of interest as it can be used to generate a secret quantum key [68], or to enhance the fidelity of conclusive teleportation using another state [69]. In the context of many-body systems, it has so far been found in thermal states [70], XY models [71] and in gapless systems [72].

We can understand the result of constant negativity for any separation of the blocks, qualitatively, using the proved area law for the entanglement entropy in 1D spin 1 VBS systems [64], namely that the entropy is proportional to the area of the system [4, 73]. In this one dimensional system with constant bond dimension, the boundary (area) changes just when we go from adjacent to separated blocks. As the area is insensitive to the separation of the blocks, we expect the same entanglement between the blocks when they are infinitely far apart as when they are separated by just one site (at least in the thermodynamic limit of infinite blocks). Assuming that there are no entangled pairs between the boundary of the blocks A and B , then we conclude that the available entanglement should be zero. In this sense our result can be understood, but still is surprising the fact that the system still possess some bound entanglement, not available for quantum communication.

The mutual entropy of this system, computed in (4.46) tells us that the work needed to erase all correlations [74] between two different blocks in the AKLT ground state decay exponentially to zero in the limit of infinite length. In this sense, all correlations between two blocks located infinitely far apart vanish (for non entangled boundary spins) which is expected from the thermodynamic limit of a gapped system.

We also studied other different boundary conditions which, altogether with the results found in [75], agree in the limit of infinite separation, except in the case when we start with an entangled pair at the spin 1 boundary of a free end AKLT ground state. In that case as shown in [75], the entanglement reduces to the entanglement of the Bell pair created from the spin 1/2 virtual particles which remain free after the antisymmetrization between different neighbor sites.

Our result is in agreement with the fact that 1D AKLT chains alone are not sufficient for universal quantum computation. This is due to the vanishing

negativity between two different non adjacent blocks. Still further coupling of many such chains can in principle implement quantum computation as shown in [76].

Chapter 5

Generalization of AKLT: AKLT_q

We study entanglement in a one-dimensional q -deformed valence-bond-solid (VBS) state with a spin- S at each site. This state, which we denote as $\text{VBS}_q(S)$, is invariant under the action of the generators of the $\text{SU}_q(2)$ quantum algebra [77, 78]. The q -generalization of the underlying algebra introduces anisotropy into the model by a continuous deformation of the usual $\text{SU}(2)$ symmetry. The first part of this chapter is devoted to the analysis of the spin-1 $\text{VBS}_q(S)$ state [79], we analytically calculated the dependence of the entanglement spectrum and entropy on the deformation parameter q . This investigation and the current one are motivated by the problem of determining how entanglement in a VBS state is changed by anisotropy. Such anisotropic effects on entanglement in VBS states is receiving attention recently [79–81].

The isotropic VBS state is the ground state of the one-dimensional Affleck-Kennedy-Lieb-Tasaki (AKLT) model [11, 61]. This model has nearest-neighbor interactions between integer spin- S 's. It is described by a Hamiltonian of the form $\mathcal{H} = \sum_i h_{i,i+1}$. The local Hamiltonian $h_{i,i+1}$ is a projector onto the subspace spanned by the $(S+1)$, $(S+2)$, \dots , and $2S$ -multiplets formed by spins at sites i and $i+1$ [11, 61, 66]. Exact results for the block entanglement entropy in the $S=1$ AKLT model were obtained in [64, 82]. Block entanglement was studied later in its higher integer spin- S [26, 83] and $\text{SU}(N)$ [84–86] generalizations.

The anisotropic q -deformed generalization of the spin-1 AKLT chain was first considered in [59, 87, 88]. The matrix product state (MPS) representation [56, 58, 89] of the ground state of the model was constructed in [59]. This ground state is separated from excited states by a gap [88]. Hence, the spin-spin correlation functions decay exponentially [59, 88]. The exact entanglement spectrum of blocks of arbitrary length in the spin-1 $\text{VBS}_q(S)$ state was calculated in [90]. The higher integer spin generalization of the q -deformed AKLT model was first proposed in [91, 92], where the spin-spin correlation

functions were calculated and where it was shown they exponential decay. To our knowledge, the entanglement spectrum and entropies of $\text{VBS}_q(S)$ states for arbitrary integer S have not yet been evaluated.

In this chapter, we calculate the entanglement spectrum and entropies of q -deformed VBS states with arbitrary integer S . Our analytical approach involves transfer matrix methods and the use of q -deformed Clebsch-Gordan coefficients and $6j$ symbols. We begin by constructing the $\text{VBS}_q(S)$ state by requiring it to be a ground state of a q -deformed spin- S AKLT Hamiltonian. We shall denote this ground state by the state vector $|\text{VBS}_q(S)\rangle$. This state is then partitioned into a block of ℓ sequential spins and the environment E . The density matrix of the whole ground state is therefore $\rho = |\text{VBS}_q(S)\rangle\langle\text{VBS}_q(S)|/\langle\text{VBS}_q(S)|\text{VBS}_q(S)\rangle$. We then compute the reduced density matrix ρ_ℓ of the block by taking the partial trace of ρ over the environment, $\rho_\ell = \text{tr}_E \rho$.

In the double scaling limit of an infinitely long block in an infinitely long chain, we are able to exactly diagonalize the reduced density matrix (5.3.1). We then use the eigenvalues of this matrix to construct the entanglement spectrum of the block (5.3.2). This entanglement spectrum (introduced in [14]) enables us to construct an effective Hamiltonian that completely describes the reduced density matrix. The eigenvalues of the reduced density matrix are further used to calculate the Rényi and von Neumann entanglement entropies

$$S_R(\alpha) \equiv \frac{\ln \text{tr} \rho_\ell^\alpha}{1 - \alpha}, \quad \alpha > 0, \quad (5.1)$$

$$S_{\text{vN}} \equiv -\text{tr}(\rho_\ell \ln \rho_\ell) = \lim_{\alpha \rightarrow 1} S_R(\alpha). \quad (5.2)$$

We thus provide exact measures of entanglement [36, 38, 39, 93] in the $|\text{VBS}_q(S)\rangle$ ground state as functions of the deformation parameter q and spin S .

We further consider the case of blocks of finite length. We obtain the exact eigenvalues of the reduced density matrix in the isotropic case $q = 1$. With this result, we calculate the leading order finite-size corrections to the entanglement spectrum and entropies (5.4.1). For a general q -deformation, we estimate the eigenvalues of the reduced density matrix in the limit of long but finite blocks by perturbation theory (5.4.2). Furthermore, we numerically investigate the properties of the reduced density matrix of the spin-2 $\text{VBS}_q(S)$ state. This result allows us to make general statements about the structure and degeneracy of the entanglement spectrum for blocks of any length.

5.1 Reduced density matrix of MPS.

We start with a pure matrix product state $|\text{MPS}\rangle$. The density matrix of the whole state is

$$\rho = |\text{MPS}\rangle\langle\text{MPS}|/\langle\text{MPS}|\text{MPS}\rangle. \quad (5.3)$$

We then partition the system into a block of ℓ sequential spins and its environment E . The reduced density matrix ρ_ℓ is the partial trace of ρ over the environment, $\rho_\ell = \text{tr}_E \rho$.

The MPS representation of a periodic chain of L identical spins is

$$|\text{MPS}\rangle = \text{tr}[\mathbf{g}_1 \cdot \mathbf{g}_2 \cdot \dots \cdot \mathbf{g}_L]. \quad (5.4)$$

The \mathbf{g}_j are $D \times D$ matrices ($D = 2$ for the examples considered below). The trace here is taken over the auxiliary matrix space (not E). The elements of \mathbf{g}_j are

$$(\mathbf{g}_j)_{\alpha\beta} = \sum_m A_{\alpha\beta}(m) |m\rangle_j. \quad (5.5)$$

The set $\{|m\rangle_j\}$ is a complete orthonormal basis for the Hilbert space of the spin at site j and the coefficients $A_{\alpha\beta}(m)$ are independent of the site index. Due to translational invariance, we drop the site label j whenever possible. We denote the matrix dual to \mathbf{g} as $\bar{\mathbf{g}}$ with elements $(\bar{\mathbf{g}})_{\alpha\beta} = \sum_m A_{\alpha\beta}^*(m) \langle m|$. Here, the coefficients are replaced by their complex conjugates and the kets are replaced by the corresponding bras. In Eq.(5.4) the matrix multiplication (\cdot) involves tensor products of vector matrix elements, i.e.,

$$(\mathbf{g}_j \cdot \mathbf{g}_{j+1})_{\alpha\gamma} = \sum_{\beta mn} A_{\alpha\beta}(m) A_{\beta\gamma}(n) |m\rangle_j \otimes |n\rangle_{j+1}. \quad (5.6)$$

The dual $(\bar{\mathbf{g}}_j \cdot \bar{\mathbf{g}}_{j+1})_{\alpha\gamma}$ is defined analogously. For products of \mathbf{g} matrices denoting a block of sequential spins we introduce an abbreviation

$$(\mathbf{g}_j \cdot \mathbf{g}_{j+1} \cdot \dots \cdot \mathbf{g}_{j'})_{\alpha\alpha'} = |\alpha\alpha'; j, j'\rangle. \quad (5.7)$$

Thus, it is sufficient to identify the states of boundary spins to specify the state of a block.

Let us construct a transfer matrix $\mathbf{G} \equiv \bar{\mathbf{g}} \otimes \mathbf{g}$ that is useful for calculating state overlaps (scalar products) and correlation functions:

$$(\mathbf{G})_{\alpha\gamma, \beta\delta} = (\bar{\mathbf{g}})_{\alpha\beta} (\mathbf{g})_{\gamma\delta} = \sum_m A_{\alpha\beta}^*(m) A_{\gamma\delta}(m). \quad (5.8)$$

For example, the square of the norm of $|\text{MPS}\rangle$ is

$$\langle \text{MPS} | \text{MPS} \rangle = \sum_{\alpha\alpha'} \langle \alpha\alpha'; 1, L | \alpha\alpha'; 1, L \rangle = \text{tr} \mathbf{G}^L. \quad (5.9)$$

The density matrix is therefore

$$\rho = \frac{\text{tr}[\mathbf{g}_1 \cdots \mathbf{g}_L] \text{tr}[\bar{\mathbf{g}}_1 \cdots \bar{\mathbf{g}}_L]}{\text{tr} \mathbf{G}^L}, \quad (5.10)$$

while the reduced density matrix is

$$\rho_\ell = \sum_{\alpha\alpha', \beta\beta'} \frac{|\alpha\alpha'; 1, \ell\rangle (\mathbf{G}^{L-\ell})_{\alpha'\beta', \alpha\beta} \langle \beta\beta'; 1, \ell|}{\text{tr} \mathbf{G}^L}. \quad (5.11)$$

We chose the block to extend from site 1 to site ℓ without loss of generality because of translational invariance. In this form, ρ_ℓ clearly acts nontrivially only in the subspace spanned by the block state vectors $\{|\alpha\alpha'; 1, \ell\rangle\}$. The dimension of this subspace is at most D^2 .

Let us consider transfer matrices with the symmetries

$$(\mathbf{G})_{\alpha\beta, \alpha'\beta'} = (\mathbf{G})_{\alpha'\beta', \alpha\beta} = (\mathbf{G})_{\beta\alpha, \beta'\alpha'}$$

This is a weak requirement because it means that the scalar product $\langle \alpha\alpha'; 1, n | \beta\beta'; 1, n \rangle$ is invariant under lattice reflections (e.g., ‘flipping’ the ring over). We construct a symmetric overlap matrix $\mathbf{K}(n)$ that is related to the n^{th} power of \mathbf{G} by $(\mathbf{K}(n))_{\alpha\alpha', \beta\beta'} \equiv (\mathbf{G}^n)_{\alpha\beta, \alpha'\beta'}$. With this definition we write ρ_ℓ as

$$\rho_\ell = \sum_{\alpha\alpha', \beta\beta'} \frac{|\alpha\alpha'; 1, \ell\rangle (\mathbf{K}(L-\ell))_{\alpha\alpha', \beta\beta'} \langle \beta\beta'; 1, \ell|}{\text{tr} \mathbf{G}^L}. \quad (5.12)$$

The indices are now matched so that we can express ρ_ℓ as a product of matrices. Suitable similarity transformations within the space spanned by $\{|\alpha\alpha'; 1, \ell\rangle\}$ finally gives

$$\rho_\ell = \frac{\mathbf{K}(L-\ell)\mathbf{K}(\ell)}{\text{tr}[\mathbf{K}(L-\ell)\mathbf{K}(\ell)]}. \quad (5.13)$$

This formula has some notable features. First, it is a general expression that is valid for a large class of MPS. Also, we find that ρ_ℓ has a small number of nonzero eigenvalues, $\text{rank} \rho_\ell \leq D^2$. Furthermore, it is evident that ρ_ℓ and $\rho_{L-\ell}$ are isospectral. Thus, the entanglement entropies of the block and environment

are the same.

5.2 AKLT_q model.

The spin 1 AKLT_q Hamiltonian is

$$\begin{aligned}
\mathcal{H} = b \sum_j & \left\{ c \mathbf{S}_j \cdot \mathbf{S}_{j+1} + [\mathbf{S}_j \cdot \mathbf{S}_{j+1} + \frac{1}{2}(1-c)(q+q^{-1}-2)S_j^z S_{j+1}^z \right. \\
& + \frac{1}{4}(1+c)(q-q^{-1})(S_{j+1}^z - S_j^z)]^2 + \frac{1}{4}c(1-c)(q+q^{-1}-2)^2(S_j^z S_{j+1}^z)^2 \\
& + \frac{1}{4}c(1+c)(q-q^{-1})(q+q^{-1}-2)S_j^z S_{j+1}^z (S_{j+1}^z - S_j^z) \\
& + \frac{1}{4}(c-3) \left[(c-1 + \frac{1}{2}(1+c)^2)S_j^z S_{j+1}^z + 2(c - \frac{1}{8}(1+c)^2)((S_{j+1}^z)^2 + (S_j^z)^2) \right] \\
& \left. + (c-1) + \frac{1}{2}c(q^2 - q^{-2})(S_{j+1}^z - S_j^z) \right\}, \tag{5.14}
\end{aligned}$$

with $c = 1 + q^2 + q^{-2}$ and $b = [c(c-1)]^{-1}$ [87, 88]. It is hermitian for real q . It commutes with the generators $\mathbb{S}^{z,\pm} \equiv \sum_j S_j^{z,\pm}$ of the $SU_q(2)$ quantum algebra [77, 78]. These generators have commutators

$$[\mathbb{S}^+, \mathbb{S}^-] = \frac{q^{2\mathbb{S}^z} - q^{-2\mathbb{S}^z}}{q - q^{-1}}, \quad [\mathbb{S}^z, \mathbb{S}^\pm] = \pm \mathbb{S}^\pm. \tag{5.15}$$

The q -deformed spin-1 operators at site j are $\mathbb{S}_j^z = S_j^z$ and

$$\mathbb{S}_j^\pm = \sqrt{\frac{q + q^{-1}}{2}} (q^{-S_j^z} \otimes \dots \otimes q^{-S_{j-1}^z} \otimes S_j^\pm \otimes q^{S_{j+1}^z} \otimes \dots). \tag{5.16}$$

Here $S_j^{z,\pm}$ are undeformed spin-1 operators at site j . Eq. (5.16) has similarities with Jordan-Wigner transformations. We recover the isotropic AKLT model at $q = 1$.

The entanglement spectrum does not depend on the sign of q and is invariant under the transformation $q \rightarrow q^{-1}$. Thus, we will only consider $q \in (0, 1]$.

The unique ground state of the periodic AKLT_q model is a VBS_q state. Its MPS representation was constructed in Ref. [59]. The properties of this state and its spin-spin correlation functions have been studied [59, 88]. This approach was later extended to obtain the spin-spin correlators of higher integer spin- S AKLT_q chains [91, 92].

The local Hamiltonian $h_{j,j+1}$ is a **projector** onto the subspace of the q -deformed spin-2 quintuplet formed by adjacent spins [59]. The MPS form of the VBS_q ground state is obtained by requiring $h_{j,j+1}$ to annihilate the

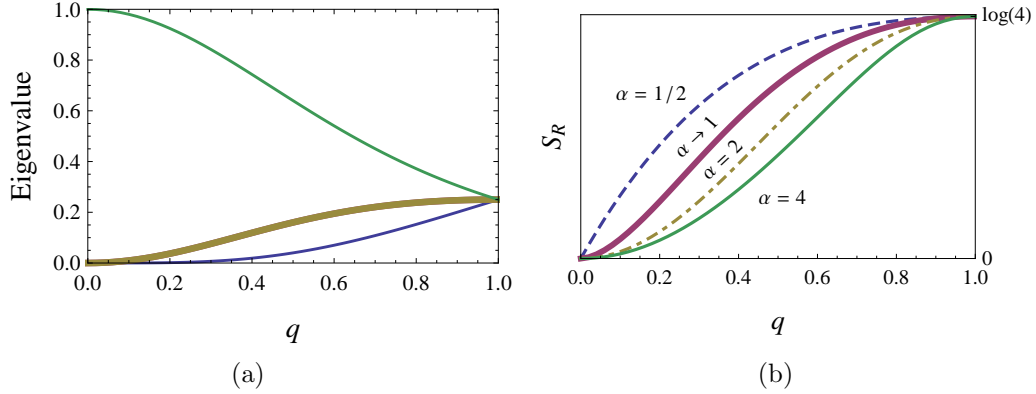


Figure 5.1: (a) In the double scaling limit the reduced density matrix of $|\text{VBS}_q\rangle$ has four degenerate eigenvalues at the isotropic $q = 1$ point. The two middle eigenvalues are always degenerate (bold line). In the classical limit $q \rightarrow 0$ the ground state is a product state and the only nonzero eigenvalue is unity. (b) The Rényi entropy S_R vanishes as $q \rightarrow 0$. It saturates to the maximally entangled value $S_R = \log 4$ at the AKLT point $q = 1$. The von Neumann entropy (bold line) is obtained at $\lim_{\alpha \rightarrow 1} S_R(\alpha)$.

elements of the matrix $\mathbf{g}_j \cdot \mathbf{g}_{j+1}$. This condition leads to

$$\mathbf{g} = \begin{pmatrix} q^{-1}|0\rangle & -\sqrt{q + q^{-1}}|+\rangle \\ \sqrt{q + q^{-1}}|-\rangle & -q|0\rangle \end{pmatrix}, \quad (5.17)$$

where the vector elements are eigenstates of S^z . This yields the MPS representation

$$|\text{VBS}_q\rangle = \text{tr}[\mathbf{g}_1 \cdot \mathbf{g}_2 \cdot \dots \cdot \mathbf{g}_L]. \quad (5.18)$$

Since \mathbf{g} is a 2×2 matrix, the reduced density matrix has at most four nonzero eigenvalues.

In the limit $q \rightarrow 0$, the AKLT_q Hamiltonian is dominated by (classical) Ising-type interactions. In this case the \mathbf{g} matrix has only one diagonal element $|0\rangle$. The resulting ground state is a product state $\bigotimes_j |0\rangle_j$ describing a magnet polarized in the transverse direction. In this classical limit all spins are in the $S_j^z = 0$ state. Hence, any block in the chain has zero entropy.

The transfer matrix (5.8) for the $|\text{VBS}_q\rangle$ state is

$$\mathbf{G} \equiv \bar{g} \otimes g = \begin{pmatrix} q^{-2} & 0 & 0 & q + q^{-1} \\ 0 & -1 & 0 & 0 \\ 0 & 0 & -1 & 0 \\ q + q^{-1} & 0 & 0 & q^2 \end{pmatrix}. \quad (5.19)$$

The eigenvalues of this matrix are $\{\Lambda, -1, -1, -1\}$ and the dominant eigenvalue is $\Lambda = 1 + q^2 + q^{-2} \geq 3$. The overlap matrix $\mathbf{K}(\ell)$ is therefore

$$\mathbf{K}(\ell) = \frac{\Lambda^\ell}{q + q^{-1}} \text{diag}\{q^{-1}, 1, 1, q\} \quad (5.20)$$

$$+ \frac{(-1)^\ell}{q + q^{-1}} \begin{pmatrix} q & 0 & 0 & q + q^{-1} \\ 0 & -1 & 0 & 0 \\ 0 & 0 & -1 & 0 \\ q + q^{-1} & 0 & 0 & q^{-1} \end{pmatrix}. \quad (5.21)$$

Eq. (5.13) gives the reduced density matrix

$$\rho_\ell = \frac{\mathbf{K}(L - \ell)\mathbf{K}(\ell)}{\Lambda^L + 3(-1)^L}. \quad (5.22)$$

In the double scaling limit of an infinite block $\ell \rightarrow \infty$ in an infinite chain $(L - \ell) \rightarrow \infty$, the reduced density matrix becomes diagonal. Thus, the block states $|\alpha\alpha'; 1, \ell\rangle$ are orthogonal to each other. The eigenvalues $\{p_i\}$ of the reduced density matrix $\rho_{\ell \rightarrow \infty}$ are

$$p_{1,4} = \frac{q^{\pm 2}}{(q + q^{-1})^2}, \quad p_2 = p_3 = \frac{1}{(q + q^{-1})^2}, \quad \ell \rightarrow \infty. \quad (5.23)$$

We discover an important consequence of q -deformation: The degeneracy of the entanglement spectrum changes between the classical and isotropic AKLT points. This result is depicted in Fig.(5.1a).

To obtain an intuitive picture for the mixed state of the block we write $\rho_{\ell \rightarrow \infty} = e^{-\beta H_e} / \text{tr} e^{-\beta H_e}$. Here, H_e is an effective Hamiltonian and $1/\beta$ an effective temperature. The eigenvalues of H_e form the entanglement spectrum [14]. Doing so gives the effective temperature $1/\beta = 1/|\ln q|$ and effective Hamiltonian

$$H_e = \sigma_1^x \sigma_\ell^x + \sigma_1^y \sigma_\ell^y, \quad (5.24)$$

where σ_j^i are Pauli operators at site j . Thus, $\rho_{\ell \rightarrow \infty}$ describes a thermal ensemble of two spin-1/2's at the block boundaries with Heisenberg (XX) interaction.

The anisotropy parameter q determines the effective boundary temperature $T_e = 1/|\ln q|$. For the original AKLT model ($q = 1$) the effective boundary spins are in a maximally mixed state ($T_e \rightarrow \infty$), while in the classical limit $q \rightarrow 0$ they are in a pure state ($T_e = 0$).

This result for the effective Hamiltonian is consistent with the area law for gapped models [4, 73]. It is similar to the effective boundary spin chain proposed for 2D AKLT models [15, 94]. However, in the AKLT $_q$ chain the effective boundary spin interaction is long-ranged and exists for arbitrarily large blocks. The long range of this interaction follows from the non-local nature of the SU $_q$ (2) symmetry (5.16) of the model.

The Rényi and von Neumann entropies in the double scaling limit are

$$S_R^{\ell \rightarrow \infty} = \frac{2}{1 - \alpha} \log \frac{q^\alpha + q^{-\alpha}}{(q + q^{-1})^\alpha}, \quad (5.25)$$

$$S_{\text{vN}}^{\ell \rightarrow \infty} = \log(q + q^{-1})^2 - \frac{q - q^{-1}}{q + q^{-1}} \log q^2. \quad (5.26)$$

We plot these entropies in Fig.(5.1b) and observe the effects of q -deformation even in the large block limit. Anisotropy reduces entanglement entropy from its maximum value $S_R = \log 4$. This maximum is reached at the AKLT point.

For blocks of finite length $\ell < \infty$ in an infinite chain $L \rightarrow \infty$, the overlap matrix $\mathbf{K}(\ell)$ has off-diagonal terms. In this case, the eigenvalues of ρ_ℓ acquire finite-size corrections:

$$p_{1,4} = \frac{q^2 + q^{-2} + 2(-\Lambda)^{-\ell}}{2(q + q^{-1})^2} \pm \sqrt{\frac{1}{4} - \frac{1 - (-\Lambda)^{-2\ell}}{(q + q^{-1})^2}},$$

$$p_2 = p_3 = \frac{1 - (-\Lambda)^{-\ell}}{(q + q^{-1})^2}, \quad \Lambda = 1 + q^2 + q^{-2}. \quad (5.27)$$

These eigenvalues are exact. The corrections decay exponentially as expected for a gapped system. At $q = 1$ we recover the eigenvalues

$$p_1 = \frac{1 + 3(-3)^{-\ell}}{4}, \quad p_2 = p_3 = p_4 = \frac{1 - (-3)^{-\ell}}{4}, \quad (5.28)$$

for the isotropic AKLT chain [64]. Figure (5.2a) shows how q -deformation reduces the von Neumann entropy. For a block consisting of one spin ($\ell = 1$) one eigenvalue is identically zero. Thus, the maximum single-site von Neumann entropy is $\log 3$. This value is reached at the isotropic point $q = 1$ where there is a uniform mixture of three spin-1 states.

For large but finite blocks $1 \ll \ell < \infty$ and $q \neq 1$, an expansion of the

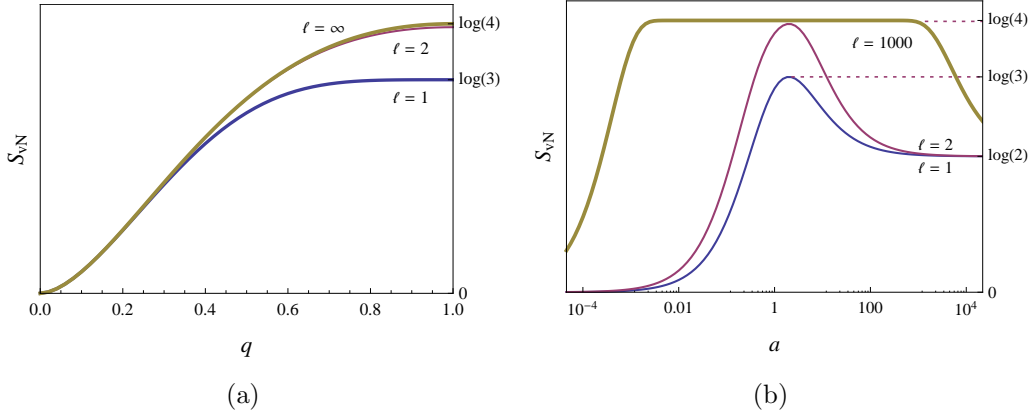


Figure 5.2: The von Neumann entropy decreases away from the isotropic AKLT points $q = 1$ for $|\text{VBS}_q\rangle$ (a) and $a = 2$ for $|\text{KSZ}_a\rangle$ (b). At the isotropic point finite-size corrections are largest for $|\text{VBS}_q\rangle$ and smallest for $|\text{KSZ}_a\rangle$.

eigenvalues (5.27) gives the leading order corrections $\pm(-1)^\ell(q + q^{-1})^{-2}e^{-\ell/\xi}$. The characteristic length of these corrections is $\xi = 1/\ln(1 + q^2 + q^{-2})$. This quantity is equal to the correlation length of the spin-spin correlators of the VBS_q state [59, 88, 92].

5.2.1 General Spin S, Quantum algebra

In this section we generalize the results obtained in the previous section, going from $S = 1$, to general spin. The deformation parameter q here, relates with the one used previously by $q \rightarrow q^2$.

Let us denote states of a spin- S at site i by $|S, m\rangle_i$. Here $m \in \{-S, -S + 1, \dots, S\}$ is the magnetic quantum number denoting the z -component of the spin. The label S of the state $|S, m\rangle_i$ is invariant under the action of q -deformed angular momentum operators satisfying the $\text{SU}_q(2)$ quantum group algebra [78]

$$[J_i^+, J_i^-] = [2J_i^z], \quad [J_i^z, J_i^\pm] = \pm J_i^\pm, \quad [n] \equiv \frac{q^{n/2} - q^{-n/2}}{q^{1/2} - q^{-1/2}}. \quad (5.29)$$

This algebra has two different unitary representations for positive real q and complex q on the unit circle [95]. In this chapter we will consider the former case where $q \in \mathbb{R}^+$. The resulting algebra is invariant under the transformation $q \rightarrow q^{-1}$ so that we consider further $q \in (0, 1]$. The usual $\text{SU}(2)$ algebra is

recovered at the isotropic point $q = 1$, while full deformation occurs in the limit $q \rightarrow 0$. The q -number $[n]$ will be used extensively below.

The analogue of total angular momentum, $\mathbf{J}_{\text{tot}} = \mathbf{J}_1 + \mathbf{J}_2$ is realized at the level of operators through the definition of the coproduct

$$J_{\text{tot}}^{\pm} \equiv q^{-J_1^z/2} \otimes J_2^{\pm} + J_1^{\pm} \otimes q^{J_2^z/2}, \quad (5.30)$$

$$J_{\text{tot}}^z \equiv \mathbb{I}_1 \otimes J_2^z + J_1^z \otimes \mathbb{I}_2. \quad (5.31)$$

The operators $J_{\text{tot}}^{z,\pm}$ satisfy the quantum group algebra (5.29). A $(2J + 1)$ -dimensional irreducible representation of \mathbf{J}_{tot} is therefore spanned by the states

$$|J, m\rangle \equiv \sum_{m_1 m_2} \begin{bmatrix} j_1 & j_2 & J \\ m_1 & m_2 & m \end{bmatrix}_q |j_1, m_1\rangle \otimes |j_2, m_2\rangle, \quad (5.32)$$

which satisfies

$$J_{\text{tot}}^{\pm} |J, m\rangle = \sqrt{[J \mp m][J \pm m + 1]} |J, m \pm 1\rangle, \quad (5.33)$$

$$J_{\text{tot}}^z |J, m\rangle = m |J, m\rangle. \quad (5.34)$$

These equations define the q -deformed Clebsch-Gordan (q -CG) coefficients $\begin{bmatrix} J & K & L \\ m_j & m_k & m_l \end{bmatrix}_q$ up to a phase.

The q -CG coefficients are components of a unitary matrix (a change of basis matrix) and may be chosen to be real. These coefficients vanish if the triangle relation $|j_1 - j_2| \leq J \leq j_1 + j_2$ and selection rule $m_1 + m_2 = m$ are not satisfied (angular momentum conservation). Throughout this chapter, the summation indices m_i (lower row of q -CG symbols) are understood to run over all values compatible with the corresponding quantum number j_i (upper row of q -CG symbols). For example, in (5.32) we sum over $m_i \in \{-j_i, -j_i + 1, \dots, j_i\}$. Some identities involving the q -CG coefficients that we use in the following derivations are collected in appendix (C.1).

5.2.2 Matrix product representation

Some of the objects we describe here are conveniently represented as diagrams (5.3). The manipulation of these diagrams has been useful in the study of entanglement and correlation functions in matrix product states [86, 96].

Let us now write down the MPS representation of the $\text{VBS}_q(S)$ state. For a periodic chain of L spins we have

$$|\text{VBS}_q(S)\rangle = \text{tr}(\mathbf{g}_1 \mathbf{g}_2 \dots \mathbf{g}_L), \quad (5.35)$$

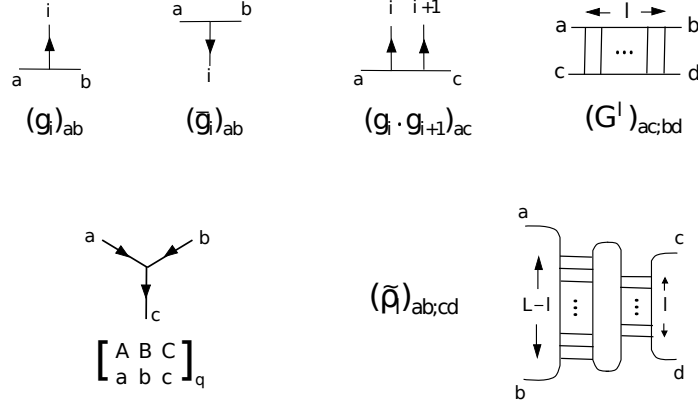


Figure 5.3: Diagrammatic representations of matrices used in the MPS description of the $\text{VBS}_q(S)$ state (upper row). The q -deformed Clebsch-Gordan coefficients (lower left) are important in the diagonalization of the transfer matrix. The matrix $\tilde{\rho}_l$ (lower right) is related to the reduced density matrix ρ_l of l sequential spins in a chain of L sites by $\rho_l = \tilde{\rho}_l / \text{tr} \mathbf{G}^L$.

where \mathbf{g}_i are $(S+1) \times (S+1)$ matrices. The trace here is done over the auxiliary matrix space. The elements of \mathbf{g}_i and its dual $\bar{\mathbf{g}}_i$ are state vectors:

$$(\mathbf{g}_i)_{ab} = \sum_m \begin{bmatrix} \frac{S}{2} & \frac{S}{2} & S \\ a & -b & m \end{bmatrix}_q (-1)^b q^{-b/2} |S, m\rangle_i, \quad (5.36)$$

$$(\bar{\mathbf{g}}_i)_{ab} = \sum_m \begin{bmatrix} \frac{S}{2} & \frac{S}{2} & S \\ a & -b & m \end{bmatrix}_q (-1)^b q^{-b/2} \langle S, m|_i. \quad (5.37)$$

The $|\text{VBS}_q(S)\rangle$ state (5.35) is annihilated by the q -deformed AKLT Hamiltonian (periodic boundary conditions)

$$\mathcal{H} = \sum_{i=1}^L h_{i,i+1} = \sum_{i=1}^L \sum_{s=S+1}^{2S} \Pi_s(i, i+1), \quad (5.38)$$

where $\Pi_s(i, i+1)$ is a projector onto the subspace spanned by the q -deformed s -multiplet formed by spins at i and $i+1$. To prove this, we look at the overlap

between the two states

$$(\mathbf{g}_i \mathbf{g}_{i+1})_{ac} = \sum_{bm'm} (-1)^{c-b} q^{\frac{1}{2}(b-c)} \begin{bmatrix} \frac{S}{2} & \frac{S}{2} & S \\ a & b & m' \end{bmatrix}_q \begin{bmatrix} \frac{S}{2} & \frac{S}{2} & S \\ -b & -c & m \end{bmatrix}_q |S, m'\rangle_i \otimes |S, m\rangle_{i+1} \quad (5.39)$$

$$|J, m\rangle = \sum_{m_1 m_2} \begin{bmatrix} j_1 & j_2 & J \\ m_1 & m_2 & m \end{bmatrix}_q |j_1, m_1\rangle_i \otimes |j_2, m_2\rangle_{i+1} \quad (5.40)$$

Since the states $\{|j, m\rangle_i\}$ are orthonormal to each other, we obtain

$$\langle J, m | (\mathbf{g}_i \mathbf{g}_{i+1})_{ac} = \sum_{bm_1 m_2} (-1)^{c-b} q^{\frac{1}{2}(b-c)} \begin{bmatrix} \frac{S}{2} & \frac{S}{2} & S \\ a & b & m_1 \end{bmatrix}_q \begin{bmatrix} \frac{S}{2} & \frac{S}{2} & S \\ -b & -c & m_2 \end{bmatrix}_q \begin{bmatrix} S & S & J \\ m_1 & m_2 & m \end{bmatrix}_q. \quad (5.41)$$

Using an identity (C.7) derived in (C.2) yields

$$\langle J, m | (\mathbf{g}_i \mathbf{g}_{i+1})_{ac} = (-1)^{c-S/2} q^{-c/2} \sqrt{\frac{[2S+1]}{[S+1]}} F_q \left[S \frac{S}{2} J \frac{S}{2}; \frac{S}{2} S \right] \begin{bmatrix} \frac{S}{2} & \frac{S}{2} & J \\ a & -c & m \end{bmatrix}_q. \quad (5.42)$$

The elements $F_q[DBJC; NK]$ of the q -deformed F -matrix are defined diagrammatically in (5.4). The q -CG coefficient in the overlap (5.42) vanishes when $J > \frac{S}{2} + \frac{S}{2}$ proving that $h_{i,i+1} |\text{VBS}_q(S)\rangle = 0$. Furthermore, $h_{i,i+1}$ has nonnegative eigenvalues because it is a sum of projectors. Thus, $|\text{VBS}_q(S)\rangle$ is a ground state of the Hamiltonian (5.38).

5.2.3 Transfer matrix

We now construct a transfer matrix \mathbf{G} that is defined in terms of \mathbf{g} and $\bar{\mathbf{g}}$ by $(\mathbf{G})_{aa';bb'} = (\bar{\mathbf{g}})_{ab}(\mathbf{g})_{a'b'}$. Explicitly, its elements are

$$(\mathbf{G})_{aa';bb'} = \sum_{m'} \begin{bmatrix} \frac{S}{2} & \frac{S}{2} & S \\ a & -b & m' \end{bmatrix}_q \begin{bmatrix} \frac{S}{2} & \frac{S}{2} & S \\ a' & -b' & m' \end{bmatrix}_q (-1)^{b+b'} q^{-(b+b')/2}. \quad (5.43)$$

This transfer matrix is an important object that appears in the calculation of correlation functions and the reduced density matrix of MPS. Let us diagonalize this matrix through an approach based on the q -deformed F -matrix (C.2). As depicted in (5.4), we construct the eigenvalue equation $(\mathbf{G})_{aa';bb'} e_{bb'} = \lambda e_{aa'}$ using the q -CG coefficients as an ansatz for the elements of the eigenvector

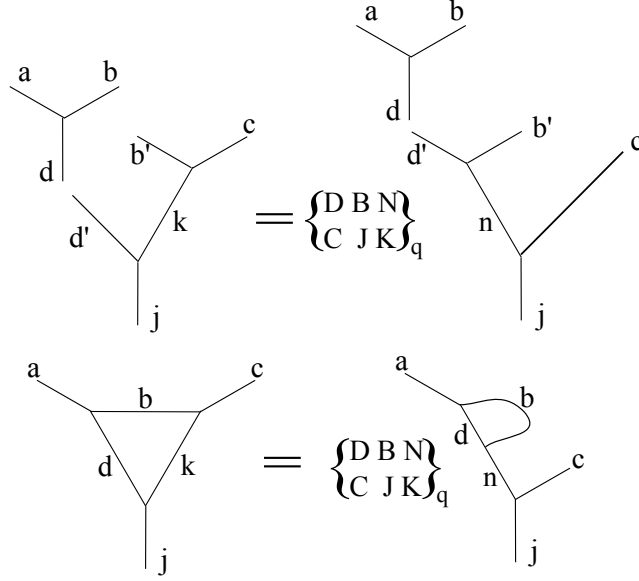


Figure 5.4: Diagrams representing the contraction of the transfer matrix \mathbf{G} with a q -deformed Clebsch-Gordan coefficient. The q -deformed F -matrix is defined according to the upper diagram in which the leg labeled by b' is shifted. The lower diagram represents the eigenvalue equation (5.45). In these diagrams internal lowercase indices are summed over.

$e_{aa'}$. The resulting equation is

$$(\mathbf{G})_{aa';bb'}e_{bb'} = \sum_{bb'm'} \begin{bmatrix} \frac{S}{2} & \frac{S}{2} & S \\ a & -b & m' \end{bmatrix}_q \begin{bmatrix} \frac{S}{2} & j & \frac{S}{2} \\ b & m & b' \end{bmatrix}_q \begin{bmatrix} \frac{S}{2} & \frac{S}{2} & S \\ a' & -b' & m' \end{bmatrix}_q (-1)^{b+b'} q^{-(b+b')/2}. \quad (5.44)$$

Transposing columns in the third q -CG coefficient in order to match the identity (C.7) leads to

$$\begin{aligned} (\mathbf{G})_{aa';bb'}e_{bb'} &= \sum_{bb'm'} \begin{bmatrix} \frac{S}{2} & \frac{S}{2} & S \\ a & b & m' \end{bmatrix}_q \begin{bmatrix} \frac{S}{2} & j & \frac{S}{2} \\ -b & m & b' \end{bmatrix}_q \begin{bmatrix} S & \frac{S}{2} & \frac{S}{2} \\ m' & b' & a' \end{bmatrix}_q (-1)^{-\frac{S}{2}-b} q^{b/2} \sqrt{\frac{[2S+1]}{[S+1]}} \\ &= (-1)^{-S} \frac{[2S+1]}{[S+1]} F_q \left[S \frac{S}{2} \frac{S}{2} j; \frac{S}{2} \frac{S}{2} \right] \begin{bmatrix} \frac{S}{2} & j & \frac{S}{2} \\ a & m & a' \end{bmatrix}_q = \lambda e_{aa'}. \end{aligned} \quad (5.45)$$

We see that the elements of the eigenvectors of \mathbf{G} are $e_{aa'} = (e_{jm})_{aa'} = \begin{bmatrix} S/2 & j & S/2 \\ a & m & a' \end{bmatrix}_q$. A suitable similarity transformation on \mathbf{G} gives the orthonormal set of eigenvectors

$$(\hat{e}_{jm})_{aa'} = \begin{bmatrix} \frac{S}{2} & \frac{S}{2} & j \\ -a & a' & m \end{bmatrix}_q. \quad (5.46)$$

To obtain this set we transposed the middle and last rows of $(e_{jm})_{aa'}$ and considered the orthogonality relation (C.2). The eigenvalues associated with these eigenvectors are

$$\lambda_j = (-1)^{-S} \frac{[2S+1]}{[S+1]} F_q \left[S \frac{S}{2} \frac{S}{2} j; \frac{S}{2} \frac{S}{2} \right], \quad (5.47)$$

$$= (-1)^{j+S} [2S+1] \left\{ \begin{matrix} \frac{S}{2} & \frac{S}{2} \\ j & \frac{S}{2} \end{matrix} \right\}_q, \quad (5.48)$$

where the q -deformed $6j$ symbol in the second line is defined in (C.9). The eigenvalue λ_j is $(2j+1)$ -fold degenerate and $0 \leq j \leq S$. The absolute value of λ_j decreases with increasing j . These expressions match the results of [91, 92] (except for a multiplicative constant).

5.2.4 Reduced Density Matrix

In this subsection we calculate the reduced density matrix ρ_ℓ of ℓ sequential spins in a chain of infinite length $L \rightarrow \infty$. Using the formalism developed in [97] for matrix product states, we obtain

$$(\rho_\ell)_{ab;cd} = \frac{1}{\text{tr} \mathbf{G}^L} \sum_{a'b'} (\mathbf{G}^{L-\ell})_{aa';bb'} (\mathbf{G}^\ell)_{a'c;b'd}. \quad (5.49)$$

Integer powers of the transfer matrix \mathbf{G} may be written as

$$\mathbf{G}^n = \sum_j \lambda_j^n \mathbf{P}_j, \quad (5.50)$$

where \mathbf{P}_j is a projection matrix onto the subspace spanned by the eigenvectors \hat{e}_{jm} of \mathbf{G} . Since the dominant (largest magnitude) eigenvalue of \mathbf{G} is $\lambda_{j=0}$, large integer powers of \mathbf{G} simplify to $\mathbf{G}^n \rightarrow \lambda_0^n \mathbf{P}_0$ as $n \rightarrow \infty$. Thus, in the limit of infinite chains $L \rightarrow \infty$ the reduced density matrix (5.49) simplifies to

$$(\rho_\ell)_{ab;cd} = \sum_{a'b'} (\mathbf{P}_0)_{aa';bb'} \sum_{j=0}^S \frac{\lambda_j^\ell}{\lambda_0^\ell} (\mathbf{P}_j)_{a'c;b'd}. \quad (5.51)$$

Constructing the projectors \mathbf{P}_j from the eigenvectors of \mathbf{G} (5.46) yields

$$(\rho_\ell)_{ab;cd} = \frac{q^{-(a+b)/2} (-1)^{a+b+S}}{[S+1]} \sum_{j=0}^S \frac{\lambda_j^\ell}{\lambda_0^\ell} \sum_{m=-j}^j \begin{bmatrix} \frac{S}{2} & \frac{S}{2} & j \\ -a & c & m \end{bmatrix}_q \begin{bmatrix} \frac{S}{2} & \frac{S}{2} & j \\ -b & d & m \end{bmatrix}_q, \quad (5.52)$$

where the projector \mathbf{P}_0 is simplified by the explicit formula [95]

$$\begin{bmatrix} \frac{S}{2} & \frac{S}{2} & 0 \\ -a & a & 0 \end{bmatrix}_q = \frac{(-1)^{a+S/2} q^{-a/2}}{\sqrt{[S+1]}}. \quad (5.53)$$

We can further express the reduced density matrix as a sum of tensor products by defining the $(S+1) \times (S+1)$ matrix

$$(\mathbf{Q}_{jm})_{ac} \equiv \frac{(-1)^{a+S/2} q^{-a/2}}{\sqrt{[S+1]}} \begin{bmatrix} \frac{S}{2} & \frac{S}{2} & j \\ -a & c & m \end{bmatrix}_q \delta_{m,c-a}. \quad (5.54)$$

The Kronecker delta here enforces the triangle relation. Finally, making the necessary substitutions gives

$$\rho_\ell = \sum_{j=0}^S \frac{\lambda_j^\ell}{\lambda_0^\ell} \sum_{m=-j}^j \mathbf{Q}_{jm} \otimes \mathbf{Q}_{jm}. \quad (5.55)$$

5.3 Double scaling limit

5.3.1 Eigenvalues of reduced density matrix

In the double scaling limit, we consider infinitely long blocks and take $\ell \rightarrow \infty$. The reduced density matrix ρ_ℓ (5.55) simplifies to a tensor product of diagonal matrices $\rho_\infty = \mathbf{Q}_{00} \otimes \mathbf{Q}_{00}$. Explicitly, we have:

$$(\rho_\infty)_{ab;cd} = \frac{(-1)^{a+b+S} q^{-(a+b)/2}}{[S+1]} \begin{bmatrix} \frac{S}{2} & \frac{S}{2} & 0 \\ -a & a & 0 \end{bmatrix}_q \begin{bmatrix} \frac{S}{2} & \frac{S}{2} & 0 \\ -b & b & 0 \end{bmatrix}_q \delta_{ac} \delta_{bd}. \quad (5.56)$$

Remembering that $-S/2 \leq a, b, c, d \leq S/2$, with integer steps, we arrive at the final expression for the reduced density matrix,

$$(\rho_\infty)_{ab;cd} = \frac{q^{-(a+b)}}{[S+1]^2} \delta_{ac} \delta_{bd}. \quad (5.57)$$

From this expression we can compute all eigenvalues of ρ_∞ . For example, in the case of a q -deformed spin-2 VBS state we have

$$\rho_\infty = \frac{1}{(q+1+q^{-1})^2} \begin{pmatrix} q^{-1} & 0 & 0 \\ 0 & 1 & 0 \\ 0 & 0 & q \end{pmatrix} \otimes \begin{pmatrix} q^{-1} & 0 & 0 \\ 0 & 1 & 0 \\ 0 & 0 & q \end{pmatrix}. \quad (5.58)$$

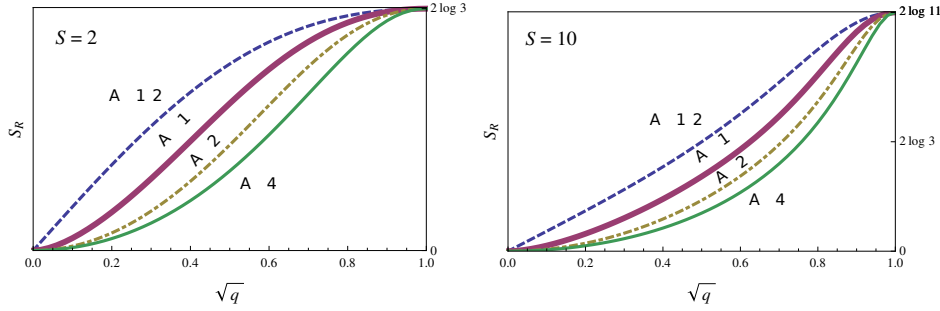


Figure 5.5: The Rényi entropy $S_R(\alpha)$ of a q -deformed spin- S VBS state vanishes in the limit $q \rightarrow 0^+$. At the isotropic point $q = 1$, large blocks are maximally entangled $S_R(\alpha) = 2 \ln(S + 1)$. The von Neumann entropy is obtained in the limit $\alpha \rightarrow 1$ (bold line).

5.3.2 Entanglement spectrum and entropy

We now write $\rho_\infty = e^{-\beta H_e} / \text{tr} e^{-\beta H_e}$, where H_e is an effective Hamiltonian and $1/\beta$ an effective temperature. The eigenvalues of the Hamiltonian H_e constitute the entanglement spectrum of the block [14]. The tensor product form of ρ_∞ (5.57) yields the simple paramagnetic model

$$-\beta H_e = -\beta(H_e^{(1)} + H_e^{(2)}) \equiv \beta h(S_1^z + S_2^z), \quad \mathbf{S}_i^2 = \frac{S}{2}(\frac{S}{2} + 1), \quad (5.59)$$

$$\beta h = |\ln q|. \quad (5.60)$$

Here h is the magnitude of an effective magnetic field along the z -axis, while \mathbf{S}_i are spin- $S/2$ operators of the undeformed $SU(2)$ algebra. We can thus identify $|\ln q|$ as the ratio h/T_e between the magnitude of the magnetic field and effective temperature T_e . We observe that the spectrum of $H_e^{(i)}$ consists of $S + 1$ equidistant energy levels. Thus, in the limit $S \rightarrow \infty$ the entanglement spectrum of the block is equal to the energy spectrum of two harmonic oscillators with frequency ω (with an S -dependent energy shift). This frequency is related to the deformation parameter through $|\ln q| = \omega/T_e$.

In this effective picture, the isotropic case $q = 1$ corresponds to infinite temperature or zero field strength. The block is therefore maximally mixed. The reduced density matrix ρ_∞ has $(S + 1)^2$ nonzero identical eigenvalues. In the opposite limit $q \rightarrow 0^+$ the effective model corresponds to zero temperature or infinite field magnitude. Hence, the block is in a pure state with zero entanglement.

We use the eigenvalues of the reduced density matrix (5.57) to compute

the Rényi entropy

$$\begin{aligned}
S_{\text{R}}(\alpha) &= \frac{\ln \text{tr} \rho^\alpha}{1-\alpha} = \frac{2}{1-\alpha} \ln \left\{ \frac{q^{\frac{\alpha(S+1)}{2}} - q^{-\frac{\alpha(S+1)}{2}}}{q^{\frac{\alpha}{2}} - q^{-\frac{\alpha}{2}}} \frac{1}{[S+1]^\alpha} \right\}, \\
&= \frac{2}{1-\alpha} \ln \left\{ \frac{q^{\frac{\alpha(S+1)}{2}} - q^{-\frac{\alpha(S+1)}{2}}}{q^{\frac{\alpha}{2}} - q^{-\frac{\alpha}{2}}} \left(\frac{q^{\frac{1}{2}} - q^{-\frac{1}{2}}}{q^{\frac{S+1}{2}} - q^{-\frac{S+1}{2}}} \right)^\alpha \right\}. \tag{5.61}
\end{aligned}$$

This is an exact expression in the double scaling limit (infinite block). Taking the limit $\alpha \rightarrow 1$ gives the von Neumann entropy

$$\begin{aligned}
S_{\text{vN}} &= 2 \ln([S+1]) + \left\{ \frac{q^{\frac{1}{2}} + q^{-\frac{1}{2}}}{q^{\frac{1}{2}} - q^{-\frac{1}{2}}} - (S+1) \frac{q^{\frac{S+1}{2}} + q^{-\frac{S+1}{2}}}{q^{\frac{S+1}{2}} - q^{-\frac{S+1}{2}}} \right\} \ln q, \\
&= 2 \ln \left\{ \frac{q^{\frac{S+1}{2}} - q^{-\frac{S+1}{2}}}{q^{\frac{1}{2}} - q^{-\frac{1}{2}}} \right\} + \left\{ \frac{q^{\frac{1}{2}} + q^{-\frac{1}{2}}}{q^{\frac{1}{2}} - q^{-\frac{1}{2}}} - (S+1) \frac{q^{\frac{S+1}{2}} + q^{-\frac{S+1}{2}}}{q^{\frac{S+1}{2}} - q^{-\frac{S+1}{2}}} \right\} \ln q. \tag{5.62}
\end{aligned}$$

In order to recover previous results for the spin-1 case [97], we have to rescale $q \rightarrow q^2$ in (5.61) and (5.62). This transformation is necessary because of the different definition (5.29) used here for the deformation parameter q .

These entanglement entropies are graphed in (5.5) as functions of the parameter q for the cases $S = 2, 10$. At the isotropic point $q = 1$, the entanglement entropies simplify to

$$S_{\text{R}}(\alpha) = S_{\text{vN}} = 2 \ln(S+1), \quad q = 1. \tag{5.63}$$

We thus recover previous results [26, 98] for isotropic spin- S VBS states. In the limit of full deformation $q \rightarrow 0^+$ the entanglement entropy for any spin S vanishes.

Finally, let us consider the case of very high spin at fixed $0 < q < 1$. Taking the limit $S \rightarrow \infty$ in (5.61) and (5.62) gives

$$S_{\text{R}}(\alpha) = \frac{2}{1-\alpha} \ln \left\{ \frac{(q^{-1/2} - q^{1/2})^\alpha}{q^{-\alpha/2} - q^{\alpha/2}} \right\}, \tag{5.64}$$

$$S_{\text{vN}} = 2 \ln \left(\frac{1}{q^{-1/2} - q^{1/2}} \right) + \left(\frac{q^{1/2} + q^{-1/2}}{q^{1/2} - q^{-1/2}} \right) \ln q, \quad S \rightarrow \infty. \tag{5.65}$$

We find that the entanglement entropy is bounded for any q -deformed AKLT chain of arbitrary spin S . It diverges only at the isotropic point $q = 1$.

5.4 Finite-size corrections

We now look at the case of finite blocks in an infinite chain. The reduced density matrix (5.55) of a block of ℓ spins may be written as

$$\rho_\ell = \rho_\infty + \sum_{j=1}^S \frac{\lambda_j^\ell}{\lambda_0^\ell} \sum_{m=-j}^j \mathbf{Q}_{jm} \otimes \mathbf{Q}_{jm}. \quad (5.66)$$

Finding the eigenvalues of ρ_ℓ thus involves the diagonalization of an $(S+1) \times (S+1)$ matrix with nonzero elements (q -CG coefficients). Let us try right-multiplying the reduced density matrix by a vector with components $(\mathbf{v}_{JM})_{cd} = (-1)^{-(c+d)} q^{(c+d)/2} \begin{bmatrix} S/2 & J & S/2 \\ -c & M & -d \end{bmatrix}_q$. Using the identity (C.7) gives

$$(\rho_\ell \mathbf{v}_{JM})_{ab} = \frac{q^{-2a+M}}{[S+1]^2} \left(1 + \sum_{j=1}^S [2j+1] \frac{\lambda_j^\ell}{\lambda_0^\ell} F_q \left[j \frac{S}{2} \frac{S}{2} J; \frac{S}{2} \frac{S}{2} \right] \right) (\mathbf{v}_{JM})_{ab}. \quad (5.67)$$

For arbitrary q , this equation is not a proper eigenvalue equation because of the factor q^{-2a} . However, we discover that \mathbf{v}_{JM} is an eigenvector of ρ_ℓ for $q = 1$. We treat the isotropic case analytically in (5.4.1). For $0 < q < 1$, we calculate the eigenvalues of ρ_ℓ using first-order perturbation theory and compare this approximation with numerical results in (5.4.2).

5.4.1 Isotropic case

When $q = 1$, making the appropriate substitutions yields the exact $(2J+1)$ -fold degenerate eigenvalues

$$p_{JM} = \frac{1}{(S+1)^2} \left(1 + \sum_{j=1}^S (2j+1) \frac{\lambda_j^\ell}{\lambda_0^\ell} F_1 \left[j \frac{S}{2} \frac{S}{2} J; \frac{S}{2} \frac{S}{2} \right] \right), \quad (5.68)$$

$$= \frac{1}{(S+1)^2} + \frac{(-1)^{J+S}}{S+1} \sum_{j=1}^S (-1)^j (2j+1) \frac{\lambda_j^\ell}{\lambda_0^\ell} \left\{ \begin{matrix} \frac{S}{2} & \frac{S}{2} \\ J & \frac{S}{2} \end{matrix} \right\}_1. \quad (5.69)$$

with $0 \leq J \leq S$ and $M \in \{-J, -J+1, \dots, J\}$. For instance, taking $S = 2$ gives the exact eigenvalues

$$p_{00} = \frac{1}{9} \left(1 + 3(-2)^{-\ell} + 5(10)^{-\ell} \right), \quad (\text{degeneracy } 1), \quad (5.70)$$

$$p_{1M} = \frac{1}{9} \left(1 + \frac{3}{2}(-2)^{-\ell} - \frac{5}{2}(10)^{-\ell} \right), \quad (\text{degeneracy } 3), \quad (5.71)$$

$$p_{2M} = \frac{1}{9} \left(1 - \frac{3}{2}(-2)^{-\ell} + \frac{1}{2}(10)^{-\ell} \right), \quad (\text{degeneracy } 5). \quad (5.72)$$

The formula (5.69) reproduces the results of [26, 98] for undeformed spin- S AKLT chains obtained from the Schwinger boson representation of the VBS state. Our approach, however, emphasizes the role of $6j$ symbols in determining finite-size effects on entanglement in these states. Additionally, this result solves a recursive formula in [26, 98] for the coefficients in the sums for the eigenvalues p_{JM} .

The leading finite-size correction to the eigenvalue p_{JM} is proportional to the exponential factor $(\lambda_1/\lambda_0)^\ell \equiv (-1)^\ell e^{-\ell/\xi}$. Using the formula

$$\left\{ \begin{matrix} S & \frac{S}{2} & \frac{S}{2} \\ j & \frac{S}{2} & \frac{S}{2} \end{matrix} \right\}_1 = \frac{(S!)^2}{(S-j)!(S+j+1)!}, \quad (5.73)$$

gives the characteristic length of decay $\xi = 1/\ln((S+2)/S)$. This length is equal to the correlation length of the spin-spin correlation functions in the spin- S VBS state [92].

Let us construct an effective Hamiltonian for long blocks $1 \ll \ell < \infty$ in the isotropic case. Considering only the leading-order correction to the eigenvalues (5.69) gives

$$p_{JM} \approx \frac{1}{(S+1)^2} \left\{ 1 - \frac{3}{S(S+2)} \left(\frac{-S}{S+2} \right)^\ell (2J(J+1) - S(S+2)) \right\}. \quad (5.74)$$

Since the reduced density matrix is diagonal in the $\{\mathbf{v}_{JM}\}$ basis, we can write the effective Hamiltonian H_e as

$$\begin{aligned} -\beta H_e &\approx \ln \left\{ 1 - \frac{3}{S(S+2)} \left(\frac{-S}{S+2} \right)^\ell (2J(J+1) - S(S+2)) \right\}, \\ &\approx -\frac{12}{S(S+2)} \left(\frac{-S}{S+2} \right)^\ell \times \frac{1}{2} \{ J(J+1) - S(\frac{S}{2} + 1) \}. \end{aligned} \quad (5.75)$$

This expression is valid for $3S^\ell(S+2)^{-\ell} \ll 1$. If we define an undeformed spin- S operator $\mathbf{J} \equiv \mathbf{S}_1 + \mathbf{S}_\ell$ as the sum of two spin- $\frac{S}{2}$ operators \mathbf{S}_1 and \mathbf{S}_ℓ on the block boundaries, we obtain the Heisenberg model

$$\beta H_e = \gamma(S, \ell) (-1)^\ell \mathbf{S}_1 \mathbf{S}_\ell, \quad \gamma(S, \ell) = \frac{12}{S(S+2)} \left(\frac{S}{S+2} \right)^\ell. \quad (5.76)$$

We can identify $T_e = 1/\gamma(S, \ell)$ as an effective temperature that depends on the length of the block. The double scaling limit $\ell \rightarrow \infty$ therefore corresponds to a maximally mixed state (infinite temperature). In this picture, we fur-

then observe that the sign of the coupling strength changes with block length (alternation between ferromagnetic and antiferromagnetic interactions). This implies that the dominant eigenvalue of the reduced density matrix alternates between the p_{00} singlet (even ℓ) and p_{SM} multiplet (odd ℓ).

Let us now consider the entanglement entropy of a block consisting of a single spin ($\ell = 1$) for the case $q = 1$. The eigenvalues of the reduced density matrix may be written as

$$p_{JM}(\ell = 1) = \frac{1}{(S+1)^2} + \frac{(-1)^{J+S}}{\left\{ \begin{smallmatrix} S & S/2 & S/2 \\ 0 & S/2 & S/2 \end{smallmatrix} \right\}_1} \sum_{j=1}^S \frac{2j+1}{S+1} \left\{ \begin{smallmatrix} S & S/2 & S/2 \\ j & S/2 & S/2 \end{smallmatrix} \right\}_1 \left\{ \begin{smallmatrix} j & S/2 & S/2 \\ J & S/2 & S/2 \end{smallmatrix} \right\}_1. \quad (5.77)$$

Making use of the identity (5.73) and

$$\left\{ \begin{smallmatrix} S & S/2 & S/2 \\ 0 & S/2 & S/2 \end{smallmatrix} \right\}_1 \left\{ \begin{smallmatrix} J & S/2 & S/2 \\ 0 & S/2 & S/2 \end{smallmatrix} \right\}_1 = \frac{(-1)^{J+S}}{(S+1)^2}, \quad (5.78)$$

$$\sum_{j=0}^S (2j+1) \left\{ \begin{smallmatrix} S & S/2 & S/2 \\ j & S/2 & S/2 \end{smallmatrix} \right\}_1 \left\{ \begin{smallmatrix} j & S/2 & S/2 \\ J & S/2 & S/2 \end{smallmatrix} \right\}_1 = \frac{\delta_{SJ}}{2S+1}, \quad (5.79)$$

gives the desired result

$$p_{JM}(\ell = 1) = \frac{\delta_{SJ}}{2S+1}, \quad q = 1. \quad (5.80)$$

Thus, the single-site reduced density matrix has $(2S+1)$ nonzero identical eigenvalues. This result proves that the block is a uniform mixture of the $(2S+1)$ states of a single spin- S as expected. The entanglement entropy in this case is $S_R(\alpha) = S_{vN} = \ln(2S+1)$.

For long blocks satisfying $\ell \gg \xi$, the leading nonvanishing correction to the entanglement entropy is proportional to $(\lambda_1/\lambda_0)^{2\ell}$. The approximate Rényi entropy in this case is

$$S_R(\alpha) \approx 2\ln(S+1) - \frac{3\alpha}{2} \left(\frac{S}{S+2} \right)^{2\ell} S(S+1)(S+2). \quad (5.81)$$

Finite-size corrections to the von Neumann entropy can be obtained from this result by taking the limit $\alpha \rightarrow 1$.

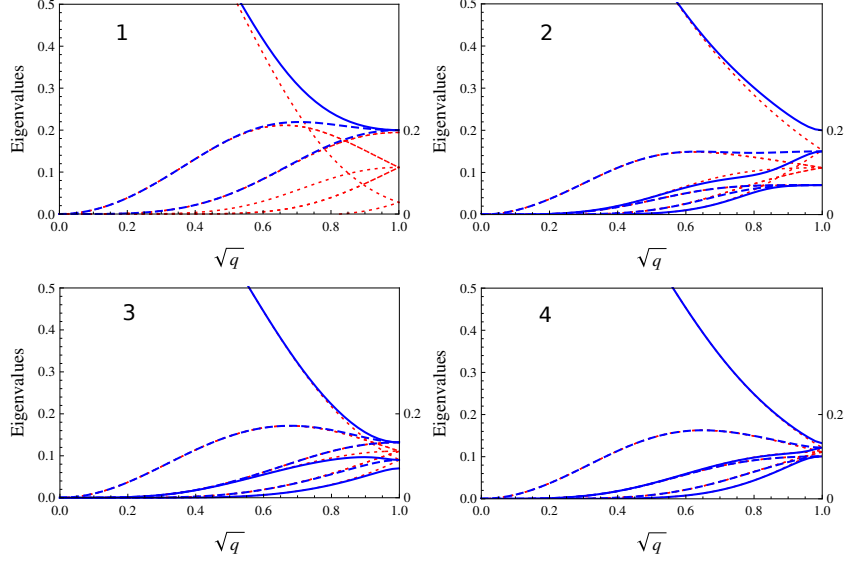


Figure 5.6: The eigenvalues of the reduced density matrix of a block of ℓ spins in a spin-2 VBS $_q$ state (solid and dashed blue lines) are compared to the perturbation result (red dotted lines). Solid blue lines denote nondegenerate eigenvalues while dashed blue lines denote doubly degenerate ones. The dominant eigenvalue approaches unity as $q \rightarrow 0$. For $\ell = 1$ four eigenvalues are zero for all q .

5.4.2 Anisotropic case

For arbitrary values of q , the dominant characteristic length of finite-size corrections generalizes to $\xi = 1/\ln([S+2]/[S])$. That is, we have $|\lambda_1/\lambda_0| = [S]/[S+2] < 1$. For blocks of length $\ell \gg \xi$, we may therefore approximate the reduced density matrix as

$$\rho_\ell \approx \mathbf{Q}_{00} \otimes \mathbf{Q}_{00} + \frac{\lambda_1^\ell}{\lambda_0^\ell} \sum_{m=-1}^1 \mathbf{Q}_{1m} \otimes \mathbf{Q}_{1m}. \quad (5.82)$$

We have already determined that \mathbf{Q}_{00} is diagonal with nondegenerate eigenvalues (5.54). This means that first-order perturbation theory within each sector of the preceding equation involves only the diagonal elements of \mathbf{Q}_{1m} . From (5.54) we know that only \mathbf{Q}_{10} has nonzero diagonal elements and hence we obtain the approximate eigenvalues

$$p_{\mu\nu} = p_{\nu\mu} \approx \frac{q^{-(\mu+\nu)}}{[S+1]^2} \left(1 + [3] \frac{\lambda_1^\ell}{\lambda_0^\ell} \begin{bmatrix} \frac{S}{2} & 1 & \frac{S}{2} \\ \mu & 0 & \mu \end{bmatrix}_q \begin{bmatrix} \frac{S}{2} & 1 & \frac{S}{2} \\ \nu & 0 & \nu \end{bmatrix}_q \right). \quad (5.83)$$

The labels μ and ν are quantum numbers that run from $-\frac{S}{2}$ to $\frac{S}{2}$ with integer steps. The second term in (5.83) involving the q -CG coefficients may be evaluated explicitly with the identity [95]

$$\left[\begin{matrix} \frac{S}{2} & 1 & \frac{S}{2} \\ \mu & 0 & \mu \end{matrix} \right]_q = \frac{q^{-\mu/2}}{\sqrt{[S][S+2]}} \left\{ q^{\frac{1}{2}(1+S/2)} \left[\frac{S}{2} + \mu \right] - q^{-\frac{1}{2}(1+S/2)} \left[\frac{S}{2} - \mu \right] \right\}. \quad (5.84)$$

These approximate eigenvalues are compared to exact numerical results for the spin-2 case in (5.6). We observe a rapid improvement in the accuracy of the perturbation result with increasing block length ℓ . Furthermore, these numerical results reveal how q -deformation modifies the degeneracy of the entanglement spectrum by breaking the multiplet structure present in the isotropic case.

5.5 KSZ model

Using the tools developed before, we can analyze quite easily another model defined by MPS in one dimension. This model is known as the Klümper Schadschneider Zittartz (KSZ) model. The local KSZ Hamiltonian is given by

$$h_{j,j+1} = \alpha_0 A_j^2 + \alpha_1 (A_j B_j + B_j A_j) + \alpha_2 B_j^2 + \alpha_3 A_j + \alpha_4 B_j (1 + B_j) + \alpha_5 [(S_j^z)^2 + (S_{j+1}^z)^2] + \alpha_6, \quad (5.85)$$

with a transverse interaction term $A_j = S_j^x S_{j+1}^x + S_j^y S_{j+1}^y$, longitudinal interaction term $B_j = S_j^z S_{j+1}^z$, and constants α_i . Requiring $h_{j,j+1}$ to have nonnegative eigenvalues and annihilate an MPS ground state $|\text{KSZ}_a\rangle$ leads to a submanifold of Hamiltonians with restrictions on the constants α_i [99]. The correlation functions and low-lying excitations of this model have been studied [99, 100], but its entanglement spectrum has not yet been investigated.

We obtain the MPS form of $|\text{KSZ}_a\rangle$ from the \mathbf{g} matrix

$$\mathbf{g} = \begin{pmatrix} |0\rangle & -\sqrt{a}|+\rangle \\ \sqrt{a}|-\rangle & -\sigma|0\rangle \end{pmatrix}, \quad (5.86)$$

where $a > 0$ is an anisotropy parameter and $\sigma = \text{sign}\alpha_3$. The corresponding transfer matrix is

$$\mathbf{G} = \begin{pmatrix} 1 & 0 & 0 & a \\ 0 & -\sigma & 0 & 0 \\ 0 & 0 & -\sigma & 0 \\ a & 0 & 0 & 1 \end{pmatrix}. \quad (5.87)$$

The unique ground state is $|\text{KSZ}_a\rangle = \text{tr}[\mathbf{g}_1 \cdot \mathbf{g}_2 \cdot \dots \cdot \mathbf{g}_L]$ (periodic boundary conditions). It reduces to the isotropic VBS state at $a = 2$ and $\sigma = 1$.

The eigenvalues of ρ_ℓ for an infinite chain $L \rightarrow \infty$ are

$$\begin{aligned} p_{1,4} &= \frac{1}{4} \left[1 + \left(\frac{1-a}{1+a} \right)^\ell \pm 2 \left(\frac{-\sigma}{1+a} \right)^\ell \right], \\ p_2 = p_3 &= \frac{1}{4} \left[1 - \left(\frac{1-a}{1+a} \right)^\ell \right]. \end{aligned} \quad (5.88)$$

We observe that the entanglement spectrum is the same for $\sigma = \pm 1$. In the double scaling limit the eigenvalues of $\rho_{\ell \rightarrow \infty}$ are four-fold degenerate $p_i^{\ell \rightarrow \infty} = \frac{1}{4}$. The block is maximally entangled with $S_R = \log 4$. The entanglement spectrum therefore corresponds to a four-level system at infinite temperature.

Let us now consider blocks of finite length. The von Neumann entropy is a maximum at the isotropic point $a = 2$. This property is depicted in Fig. (5.2b). For a block of one spin ($\ell = 1$) one eigenvalue of ρ_ℓ vanishes and the maximum entanglement entropy is $\log 3$. In the limit $a \rightarrow 0$, the $|\text{KSZ}_a\rangle$ ground state approaches the transverse ferromagnet $\bigotimes_j |0\rangle_j$. This is a (classical) product state with no entanglement. In the opposite limit $a \rightarrow \infty$ the reduced density matrix represents a uniform mixture of two degenerate Néel ordered states. In this limit the von Neumann entropy approaches $\log 2$.

Finite-size corrections to the eigenvalues (5.88) are exponential in ℓ . The characteristic lengths of these corrections are $\xi_{\parallel} = 1/\ln|(1+a)/(1-a)|$ and $\xi_{\perp} = 1/\ln(1+a)$. These quantities are equal to the longitudinal (ξ_{\parallel}) and transverse (ξ_{\perp}) correlation lengths of the spin-spin correlation functions [99]:

$$\langle S_1^z S_\ell^z \rangle = -\frac{a^2}{(1-a)^2} [\text{sign}(1-a)]^\ell \times e^{-\ell/\xi_{\parallel}}, \quad (5.89)$$

$$\langle S_1^x S_\ell^x \rangle = -a(\sigma+1) [\text{sign}(-\sigma)]^\ell \times e^{-\ell/\xi_{\perp}}, \quad \ell \geq 2. \quad (5.90)$$

5.6 Conclusions

We exactly calculated the reduced density matrix of q -deformed VBS states with arbitrary integer spin- S in the double scaling limit. We discovered that the entanglement spectrum corresponds to a thermal ensemble of two spin- $S/2$'s in a uniform magnetic field. We also derived exact expressions for the Rényi and von Neumann entropies as functions of the deformation parameter q and spin S . We found the exact dependence of entanglement entropy on the q -deformation parameter in the double scaling limit.

Furthermore, we constructed the exact reduced density matrix of finite blocks in an infinite chain. We diagonalized this matrix for the isotropic case

and obtained its exact spectrum in terms of $6j$ symbols. We found that degenerate eigenvalues of the reduced density matrix are grouped into multiplets. An approximate effective Hamiltonian describing this undeformed case consists of two spin- $S/2$'s with a Heisenberg interaction. For arbitrary values of the deformation parameter q , we made approximations for the eigenvalues of the reduced density matrix using first-order perturbation theory. Finally, we numerically investigated the finite block eigenvalue spectrum of the q -deformed spin-2 VBS state. In this case we discovered that q -deformation partially breaks the degeneracy of eigenvalues within each multiplet.

Chapter 6

Bulk-Edge Correspondence of Entanglement Spectrum

So far we have studied one dimensional systems, that in the gapped phase follow an area law which saturates to a constant regardless of the length of the system. This has been reinterpreted in the case of the AKLT model in terms of a boundary Hamiltonian which is local and acts on spin $1/2$ particles located at both ends of the interval. The natural question is then to ask what happens in two dimensions, where correlations along boundary degrees of freedom arise, creating subleading corrections to the area law. In this chapter we attempt to answer this question focusing again in the AKLT model, now in two spatial dimensions, defined in the hexagonal (honeycomb) lattice.

In this chapter we introduce the spin S model in section 6.1, defined on a two dimensional lattice wrapped on a torus and construct its explicit VBS ground state following [101, 102]. Then, we derive an expression for the RDM (also called partial density matrix) ρ_A in section 6.2. This operator is expressed in terms of classical variables in section 6.3. In this representation, the operator can be expanded in different graph contributions of the classical $O(3)$ model as presented in section 6.4. From this expression we identify the Heisenberg Hamiltonian for spin $1/2$ particles in the boundary as the leading term in a sequence of boundary Hamiltonians. Evidence for the structure of the entanglement Hamiltonian is given in section 6.5 based on the analysis in the continuous limit. From Section 6.6 on, we discuss another model based on the partition function of Ising model, where we can see the change of the boundary Hamiltonian across a phase transition.

6.1 Spin S VBS ground state on a two dimensional torus

As discussed on [11, 102, 103] it is possible to construct a valence bond solid (VBS) ground state in a planar graph \mathcal{G} (without edges starting and ending in the same site) in the following way: Given a planar graph \mathcal{G} , consisting of a set of vertices (sites) V and edges E , with z_i edges arriving to vertex i (in graph theoretical language, z_i is called coordination number), we place a local spin S_i on the vertex with the condition $S_i = z_i/2$. The local spin state is constructed from the symmetric subspace of z_i spins $1/2$ (doing this we obtain a higher spin representation of dimension $2S_i + 1$ from $2S_i$ fundamental representations of $SU(2)$). Finally we antisymmetrize between nearest neighbors. Representing the spin $1/2$ constituents of the spin S_i at site i as black dots, using a circle to indicate symmetrization and a bond between antisymmetric neighbors, we obtain a planar graph \mathcal{G}' isomorphic to \mathcal{G} , see Fig 6.1.

The AKLT Hamiltonian for which the VBS state constructed is a ground state is a sum over interactions on all edges E of \mathcal{G} , $H = \sum_{\langle k,l \rangle \in E} H_{kl}(\mathbf{S}_k + \mathbf{S}_l)$, where the Hamiltonian density H_{kl} is

$$H_{kl}(\mathbf{S}_k + \mathbf{S}_l) = \sum_{J=S_k+S_l+1-M_{kl}}^{S_k+S_l} A_{kl}^J \pi_{kl}^J(\mathbf{S}_k + \mathbf{S}_l), \quad (6.1)$$

the coefficients $A_{kl}^J > 0$ are arbitrary and can depend on the edge $\langle k, l \rangle$, while the positive number M_{kl} is the number of bonds (edges) connecting the sites k and l . The operator $\pi_{kl}^J(\mathbf{S}_k + \mathbf{S}_l)$ is a projector of the total spin $\mathbf{J}_{kl} = \mathbf{S}_l + \mathbf{S}_k$ of the edge $\langle k, l \rangle$ on the subspace of spin value J , its explicit form is

$$\pi_{kl}^J(\mathbf{J}_{kl}) = \prod_{j=|S_k-S_l|, j \neq J}^{S_k+S_l} \frac{(\mathbf{J}_{kl})^2 - j(j+1)}{J_{kl}(J_{kl}+1) - j(j+1)}, \quad (6.2)$$

The VBS state is the *unique* ground state of H [66]. While this construction is totally general, in the rest of this discussion we will focus on graphs without boundaries, which can be embedded on a two dimensional torus, with $M_{ij} = 1$ for all edges.

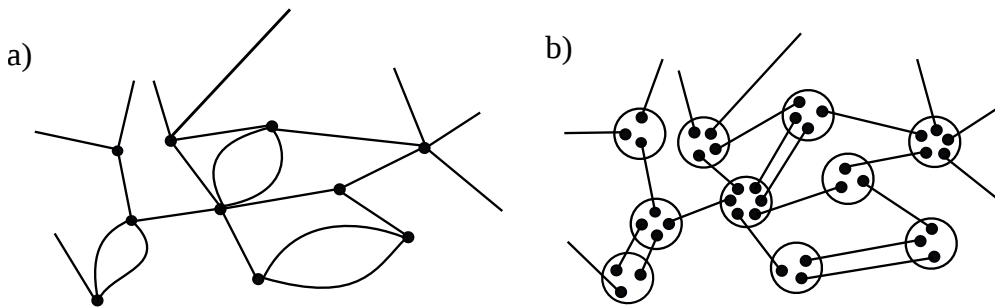


Figure 6.1: a) Original planar graph \mathcal{G} , vertices represented with black dots. b) VBS state on \mathcal{G}' , circles (vertices of \mathcal{G}') represent symmetrization of constituents spin 1/2 (black dots) particles, while bonds represent anti-symmetrization of neighboring spins. Note that any loop in \mathcal{G} would make the associated VBS state vanish, as it would correspond to the antisymmetrization of a state with itself.

6.2 Partial density matrix and Schwinger boson representation of VBS ground state

In this section, we introduce a general way of writing the reduced density matrix of a pure system in terms of overlap matrices. These matrices have elements which correspond to overlap amplitudes between states spanning the ground space of Hamiltonians defined entirely in the subsystems. We apply these results to the VBS case introduced in the previous section.

Using the Schmidt decomposition, any ground state $|\Psi\rangle$ of a system can be written as

$$|\Psi\rangle = \sum_{\alpha} |A_{\alpha}\rangle \otimes |B_{\alpha}\rangle, \quad (6.3)$$

where the states $|A_{\alpha}\rangle$ and $|B_{\alpha}\rangle$ are related to the usual states appearing in the Schmidt decomposition by a scale factor. $|A_{\alpha}\rangle$ and $|B_{\alpha}\rangle$ are states defined in the subsystems A and B , with associated Hilbert spaces \mathcal{H}_A and \mathcal{H}_B respectively. The total system has a Hilbert space $\mathcal{H} = \mathcal{H}_A \cup \mathcal{H}_B$. The set of states $\{|A_{\alpha}\rangle, |B_{\alpha}\rangle\}$ is a complete, linear independent but not orthonormal basis (in principle). The density matrix for this pure state is the projector onto the ground state $\rho = \mathcal{N}|\Psi\rangle\langle\Psi|$, with $\mathcal{N}^{-1} = \langle\Psi|\Psi\rangle$. Tracing out the sites belonging to the subsystem B , we obtain the partial density matrix, which describe the system A , $\rho_A = \text{Tr}_B \rho$. Using (6.37) the partial density matrix becomes $\rho_A = \mathcal{N} \sum_{\alpha\beta} \langle B_{\beta}|B_{\alpha}\rangle |A_{\alpha}\rangle \otimes \langle A_{\beta}|$.

We can write the operator ρ_A as a matrix using the basis $|i\rangle = \sum_{\alpha} U_{i\alpha} |A_{\alpha}\rangle$

and its dual $\langle j| = \sum_{\gamma} V_{j\gamma} \langle A_{\gamma}|$, where U and V are matrices of change of basis and $\langle j|i\rangle = \delta_{ij}$. We have

$$\langle j|\rho_A|i\rangle = (\rho_A)_{ji} = \mathcal{N} \sum_{\alpha\beta\mu\gamma} \langle B_{\beta}|B_{\alpha}\rangle V_{j\gamma} \langle A_{\gamma}|A_{\alpha}\rangle U_{i\mu} \langle A_{\beta}|A_{\mu}\rangle. \quad (6.4)$$

However from the orthonormality condition $\langle j|i\rangle = \delta_{ij}$ follows the relation $\sum_{\gamma} V_{j\gamma} \langle A_{\gamma}|A_{\alpha}\rangle = (U^{-1})_{\alpha j}$ which inserted back in the expression for $(\rho_A)_{ji}$ simplifies it to $\langle j|\rho_A|i\rangle = \mathcal{N} \sum_{\alpha\beta\mu} U_{i\mu} (\langle A_{\mu}|A_{\beta}\rangle)^* \langle B_{\beta}|B_{\alpha}\rangle (U^{-1})_{\alpha j}$. Using this, the partial density matrix can be written as

$$(\rho_A)_{\mu\alpha} = \sum_{\gamma} \frac{\langle (A_{\mu}|A_{\gamma})\rangle^* \langle B_{\gamma}|B_{\alpha}\rangle}{\langle \Psi|\Psi\rangle}. \quad (6.5)$$

From the Schmidt decomposition, we know that the dimension of this operator is the minimum between the dimensions of \mathcal{H}_A and \mathcal{H}_B . Let's assume $\dim \mathcal{H}_A \leq \dim \mathcal{H}_B$. The dimension of ρ_A is then $\dim \mathcal{H}_A \times \dim \mathcal{H}_A$. This matrix is not hermitian in the usual sense $O^{\dagger} = O$, but it is isospectral with $(\rho_A)^{\dagger}$.

Using the Schwinger boson representation for spin operators, the VBS state on \mathcal{G} can be written as [65, 66]

$$|\Psi_{vbs}\rangle = \prod_{\langle i,j\rangle \in E_{\mathcal{G}}} (a_i^{\dagger} b_j^{\dagger} - a_j^{\dagger} b_i^{\dagger}) |0\rangle, \quad (6.6)$$

where $E_{\mathcal{G}}$ is the set of all edges (bonds) of \mathcal{G} and $|0\rangle$ is the state annihilated by all the a_i and b_i operators, i.e. $a_i|0\rangle = b_i|0\rangle = 0, \forall i$. For a generic partition of the system into two subsystems A and B (we assume both of them to be connected regions) with boundaries ∂A and ∂B , we have a collection of vertices V_A, V_B such that $V_A \cup V_B = V_{\mathcal{G}}$ and a collection of edges (bonds) which endpoints live either both in A (B) or one in A and the other in B . For bonds which both endpoints live in A we will say $\langle i,j\rangle \in E_A$ (similarly for B), while for shared bonds with endpoints i and j we use $i \in \partial A, j \in \partial B$. The set of shared bonds we will call it ∂ (and is the same for A and B). Finally the cardinality of a set M is denoted by $|M|$. Using this definitions, we can write the state $|\Psi_{vbs}\rangle$ in the form (6.3) as follows; first we write

$$|\Psi_{vbs}\rangle = \prod_{\substack{\langle i,j\rangle \in \\ E_A \cup E_B}} (a_i^{\dagger} b_j^{\dagger} - a_j^{\dagger} b_i^{\dagger}) \prod_{\substack{i \in \partial A \\ j \in \partial B}} (a_i^{\dagger} a_j^{\dagger} + b_j^{\dagger} b_i^{\dagger}) |0\rangle, \quad (6.7)$$

where we have applied a local basis transformation on the sites (vertices) in

B , $a_i^\dagger \rightarrow -b_i^\dagger$ and $b_j^\dagger \rightarrow a_j^\dagger$ just for later convenience. In the shared bonds, we can assign to an endpoint j of a bond, it's partner in the other end of the bond to be \bar{j} . Doing this we can expand (6.7) in the form [103]

$$\begin{aligned}
|\Psi_{vbs}\rangle &= \sum_{\{\alpha\}} \prod_{i \in \partial} (a_i^\dagger)^{\alpha_i} (b_i^\dagger)^{1-\alpha_i} (a_{\bar{i}}^\dagger)^{\alpha_i} (b_{\bar{i}}^\dagger)^{1-\alpha_i} \\
&\times \prod_{\langle i,j \rangle \in E_A \cup E_B} (a_i^\dagger b_j^\dagger - a_j^\dagger b_i^\dagger) |0\rangle \\
&= \sum_{\{\alpha\}} |A_{\{\alpha\}}\rangle \otimes |B_{\{\alpha\}}\rangle, \tag{6.8}
\end{aligned}$$

here $\{\alpha\} = \{\alpha_1, \alpha_2, \dots, \alpha_{|\partial|}\}$ with $\alpha_i = 0, 1$, labels the different ground states of the subsystems, which span a Hilbert space of dimension $2^{|\partial|}$. The Hamiltonian in subsystem A is defined by $H_A \equiv \sum_{\langle k,l \rangle \in E_A} H_{kl}$ (and similarly for B), with H_{kl} given by (6.1). From (6.8), we can read off the form of the states $|A_{\{\alpha\}}\rangle$

$$|A_{\{\alpha\}}\rangle = \prod_{\langle i,j \rangle \in E_A} (a_i^\dagger b_j^\dagger - a_j^\dagger b_i^\dagger) \prod_{i \in \partial} (b_i^\dagger)^{1-\alpha_i} (a_i^\dagger)^{\alpha_i} |0\rangle, \tag{6.9}$$

using (6.5) and (6.9), we can compute the density matrix ρ_A in terms of the overlap matrices $M_{\{\alpha\},\{\beta\}}^{[A]} = \langle A_{\{\alpha\}} | A_{\{\beta\}} \rangle$. From eq. (6.5), the partial density matrix is constructed gluing together two of these overlap matrices, one for each subsystem, along the boundary of the partition, leaving one index free in each overlap matrix, obtaining a torus with a cut along the partition (see Fig. 6.2).

From this construction, we see that we can write ρ_A as a block diagonal operator, with a nontrivial block of dimension $2^{|\partial|} \times 2^{|\partial|}$, and a trivial block (full of zeros), of dimension $(\dim \mathcal{H}_A - 2^{|\partial|}) \times (\dim \mathcal{H}_A - 2^{|\partial|})$. This result can be understood from the properties of the VBS state. This state is annihilated at each and every site by the action of the Hamiltonian density H_{kl} . After making the partition the states defined in the subsystems are still annihilated by the local Hamiltonians defined in each partition, but the states of the sites at the edges who cross from one subsystem to the other (in our notation, the edges belonging to the set ∂) are free to have any possible state on them, as no local Hamiltonian defined in just one subsystem can act on this edges. This feature has been encountered before in the study of AKLT chains, where the dimension of the partial density matrix does not increase with the size of the system [64].

The computation of this overlap matrix can be mapped to the computation of partition and correlation functions in an $O(3)$ model, by means of the

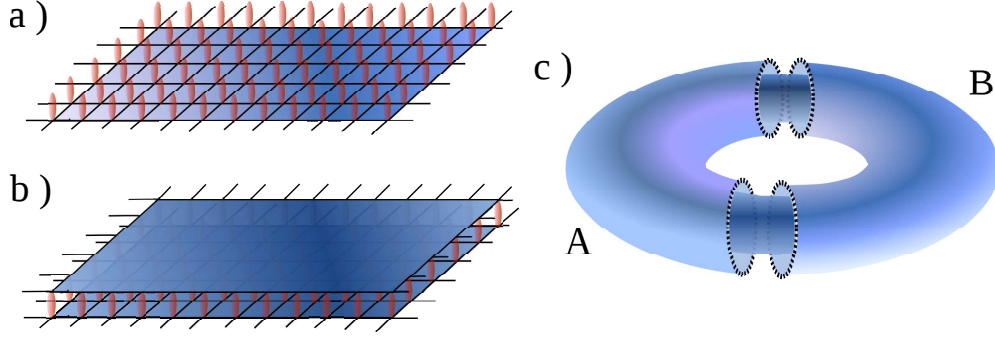


Figure 6.2: a.- The VBS ground state in its tensor product representation can be viewed as a two dimensional lattice build up from contractions of virtual indices (black lines in the plane). The physical indices stick out of the plane. After making the partition, virtual indices at the boundary are free. b.- The overlap matrix $M_{\alpha\beta}^{[A]} = \langle A_\alpha | A_\beta \rangle$ can be obtained by stacking two of this systems and contracting their physical index. This creates a two layer stack. c.- Graphical representation of the partial density matrix ρ_A , for a particular partition. For periodic boundary conditions, the overlap matrix corresponds to a section of the torus with two different, inner and outer, layers. To compute $(\rho_A)_{\alpha\beta}$, we glue the inner layers of the overlap matrices $M^{[A]}$ and $M^{[B]}$ (contracting the virtual indices), obtaining a two layer torus with a cut in the outer sheet along the boundary of the partition. The cut here is represented by the dashed line.

classical representation of the VBS state [65], as we show in the next section.

6.3 Quantum to Classical mapping

Introducing the spinor coordinates

$$\phi_k^a = (u_k, v_k) = \left(e^{i\varphi_k/2} \cos \frac{\theta_k}{2}, e^{-i\varphi_k/2} \sin \frac{\theta_k}{2} \right),$$

at site k , with $\theta \in [0, 2\pi]$, $\varphi_k \in [0, 2\pi)$, we can define the the spin coherent state $|\Omega_k\rangle$ as

$$|\Omega_k\rangle = \frac{(u_k a_k^\dagger + v_k b_k^\dagger)^{2S_k}}{\sqrt{(2S_k)!}} |0_k\rangle, \quad (6.10)$$

($|0_k\rangle$ being the vacuum state at site k), these states are complete but not orthogonal. Inserting the resolution of the identity

$$1_{2S_k+1} = \frac{2S_k+1}{4\pi} \int d\Omega_k |\Omega_k\rangle \langle \Omega_k|, \quad (6.11)$$

in $M_{\{\alpha\}\{\beta\}}^{[A]}$, and using the result $\langle 0|a_k^{S_k-l} b_k^{S_k+l}|\Omega_k\rangle = \sqrt{(2S_k)!} u_k^{S_k-l} v_k^{S_k+l}$, the following form of the overlap matrix is obtained (dropping overall constant factors)

$$M_{\{\alpha\}\{\beta\}}^{[A]} = \int \prod_{i \in A} \frac{d\Omega_i}{4\pi} \prod_{\langle i,j \rangle \in E_A} (1 - \hat{\Omega}_i \cdot \hat{\Omega}_j) \times \prod_{k \in \partial A} (u_k)^{\alpha_k} (v_k)^{1-\alpha_k} (u_k^*)^{\beta_k} (v_k^*)^{1-\beta_k} \quad (6.12)$$

here $\hat{\Omega}_k = (\sin \theta_k \cos \varphi_k, \sin \theta_k \sin \varphi_k, \cos \theta_k)$ is the unit vector over the two dimensional sphere S^2 and u^* is the complex conjugate of u . From (6.12) we see that the overlap matrix $M^{[A]}$ is hermitian, so the partial density matrix $\rho_A = \mathcal{N}(M^{[A]})^* M^{[B]}$ is also hermitian. Using now that $(u_k)^{1-\alpha_k} (v_k)^{\alpha_k} = \phi_k^{\alpha_k}$ (abusing notation, α_k goes from being a power, to become a (supra)index, $\phi_k^0 = u_k, \phi_k^1 = v_k$) and the identity

$$2\phi_k^\alpha (\phi_k^*)^\beta = \delta_{\alpha\beta} + \hat{\Omega}_k \cdot \boldsymbol{\sigma}_{\alpha\beta}, \quad (6.13)$$

where $\delta_{\alpha\beta}$ is the Kronecker delta symbol, and $\boldsymbol{\sigma} = (\sigma_1, \sigma_2, \sigma_3)$ is a vector of Pauli matrices (no distinction is made between upper or lower greek indices); the expression for the overlap matrix can be written as

$$M_{\{\alpha\}\{\beta\}}^{[A]} = \int \prod_{i \in A} \frac{d\Omega_i}{4\pi} \prod_{\langle i,j \rangle \in E_A} (1 - \hat{\Omega}_i \cdot \hat{\Omega}_j) \times \prod_{k \in \partial A} (\mathbb{I} + \hat{\Omega}_k \cdot \boldsymbol{\sigma})_{\alpha_k \beta_k}, \quad (6.14)$$

combining this result with (6.5), the density matrix of the subsystem A becomes

$$\begin{aligned} (\rho_A)_{\{\alpha\}\{\beta\}} &= \frac{1}{Z} \int \prod_{k \in \mathcal{G}} \frac{d\Omega_k}{4\pi} \prod_{\langle i,j \rangle \in E_A \cup E_B} (1 - \hat{\Omega}_i \cdot \hat{\Omega}_j) \\ &\times \prod_{\langle k,l \rangle \in \partial} [(\mathbb{I} + \hat{\Omega}_k \cdot \boldsymbol{\sigma})(\mathbb{I} + \hat{\Omega}_l \cdot \boldsymbol{\sigma})]_{\alpha_k \beta_l}. \end{aligned} \quad (6.15)$$

with Z the proper normalization factor to make $\text{Tr} \rho_A = 1$. We can expand the matrix product inside (6.15) using the product identity for Pauli matrices

$\sigma_i \sigma_j = \delta_{ij} \mathbb{I} + i \epsilon_{ijk} \sigma_k$ (repeated index implies sum) where ϵ_{ijk} is the totally antisymmetric Levi-Civita tensor. The result of the term inside the square bracket in (6.15) is then

$$\begin{aligned} & [(\mathbb{I} + \hat{\Omega}_k \cdot \boldsymbol{\sigma})(\mathbb{I} + \hat{\Omega}_l \cdot \boldsymbol{\sigma})]_{\alpha\beta} \\ & = (1 + \hat{\Omega}_k \cdot \hat{\Omega}_l) \delta_{\alpha\beta} + (\hat{\Omega}_k + \hat{\Omega}_l + i(\hat{\Omega}_k \times \hat{\Omega}_l)) \cdot \boldsymbol{\sigma}_{\alpha\beta}, \end{aligned} \quad (6.16)$$

where $\hat{a} \times \hat{b}$ represent the cross product between vectors \hat{a} and \hat{b} .

6.4 Graph expansion of the density matrix

In this section we derive the structure of the entanglement Hamiltonian as a sequence of spin 1/2 Hamiltonians with increasing interaction length, using the quantum to classical correspondence introduced in the previous section.

From (6.16), two types of expressions can be assigned to each edge on ∂ . We draw an straight line between k and l whenever in that bond we have the expression $(1 + \hat{\Omega}_k \cdot \hat{\Omega}_l) \delta_{\alpha\beta}$, while we put a wiggly line for $(\hat{\Omega}_k + \hat{\Omega}_l + i(\hat{\Omega}_k \times \hat{\Omega}_l)) \cdot \boldsymbol{\sigma}_{\alpha\beta}$. Expanding the product over the boundary in (6.15), we obtain a sum where each term has either a wiggly or straight line corresponding to $\langle k, l \rangle \in \partial$. All the other bonds who don't belong to ∂ have an straight line associated with them.

In general, for a planar graph \mathcal{L} , the expression

$$Z_{O(N)} = \int \prod_{k \in \mathcal{L}} \frac{d\Omega_k}{S_N} \prod_{\langle i, j \rangle \in E_{\mathcal{L}}} (1 + x \hat{\Omega}_i \cdot \hat{\Omega}_j) \quad (6.17)$$

where $\hat{\Omega}$ is an N dimensional unit vector; corresponds to the partition function over \mathcal{L} of the $O(N)$ model [104] which is analogous to a model of overlapping loops. To see this, we use that

$$\int \frac{d\Omega_k}{S_N} \hat{\Omega}_k \cdot \hat{\Omega}_k = 1, \quad \int \frac{d\Omega_k}{S_N} \prod_{i=1}^{odd} (\hat{\Omega}_i \cdot \hat{\Omega}_k) = 0, \quad (6.18)$$

where S_N is the area of the S^{N-1} sphere and the second property follows from the invariance of the integration measure under change $\hat{\Omega}_k \rightarrow -\hat{\Omega}_k$. As the only terms that contribute to $Z_{O(N)}$ are the ones with a product of even $(\hat{\Omega}_i \cdot \hat{\Omega}_k)$ terms at each site of the graph, the whole partition function can be written as [105]

$$Z_{O(N)} = \sum_{\mathcal{C}} w(\zeta, \mathcal{C}) x^{\Gamma(\mathcal{C})} \quad (6.19)$$

with \mathcal{C} a particular configuration of loops of total length $\Gamma(\mathcal{C})$ that can be embedded in the graph \mathcal{L} , and $w(l, \mathcal{C})$ being the corresponding weight associated with a loop ζ and with the particular configuration of loops \mathcal{C} . For example, for the hexagonal lattice (coordination number $z_i = 3$) each site has associated just two bonds, and each integration of a site gives a factor of $\frac{1}{N}$, except the last integration which closes the loop. The partition function is then $Z_{O(N)} = \sum_{\mathcal{C}} \left(\frac{x}{N}\right)^{\Gamma(\mathcal{C})} N^{n(\mathcal{C})}$, with $n(\mathcal{C})$ the number of loops in the configuration \mathcal{C} . The computation of spin correlations $\langle \hat{\Omega}_m \cdot \hat{\Omega}_k \rangle$ corresponds then to the computation of $Z_{O(N)}$, with configurations that allow loops and open paths that begin at site m and end at site k . From (6.15) expanding the product over the partition's boundary we get a sum over different configurations of loops and open strands in the $O(N)$ model, over the graph \mathcal{L} with defects (wiggly lines). In the present case, $x = -1$ and $N = 3$ for the classical partition function of the VBS ground state.

So far we have developed our ideas for general planar graphs with no loops and no more than one bond shared between neighbors ($M_{ij} = 1$), but from now on we will focus the discussion on translation invariant lattices with the previous restrictions. The discussion will remain general for lattices subject to the mentioned restrictions, that can be embedded on a torus. Using translation symmetry, we can expand the product over the boundary in (6.15) in different contributions of translational invariant Hamiltonians along the boundary, with increasing number of non-trivial operators (Pauli matrices) acting on the local Hilbert space associated with a bond. The first term of the expansion correspond to the identity in the $2^{|\partial|}$ -dimensional Hilbert space of the boundary. The second term, which is proportional to a constant external magnetic field acting on the boundary chain, vanish. This follows from the observation that in this term, we have just one wiggly bond placed in the boundary - let's say at bond k with endpoints k and \bar{k} - and the rest are just straight lines, which after integration will generate all the configurations of loops, *and* open lines that start at k , travel through the lattice and end at site \bar{k} (for this type of bonds we will use dashed lines, to indicate the corresponding connection on the lattice). So we will have a term which is proportional to the spin correlation between k and \bar{k} , and an integral of the form (see fig 6.3.a)

$$\int \frac{d\Omega_k}{4\pi} \frac{d\Omega_{\bar{k}}}{4\pi} (\hat{\Omega}_i \cdot \hat{\Omega}_{\bar{k}})^m (\hat{\Omega}_k + \hat{\Omega}_{\bar{k}} + i(\hat{\Omega}_k \times \hat{\Omega}_{\bar{k}})) \cdot \sigma_{\alpha_k \beta_{\bar{k}}},$$

with m odd, which vanish trivially. The next terms in the expansion have two Pauli matrices acting on the different bonds. These terms are proportional to the only $SU(2)$ invariants that can be constructed with two vectors (of Pauli matrices), namely $\boldsymbol{\sigma}_i \cdot \boldsymbol{\sigma}_j$ (see fig 6.3.b). Depending on the separation between the wiggly bonds along the boundary, we have different contributions for which the numerical factor should decay exponentially with this distance, given that the VBS model is expected to have a mass gap (fact that is proven for linear and hexagonal lattices [11]), result which is in agreement with the $O(N)$ model being noncritical for $N > 2$ at $x = -1$ [106].

With the previous results, we can write the following expansion for the density matrix ρ_A


$$\rho_A = \frac{\mathbb{I}}{2^\partial} + \sum_{r,i} A_r \boldsymbol{\sigma}_i \cdot \boldsymbol{\sigma}_{i+r} + \sum_{ijk} A_{ijk} \boldsymbol{\sigma}_i \cdot (\boldsymbol{\sigma}_j \times \boldsymbol{\sigma}_k) + \dots \quad (6.20)$$

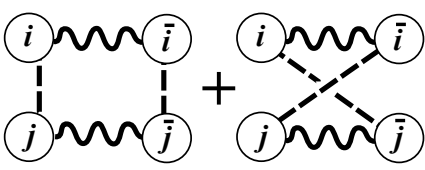
where \mathbb{I} is the $2^\partial \times 2^\partial$ identity operator and the coefficients A_r and A_{ijk} are related to the correlation functions of the $O(N)$ on the lattice \mathcal{L} , with some sites and bonds *erased* along the boundary. Specifically for the first coefficient A_r we have

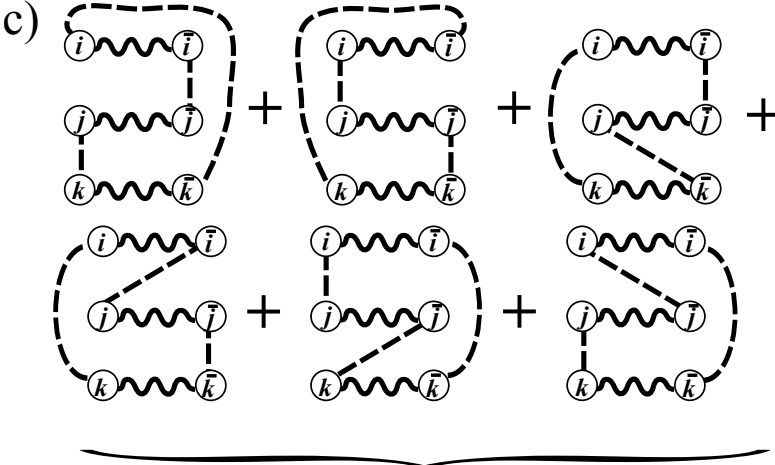
$$A_r \sim \langle (\hat{\Omega}_k \cdot \hat{\Omega}_{k+r})(\hat{\Omega}_{\bar{k}} \cdot \hat{\Omega}_{\bar{k}+r}) \rangle_{\mathcal{L}_k} - \langle (\hat{\Omega}_k \cdot \hat{\Omega}_{\bar{k}+r})(\hat{\Omega}_{\bar{k}} \cdot \hat{\Omega}_{k+r}) \rangle_{\mathcal{L}_k}. \quad (6.21)$$

Here the correlation function is computed over the lattice \mathcal{L}_k which is the same lattice \mathcal{L} but with the bonds $\langle k, \bar{k} \rangle$ and $\langle k+r, \bar{k}+r \rangle$ erased. This relation is exact for hexagonal lattices, while for other lattices with coordination number greater than 3, all the other possible contractions between even number of legs at the boundary sites have to be included. As usual with gapped systems, we expect that this correlation decays exponentially with the separation of the spins, then we have $A_r \sim \exp(-r/\xi_1)$. Numerical studies for two-leg VBS ladders have been performed [16] being in agreement with this general result. For $r = 1$, the second term in (6.21) vanishes in the thermodynamic limit when minimum distance paths joining the sites are cycles who travel the lattice. Also taking the limit of infinite size of the A and B subsystems, the interaction between the two boundary chains along different cuts of the partition vanishes. Then the total density matrix is the tensor product of matrices with the expansion (6.20), for each cut.

It is clear that the first nontrivial term in the expansion (6.20) is the XXX Heisenberg Hamiltonian. We can also determine whether this interaction is ferro or anti-ferromagnetic in the simplest hexagonal lattice, from the loop

a)  } = 0

b)  } ~ \vec{\sigma}_i \cdot \vec{\sigma}_j

c)  + ... +

~ \vec{\sigma}_i \cdot (\vec{\sigma}_j \times \vec{\sigma}_k)

Figure 6.3: First terms in the graph expansion of the RDM ρ_A . For a generic lattice, the number of bonds arriving to a boundary vertex (big circles) can be any even integer, here we show for simplicity the case corresponding to an hexagonal lattice where the number of bonds arriving to a vertex is exactly 2. Dashed lines show the remaining bonds after taking the trace over the whole lattice, except for the boundary vertices joined by wiggly lines.

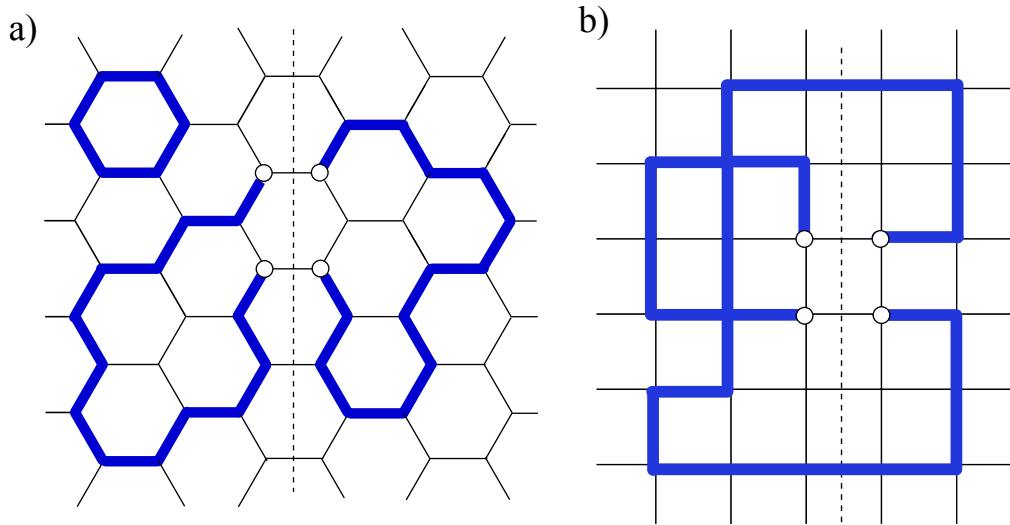


Figure 6.4: a.- Loop contribution to A_1 in the hexagonal lattice. Big circles represent boundary sites, along the partition (dashed line). b. Dashed line represent a partition in the square lattice. The contributions to A_1 consist now of configurations of overlapping loops.

expansion. The structure of the lattice determines the sign of the interaction through the number of bonds that define the allowed paths between site k and site $k + 1$ (each bond has an associated $x = -1$). An overall minus sign comes from the contraction of two wiggly lines. Then it is easy to show that for the hexagonal lattice with a partition like the one in Fig. 6.4.a, all the paths connecting the boundary sites have even number of bonds, then the sign of the boundary XXX Hamiltonian is -1 , so the boundary chain interaction is ferromagnetic. Numerical results [15, 16] in finite size square lattices for a partition like Fig 6.4.b, indicate that in the square grid the interaction is anti-ferromagnetic.

6.5 Continuous limit and Entanglement Hamiltonian

In order to unveil the structure of the entanglement Hamiltonian, we can analyze the partial density matrix (6.15) taking the lattice spacing in the original discrete model to zero, obtaining a continuous version of the model. In this

limit we can show the locality of the boundary (entanglement) Hamiltonian as presented in this section.

Starting from (6.15), using (6.16) we can write

$$(\rho_A)_{\{\alpha\}\{\beta\}} = \frac{1}{Z} \int \prod_{k \in \mathcal{G}} \frac{d\Omega_k}{4\pi} \prod_{\langle i,j \rangle} (1 - \hat{\Omega}_i \cdot \hat{\Omega}_j) \prod_{\langle k,l \rangle \in \partial} [\delta_{\alpha_k \beta_l} + \hat{\Phi}_{kl} \cdot \sigma_{\alpha_k \beta_l}]. \quad (6.22)$$

where $\hat{\Phi}_{kl}$ is a unit vector (with complex components), explicitly given by

$$\hat{\Phi}_{kl} = \frac{\hat{\Omega}_k - \hat{\Omega}_l - i(\hat{\Omega}_k \times \hat{\Omega}_l)}{1 - \hat{\Omega}_k \cdot \hat{\Omega}_l}. \quad (6.23)$$

Note that $\hat{\Phi}_{kl}^2 = 1$. We can write $\hat{\Phi}_{kl}$ in the orthogonal decomposition $\hat{\Omega}_k$ and Ω_{\perp} , with Ω_{\perp} a complex vector of vanishing square. In the continuous limit we drop the contribution from Ω_{\perp} . In this approximation we have

$$\hat{\Phi}_{kl} = \hat{\Omega}_k. \quad (6.24)$$

Putting this result back on (6.15), we obtain a generating function of a $O(3)$ model with a discrete action $\sum_{\langle i,j \rangle} \ln(1 - \hat{\Omega}_i \cdot \hat{\Omega}_j)$ and a spin 1/2 operator localized in the boundary which acts as the current for the generating function. We can study the related $O(N)$ symmetric model with action $-\sum_{\langle i,j \rangle} \hat{\Omega}_i \cdot \hat{\Omega}_j$ which is in the same universality class as (6.17). In this case, the partial density matrix reads

$$\rho_A[\sigma] = \frac{1}{Z} \int \prod_{k \in \mathcal{G}} \frac{d\Omega_k}{4\pi} \exp \left(- \sum_{\langle i,j \rangle} \hat{\Omega}_i \cdot \hat{\Omega}_j + \sum_{k \in \partial} \hat{\Omega}_k \cdot \sigma \right)$$

where $\hat{\Omega}$ is constrained to be a unit vector. In the continuous limit, the reduced density matrix becomes the generating functional of $O(3)$ nonlinear sigma model in Euclidean two dimensional space, with an external current localized at the boundary of A . This Euclidean non-linear sigma model has been well studied [107, 108] and can be solved by standard methods [109]. Here we recall these methods for completeness.

We can impose the unit vector constraint on $\hat{\Omega}$ by introducing an auxiliary field α . In sum, we have

$$\rho_A[\sigma] = \frac{1}{Z} \int \mathcal{D}\Omega \mathcal{D}\alpha \exp \left[-S[\Omega, \alpha] + \int d^2x \Omega \cdot \sigma \right] \quad (6.25)$$

with $\sigma^k(x_1, x_2) = \sigma^k(x_1)(\delta(x_2) + \delta(x_2 - L_A))$, ($k = 1..3$) an spin 1/2 field defined at the boundary of A , which we have placed conveniently at $x_2 = 0$ and $x_2 = L_A$. The action $S[\Omega, \alpha]$ is given by

$$S[\Omega, \alpha] = \frac{1}{2g_0^2} \int d^2x \{ (\nabla \Omega)^2 + i\alpha(x)(\Omega(x)^2 - 1) \}, \quad (6.26)$$

where we have introduced a bare coupling g_0 . As the discussion is essentially the same for any number of components of the Ω field, we now consider the more general N component case with the corresponding $O(N)$ global symmetry. We can integrate out the field Ω , as the action in this field is quadratic, obtaining

$$\rho_A[\sigma] = \frac{1}{Z} \int \mathcal{D}\alpha \exp S, \quad (6.27)$$

with

$$S = -\frac{g_0^2}{2} \int dx dy \sigma^k(x) \Delta^{-1}(x-y) \sigma^k(y) + \frac{i}{2g_0^2} \int d^2x \alpha(x) - \frac{N}{2} \text{tr} \ln \Delta, \quad (6.28)$$

with $\Delta(x) = -\nabla^2 + i\alpha(x)$.

In order to make progress, we now can take the $N \rightarrow \infty$ limit, keeping Ng_0^2 fixed. In this limit, we can evaluate the integral (6.27) by the method of steepest descent. The value of α that minimizes the action is given in the large N limit by $\alpha(x) = -im^2$, with m the solution of the equation

$$\int \frac{d^2k}{(2\pi)^2} \frac{1}{k^2 + m^2} = \lim_{\Lambda \rightarrow \infty} \frac{1}{2\pi} \ln \left(\frac{\Lambda}{m} \right) = \frac{1}{Ng_0^2}. \quad (6.29)$$

This equation is divergent, but can it can be made finite by renormalizing the bare coupling g_0 at an arbitrary renormalization scale M as $\frac{1}{g_0^2} = \frac{1}{g^2} + \frac{N}{2\pi} \ln \left(\frac{\Lambda}{M} \right)$. Inserting this equation back in (6.29), we get the following expression for m in terms of the physical coupling g , the renormalization scale M and the number of components N of the original Ω field,

$$m = M \exp \left[-\frac{2\pi}{g^2 N} \right]. \quad (6.30)$$

In this large N limit, we can compute the Entanglement Hamiltonian as the logarithm of the reduced density matrix, obtaining

$$H_{\text{ent}} = \ln \rho_A[\sigma] = \frac{g^2}{2} \int dx dy \sigma^k(x) \Delta^{-1}(x-y) \sigma^k(y), \quad (6.31)$$

where $\Delta^{-1}(x) = K_0(m|x|)/2\pi$ is the zeroth order modified Bessel function. The exponential decay of $K_0(m|x|)$ for large x is what defines a local interaction at the boundary of A . Although this result is obtained in the large N limit, the general features of the $N = 3$ model are believed to be captured in this limit [110].

6.6 Ising PEPS quantum model

A general method to construct quantum Hamiltonians, and to relate their ground state wavefunctions to classical partition functions was introduced in [111]. This model was also studied in [112] in the context of projected entangled pair states (PEPS), where was shown that the entanglement entropy S_A for a subsystem follows an strict area law bound $S_A \leq |\partial A|$ where $|\partial A|$ is the length of the subsystem's boundary. Also they found a Hamiltonian (Parent Hamiltonian) whose ground state wavefunction is given by the partition function of the Ising model.

For completeness in this section we present explicit results following the methods presented in [111] for a two dimensional square lattice

Given a square lattice Λ , we denote the vertices in Λ by the pair (m, n) with $0 \leq m \leq N_h$ and $0 \leq n \leq N_v$. The total number of vertices in Λ is $N_h N_v$. At each site we introduce a Hilbert space of dimension 2, spanned by the basis $\{|-1\rangle, |1\rangle\}$. The state $|\sigma_i\rangle$ is an eigenstate of the the σ_i^z operator at site $i = (m, n)$, with the natural notation $\sigma_i^z |\sigma_i\rangle = \sigma_i |\sigma_i\rangle$ ($\sigma = \{-1, 1\}$).

We define the following state in the whole lattice (assuming periodic boundary conditions in horizontal and vertical directions)

$$|Z\rangle = \sum_{\{\sigma\}} e^{-\frac{\beta}{2} h(\{\sigma\})} |\{\sigma\}\rangle, \quad (6.32)$$

where $|\{\sigma\}\rangle = \bigotimes_{i \in \Lambda} |\sigma_i\rangle$. The set $\{\sigma\}$ is just the set of all the sigma labels in the lattice $\{\sigma\} = \{\sigma_i\}_{i \in \Lambda}$. This set corresponds to the $2^{N_h N_v}$ possible

configurations of σ variables across the lattice. $h(\{\sigma\})$ denotes the Hamiltonian of the classical Ising model

$$h(\{\sigma\}) = - \sum_{m,n} J_h \sigma_{(m,n)}^z \sigma_{(m+1,n)}^z + J_v \sigma_{(m,n)}^z \sigma_{(m,n+1)}^z.$$

for ferromagnetic interactions ($J_h, J_v \geq 0$).

The state $|Z\rangle$ is the ground state of the following local quantum Hamiltonian, defined in the same square lattice Λ

$$H_Q = \sum_{m,n} e^{(-\sigma_{(m,n)}^z [2K_v(\sigma_{(m,n-1)}^z + \sigma_{(m,n+1)}^z) + 2K_h(\sigma_{(m-1,n)}^z + \sigma_{(m+1,n)}^z)])} - \sigma_{(m,n)}^x, \quad (6.33)$$

this is a local operator, considering that $(\sigma^z)^2 = 1$. Expanding we get

$$\begin{aligned} H &= \sum_{m,n} A_{00} - 2A_{01} \sigma_{(m,n)}^z \sigma_{(m+1,n)}^z - 2A_{10} \sigma_{(m,n)}^z \sigma_{(m,n+1)}^z + A_{02} \sigma_{(m,n-1)}^z \sigma_{(m,n+1)}^z \\ &+ A_{20} \sigma_{(m-1,n)}^z \sigma_{(m+1,n)}^z + A_{11} \sigma_{(m+1,n)}^z \sigma_{(m,n-1)}^z + A_{11} \sigma_{(m+1,n)}^z \sigma_{(m,n+1)}^z \\ &- A_{21} (\sigma_{(m,n)}^z \sigma_{(m+1,n)}^z \sigma_{(m,n-1)}^z \sigma_{(m,n+1)}^z + \sigma_{(m,n)}^z \sigma_{(m-1,n)}^z \sigma_{(m,n-1)}^z \sigma_{(m,n+1)}^z) \\ &- A_{12} (\sigma_{(m,n)}^z \sigma_{(m,n+1)}^z \sigma_{(m-1,n)}^z \sigma_{(m+1,n)}^z + \sigma_{(m,n)}^z \sigma_{(m,n-1)}^z \sigma_{(m-1,n)}^z \sigma_{(m+1,n)}^z) \\ &+ A_{11} (\sigma_{(m-1,n)}^z \sigma_{(m,n-1)}^z + \sigma_{(m-1,n)}^z \sigma_{(m,n+1)}^z) \\ &+ A_{22} \sigma_{(m+1,n)}^z \sigma_{(m,n+1)}^z \sigma_{(m-1,n)}^z \sigma_{(m,n-1)}^z - \sigma_{(m,n)}^x / (\cosh 2K_v \cosh 2K_h)^2 \end{aligned} \quad (6.34)$$

where σ^x, σ^z denotes the usual Pauli matrices, and

$$A_{ij}(\beta) = (\tanh 2K_v)^i (\tanh 2K_h)^j. \quad (6.35)$$

K_h and K_v are given by $K_h = \beta J_h / 2$ and $K_v = \beta J_v / 2$. A graphical depiction of each local interaction term in the Hamiltonian is given in Fig. (6.6)

Given that H_Q is a positive definite operator [111] (for real coupling constants $K_{h,v}$), and $H_Q|Z\rangle = 0$, which can be verified explicitly, we see already that $|Z\rangle$ corresponds to the ground state H_Q .

6.7 Density matrix of a subsystem

We define a bipartition on the lattice Λ (which has the topology of a torus), between regions A and B , such that A and B are topologically equivalent to

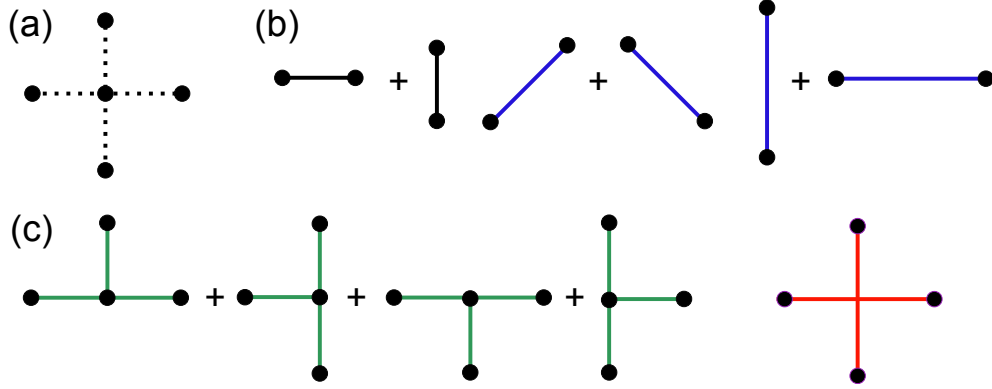


Figure 6.5: Graphical notation for the interaction terms of the Hamiltonian. Sites who interact are connected by bonds. a) Vertex and nearest neighbors in the square lattice. b) Two body interactions. c) Four body interactions. Different colors represent different interaction strengths (for $K_h = K_v$).

cylinders. For definiteness we cut along a line in the vertical direction, crossing N_v links. The boundaries of the regions are ∂A and ∂B respectively. We have the following decomposition of the original ground state $|Z\rangle$

$$|Z\rangle = \sum_{\{\sigma\}} e^{-\frac{\beta}{2}(h_A(\sigma)+h_B(\sigma))} \exp\left(K_h \sum_{\substack{i \in \partial A \\ j \in \partial B}} \sigma_i \sigma_j\right) |\{\sigma\}\rangle. \quad (6.36)$$

Here $h_A(\sigma)$ is the Ising Hamiltonian in the region A (and equivalently for B). The interaction term across the boundary of A and B can be written as a product over the boundary links of $\cosh K_h + \sigma_i \sigma_j \sinh K_h$. Defining $\phi(j)_0 = \sqrt{\cosh K_h}$ and $\phi(j)_1 = \sqrt{\sinh K_h} \sigma_j$ we can write the ground state in the form

$$|Z\rangle = \sum_{\{\alpha\}} |A_{\{\alpha\}}\rangle \otimes |B_{\{\alpha\}}\rangle. \quad (6.37)$$

The set of states in the A subsystem is $|A_{\{\alpha\}}\rangle = \sum_{\{\sigma\}_A} e^{-\frac{\beta}{2}h_A(\sigma)} \prod_{i \in \partial A} \phi(i)_{\alpha_i} |\{\sigma\}_A\rangle$, where the sum is done over the lattice sites in A . Each of these states is labeled by an element of the set $\{\alpha\} = \{\alpha_i\}_{i \in \partial A}$, whose dimension is 2^{N_v} . From [113] the partial density matrix can be written as

$$[\rho_A]_{\mu\alpha} = \sum_{\gamma} \frac{(\langle A_{\mu} | A_{\gamma} \rangle)^* \langle B_{\gamma} | B_{\alpha} \rangle}{\langle Z | Z \rangle}. \quad (6.38)$$

The overall normalization $\langle Z|Z \rangle$ is just the partition function of the Ising model $Z(\beta)$ which is dependent of the horizontal (K_h) and vertical (K_v) couplings. The numerator in (6.38) is the product of overlap matrices for each of the regions. The overlap matrix has the form

$$\langle A_\alpha | A_\beta \rangle = \sum_{\{\sigma\}_A} e^{-\beta h_A(\sigma)} \prod_{i \in \partial A} \left(\frac{e^{K_h \delta_{\alpha_i \beta_i}} + \mathbf{n}_i \cdot \boldsymbol{\tau}_{\alpha_i \beta_i}}{2} \right), \quad (6.39)$$

where $\mathbf{n}_i = (\sqrt{2 \sinh 2K_h} \sigma_i, 0, e^{-K_h})$ is a three dimensional vector, and $\boldsymbol{\tau} = (\tau_1, \tau_2, \tau_3)$ is a vector of Pauli matrices. The partial density matrix reduces to

$$[\rho_A]_{\alpha\beta} = \sum_{\{\sigma\}} \frac{e^{-\beta h(\sigma)}}{Z(\beta)} \prod_{\substack{i \in \partial A \\ j \in \partial B}} \left(\frac{\delta_{\alpha_i \beta_j} + \mathbf{s}_{ij} \cdot \boldsymbol{\tau}_{\alpha_i \beta_j}}{2} \right), \quad (6.40)$$

with

$$\begin{aligned} \mathbf{s}_{ij} &= (\lambda_x(\sigma_i + \sigma_j), -i\lambda_y(\sigma_i - \sigma_j), e^{-2K_h \sigma_i \sigma_j}), \\ \lambda_x(K_h) &= e^{-K_h} \sqrt{\frac{\sinh 2K_h}{2}}, \quad \lambda_y(K_h) = e^{K_h} \sqrt{\frac{\sinh 2K_h}{2}}. \end{aligned}$$

The operator acting across the cut is explicitly given by

$$L_{\alpha_i \beta_j}^{\sigma_i, \sigma_j} = e^{2K_h \sigma_i \sigma_j} (\delta_{\alpha_i \beta_j} + \mathbf{s}_{ij} \cdot \boldsymbol{\tau}_{\alpha_i \beta_j}). \quad (6.41)$$

It corresponds to an operator acting on two different spaces, one being the space where the α index acts, space which we will call quantum space, and the space where the transfer matrix of the classical Ising model acts, which we will call auxiliary space. This nomenclature is borrowed from the study of integrable systems [114] where the construction of the monodromy matrix has a similar structure.

After applying a change of basis uLu^{-1} , with $u = (\tau_1 + \tau_3)$, the matrix L is explicitly given by,

$$\begin{aligned} L &= (v_2^{1/2} \otimes \mathbb{I}) ((\mathbb{I} \otimes (\mathbb{I} + b\tau_1) + J_k \hat{\sigma}^k \otimes \tau_k) (v_2^{1/2} \otimes \mathbb{I}), \\ \text{with } v_2 &= \sqrt{2 \sinh 4K_h} \exp(2K_h^* \hat{\sigma}^x), \\ b &= \frac{e^{-2K_h^*}}{\sqrt{2 \sinh 4K_h}}, \quad e^{-4K_h} = \tanh 2K_h^* \quad \text{and} \end{aligned} \quad (6.42)$$

$$\mathbf{J} = \left(\frac{e^{-2K_h^*}}{\sqrt{2 \sinh 4K_h}}, \frac{-e^{-K_h}}{\sqrt{2 \cosh 2K_h}}, \frac{e^{K_h}}{\sqrt{2 \cosh 2K_h}} \right), \quad (6.43)$$

(sum implied over repeated indices). Here the first space in the tensor product is the auxiliary space Γ , while the second is the quantum space Q . The matrix \mathbb{I} is the 2×2 identity in each space. The matrices $\hat{\sigma}_{1,2,3}$ are the usual Pauli matrices.

The partial density matrix has then the following structure

$$\rho = (2^{2N_v} Z(K_h, K_v))^{-1} \text{Tr}_\Gamma (\mathbf{T}^{N_A} \mathbf{L} \mathbf{T}^{N_B} \mathbf{L}), \quad (6.44)$$

with \mathbf{T} the tensor product of the identity matrix in the quantum space Q , of dimension $2^{N_v} \times 2^{N_v}$ with the transfer matrix of the Ising model, T which has the same dimension. \mathbf{L} is the tensor product along the boundary of the L matrices, explicitly $\mathbf{L}_{\alpha,\beta}^{\sigma,\sigma'} = \prod_{ij} L_{\alpha_i\beta_j}^{\sigma_i\sigma_j}$ and has dimension $2^{2N_v} \times 2^{2N_v}$. The reduced density matrix is obtained tracing out the auxiliary space. Writing (6.44) we have assumed for the two subsystems A and B to be cylinders of circumference N_v and length N_h^A and N_h^B , with $N_h^A + N_h^B = N_h$ and $N_v(N_v^A + N_v^B)$ the total number of sites. In the thermodynamic limit, the Ising transfer matrix becomes a projector on the eigenspace associated with the maximum eigenvalue, multiplied by that eigenvalue so we can write in that limit $\rho_A = 2^{-2N_v} \langle e_0 | \mathbf{L} | e_0 \rangle \langle e_0 | \mathbf{L} | e_0 \rangle$, where $|e_0\rangle$ is the eigenvector corresponding to the maximum eigenvalue of T . As expected, the density matrix factorizes in two density matrices, one for each boundary, so we can study the spectrum of ρ_A just looking at one boundary, so from now on we concentrate our efforts in

$$\rho'_A = 2^{-N_v} \langle e_0 | \mathbf{L} | e_0 \rangle, \quad (6.45)$$

which is an operator of dimension $2^{N_v} \times 2^{N_v}$.

6.8 Expansion of ρ_A

Using (6.45) we can find a series expansion for ρ_A in terms of correlation functions of the XY model with magnetic field as follows.

The symmetric transfer matrix of the classical Ising model (6.33) defined on Γ is given by [115, 116]

$$\begin{aligned}
T &= V_2^{1/2} V_1 V_2^{1/2}, \quad V_1 = \exp\left(\sum_{i=1}^{N_v} 2K_h \hat{\sigma}_i^z \hat{\sigma}_{i+1}^z\right), \\
V_2 &= (2 \sinh 4K_h)^{N_v/2} e^{2K_h^* \sum_{i=1}^{N_v} \hat{\sigma}_i^x}.
\end{aligned} \tag{6.46}$$

The transfer matrix T adds one column to the Ising partition function $Z(K_v, K_h)$. The partition function (for periodic boundary conditions) can then be constructed by taking the trace of T^{N_h} . The transfer matrix (6.46) commutes with the Hamiltonian of the one dimensional XY model with magnetic field [116]. This Hamiltonian is explicitly given by

$$H_{XY} = - \sum_{j=1}^{N_v} \frac{1+\gamma}{2} \sigma_j^z \sigma_{j+1}^z + \frac{1-\gamma}{2} \sigma_j^y \sigma_{j+1}^y + h \sigma_j^x, \tag{6.47}$$

where the interaction constant γ and the magnetic field h are related with the original couplings in the classical Ising model by

$$\begin{aligned}
\gamma &= \frac{1}{\cosh 4K_h^*} \quad \text{and} \quad h = \frac{\tanh 4K_h^*}{\tanh 4K_v}, \\
\text{with} \quad &\sinh 4K_h \sinh 4K_h^* = 1.
\end{aligned} \tag{6.48}$$

This Hamiltonian is related with the usual XY Hamiltonian by the canonical transformation $(\sigma_x, \sigma_z) \rightarrow (\sigma_z, -\sigma_x)$.

The vector $|e_0\rangle$ in (6.45) denotes the eigenvector of T with the maximum eigenvalue. As T and H_{XY} commute, they share the same eigenvectors. It was shown in [116] that the eigenvector associated with the maximum eigenvalue corresponds to the ground state of H_{XY} which we call $|0_{XY}\rangle$. The XY Hamiltonian can be diagonalized essentially by a Jordan Wigner transformation, followed by Bogoliubov transformation in momentum space (for more details see [117]), rendering the model solvable.

In order to use the results available for the XY model, we use the expression for the operator L introduced in (6.42), which is given in terms of the observable operators in the XY model. From expression (6.45) we have

$$\rho'_A = \left\langle 0_{XY} \left| \prod_{i=0}^{N_v} \frac{\mathbb{I}^{(i)} \otimes (\mathbb{I}^{(i)} + b\tau_1^{(i)}) + J_k \hat{\sigma}_{(i)}^k \otimes \tau_k^{(i)}}{2} \right| 0_{XY} \right\rangle. \tag{6.49}$$

6.9 Small and High β expansion

6.9.1 $\beta \rightarrow \infty$ limit

We can study the $K_h \rightarrow \infty$ limit of the partial density matrix from (6.49), using the ground state associated with the XY Hamiltonian in this regime, which is just the one dimensional cat state

$$|0_{XY}\rangle_\infty = \frac{1}{\sqrt{2}} \left(\bigotimes_{i \in \partial A} |\uparrow_i\rangle + \bigotimes_{i \in \partial A} |\downarrow_i\rangle \right), \quad (6.50)$$

For $x = e^{-4K_h} \ll 1/\sqrt{N_v}$ the Hamiltonian (6.47) becomes

$$H_{XY} \approx - \sum_{j=1}^{N_v} (1 - x^2) \sigma_j^z \sigma_{j+1}^z + x^2 \sigma_j^y \sigma_{j+1}^y + 2x \sigma_j^x. \quad (6.51)$$

The unperturbed Hamiltonian $H_0 = H_{XY}(x=0)$ corresponds to the usual one dimensional Ising model. Using first order perturbation theory, the ground state of (6.51) is

$$|0_{XY}\rangle_x = |0_{XY}\rangle_\infty + \frac{x}{2} \sum_{i=1}^{N_v} |\uparrow\downarrow_i \dots \uparrow\rangle + |\downarrow\uparrow_i \dots \downarrow\rangle,$$

, where we have choose one particular ferromagnetic ground state.

To write down the expression for ρ'_A in this limit, we need to introduce some notation. The projector operators $Z_\pm^{(i)}$ acting on the site i in the quantum space Q and are defined by

$$Z_\pm^{(i)} = \frac{1^{(i)} \pm \tau_3^{(i)}}{2}. \quad (6.52)$$

These operators project on the eigenstates of τ_3 . The operator Z_\pm corresponds to the product of $Z_\pm^{(i)}$ over all sites in Q . The operator $Z_a^{[i]} = \prod_{j \neq i} Z_a^{(j)}$, acts as a projector on all the sites along the chain different from site i . In general, the sites where the projector doesn't act will be denoted in the square bracket. It turns out that just with the first order perturbation in the state, we can obtain the expansion for ρ'_a up to order x^2 . The density matrix ρ'_A is then (for $x \ll 1$, $a = \{+, -\}$)

$$\begin{aligned}
\rho'_A &= \frac{1}{2} \sum_a \left(\left(1 - \frac{x^2 N_v}{4} \right) \mathbb{Z}_a + \sum_{i=1}^{N_v} \mathbb{Z}_a^{[i]} \left[\frac{x}{2} \tau_1^{(i)} - a \left(\frac{x}{4} - \frac{3x^2}{16} \right) \tau_3^{(i)} \right] \right) \\
&+ \frac{1}{2} \sum_a \left(\frac{x^2}{4} \sum_{j>i}^{N_v} \mathbb{Z}_a^{[i,j]} \left[\tau_1^{(i)} \tau_1^{(j)} + \frac{1}{4} \tau_3^{(i)} \tau_3^{(j)} \right] \right) \\
&+ \frac{1}{2} \sum_a \left(\frac{x^2}{4} \sum_i \mathbb{Z}_a^{[i]} \mathbb{Z}_{-a}^{(i)} - a \frac{x^2}{8} \sum_{i \neq j} \mathbb{Z}_a^{[i,j]} \tau_3^{(i)} \tau_1^{(j)} \right). \tag{6.53}
\end{aligned}$$

This operator is explicitly Z_2 symmetric. We now concentrate in the excitations respect to just one ferromagnetic ground state for simplicity.

The operator (6.53) (acting now in the quantum space Q) is block diagonal with respect to the states of definite momentum and particle number,

$$\begin{aligned}
|0; 0\rangle &= |\uparrow \uparrow \dots \uparrow\rangle, \\
|1; p\rangle &= \sum_{j=1}^{N_v} e^{ipj} |\downarrow_j\rangle, \\
|2; p_1, p_2\rangle &= \frac{1}{2} \sum_{j \neq k}^{N_v} e^{ip_1 j} e^{ip_2 k} |\downarrow_j \dots \downarrow_k\rangle,
\end{aligned} \tag{6.54}$$

where $\{|\uparrow\rangle, |\downarrow\rangle\}$ correspond to the eigenstates of τ_3 , namely $\tau_3|\uparrow\rangle = |\uparrow\rangle$ and $\tau_3|\downarrow\rangle = -|\downarrow\rangle$. The state $|\downarrow_k\rangle$, indicates a spin flip from the completely magnetized state at position k . From the Z_2 symmetry of the model ρ'_A is also block diagonal respect to corresponding excitations around the other completely magnetized state $|\downarrow \downarrow \dots \downarrow\rangle$.

Up to first order in x , the density matrix can be written as

$$\rho'_A = \mathcal{N} e^{\frac{x}{2} \sum_i \tau_1^{(i)}} \exp \left(-\frac{1}{4} \sum_{i=1}^{N_v} \left[\left| \ln \frac{x}{4} \right| + x \right] \tau_3^{(i)} \tau_3^{(i+1)} \right) e^{\frac{x}{2} \sum_i \tau_1^{(i)}} \tag{6.55}$$

with normalization constant $\mathcal{N} = \exp\left(\frac{N_v}{4} \left| \ln \frac{x}{4} \right| \right)$.

6.9.2 $\beta \rightarrow 0$ limit

In the limit $\epsilon = e^{-4K_h^*} \ll 1$, the Hamiltonian (6.47) becomes

$$H_{XY} \approx - \sum_{j=1}^{N_v} \sigma_j^x + \epsilon((1 + 4\epsilon)\sigma_j^z \sigma_{j+1}^z + (1 - 4\epsilon)\sigma_j^y \sigma_{j+1}^y). \quad (6.56)$$

The ground state is given by the product state

$$|0_{XY}\rangle_0 = \bigotimes_{i \in \partial A} \frac{|\uparrow_i\rangle + |\downarrow_i\rangle}{\sqrt{2}} = \bigotimes_{i \in \partial A} |+_i\rangle, \quad (6.57)$$

this state does not receive corrections in first order (in ϵ) perturbation theory.

The expansion of ρ'_A is then

$$\rho'_A = \mathbb{X}_+ - \frac{\epsilon}{2} \sum_{i=1}^{N_v} \mathbb{X}_+^{[i]} \tau_1^{(i)} + O(\epsilon^2), \quad (6.58)$$

where the operators \mathbb{X} are defined in analogy with the \mathbb{Z} operators, but using the local projector onto the eigenstates of τ_1 , i.e

$$X_{\pm}^{(i)} = \frac{1^{(i)} \pm \tau_1^{(i)}}{2}. \quad (6.59)$$

To first order in ϵ , the density matrix (6.58) can be put in the exponential form

$$\rho'_A = \exp\left(-\left|\ln\left(\frac{\epsilon}{2}\right)\right| \sum_{i=1}^{N_v} X_-^{(i)} + N_v \epsilon\right) + O(\epsilon^2) \quad (6.60)$$

6.10 Entanglement Hamiltonian

In this section, we will analyze the structure of Entanglement Hamiltonian, which is basically the logarithm of the partial density matrix i.e $H_{ent} = \ln \rho_A$. In order to compute this operator, we start from the expression (6.49). Expanding the product in (6.49) we have

$$\rho'_A = \frac{1}{2^{N_v}} \left\langle 0_{XY} \left| \mathbf{1} + \sum_{i=1}^{N_v} M_i + \frac{1}{2} \sum_{i_1 \neq i_2} M_{i_1} M_{i_2} + \frac{1}{3!} \sum_{i_1 \neq i_2 \neq i_3} M_{i_1} M_{i_2} M_{i_3} \dots \right| 0_{XY} \right\rangle, \quad (6.61)$$

here $\mathbf{1}$ is the identity in $\Gamma \otimes Q$ and M_i is an operator acting trivially everywhere except at site i , where it acts as

$$M_i = J_1 \mathbb{I}_{(i)} \otimes \tau_1^{(i)} + J_k \hat{\sigma}_{(i)}^k \otimes \tau_k^{(i)}. \quad (6.62)$$

Taking the expectation values in the ground state of XY model, we are left with

$$\rho'_A = \frac{1}{2^{N_v}} \left(\mathbf{1}_Q + \sum_{i=1}^{N_v} \langle M_i \rangle + \frac{1}{2} \sum_{i_1 \neq i_2} \langle M_{i_1} M_{i_2} \rangle + \frac{1}{3!} \sum_{i_1 \neq i_2 \neq i_3} \langle M_{i_1} M_{i_2} M_{i_3} \rangle + \dots \right). \quad (6.63)$$

The operator $\mathbf{1}_Q$ is the unit operator in Q . The operators $\langle M_{i_1} M_{i_2} \dots M_{i_n} \rangle$ are n body operators in the quantum space Q . For example

$$\langle M_i \rangle = J_k \langle \hat{\sigma}_{(i)}^k \rangle \tau_k^{(i)} + J_1 \tau_1^{(i)} = J_1 (1 + \langle \hat{\sigma}^x \rangle) \tau_1^{(i)}, \quad (6.64)$$

$$\begin{aligned} \langle M_i M_j \rangle &= \langle (J_1 \mathbb{I}_{(i)} \otimes \tau_1^{(i)} + J_k \hat{\sigma}_{(i)}^k \otimes \tau_k^{(i)}) (J_1 \mathbb{I}_{(j)} \otimes \tau_1^{(j)} + J_k \hat{\sigma}_{(j)}^k \otimes \tau_k^{(j)}) \rangle. \\ &= J_1^2 (1 + 2 \langle \hat{\sigma}^x \rangle) \tau_1^{(i)} \tau_1^{(j)} + J_a^2 \langle \hat{\sigma}_{(i)}^a \hat{\sigma}_{(j)}^a \rangle \tau_a^{(i)} \tau_a^{(j)}. \end{aligned} \quad (6.65)$$

where we have used the translation symmetry to define $\langle \hat{\sigma}_{(i)}^x \rangle \equiv \langle \hat{\sigma}^x \rangle$ and the symmetry of the ground state correlation functions for the XY model $\langle \hat{\sigma}^{z,y} \rangle = 0$, $\langle \hat{\sigma}_{(i)}^a \hat{\sigma}_{(j)}^b \rangle \sim \delta^{ab}$.

To have a control on the different interaction terms, we add a parameter λ^p in front of each operator acting nontrivially in p sites. We recover the original expression for ρ'_A with $\lambda = 1$. Taking the logarithm of (6.63) in a series expansion, we obtain

$$\begin{aligned} \ln(\rho'_A) &= - \sum_n \frac{1}{n} (1 - \rho'_A)^n \\ &= \sum_{n=1}^{\infty} \frac{-(-1)^n}{n} \left(\lambda \sum_{i=1}^{N_v} \langle M_i \rangle + \frac{\lambda^2}{2} \sum_{i_1 \neq i_2} \langle M_{i_1} M_{i_2} \rangle + \frac{\lambda^3}{3!} \sum_{i_1 \neq i_2 \neq i_3} \langle M_{i_1} M_{i_2} M_{i_3} \rangle + \dots \right)^n \\ &= \lambda \sum_{i=1}^{N_v} \langle M_i \rangle + \frac{\lambda^2}{2} \left(\sum_{i_1 \neq i_2} \langle M_{i_1} M_{i_2} \rangle - \sum_{i_1, i_2} \langle M_{i_1} \rangle \langle M_{i_2} \rangle \right) + \dots \\ &= \lambda \sum_{i=1}^{N_v} h_\sigma \tau_1^{(i)} + \frac{\lambda^2}{2} \sum_{i_1 \neq i_2} J_a^2 G^a(i_1 - i_2) \tau_a^{(i_1)} \tau_a^{(i_2)} + O(\lambda^3) \end{aligned} \quad (6.66)$$

where h_σ and $G^a(i - j)$ are given by

$$h_\sigma = J_1(1 + \langle \hat{\sigma}^x \rangle), \quad \text{and} \quad G^a(i-j) = \langle \hat{\sigma}_{(i)}^a \hat{\sigma}_{(j)}^a \rangle_c = \langle \hat{\sigma}_{(i)}^a \hat{\sigma}_{(j)}^a \rangle - \langle \hat{\sigma}_{(i)}^a \rangle \langle \hat{\sigma}_{(j)}^a \rangle \quad (6.67)$$

The expectation value $\langle \cdot \rangle_c$ denotes the connected correlation function in the XY model ground state. Higher order terms cannot be in principle discarded as λ is not an expansion parameter ($\lambda = 1$). Nevertheless, n -body interaction terms in (6.66) are proportional to J_a^n . Then (6.66) can be thought as a perturbative expansion in terms of J_a (see Fig 6.6).

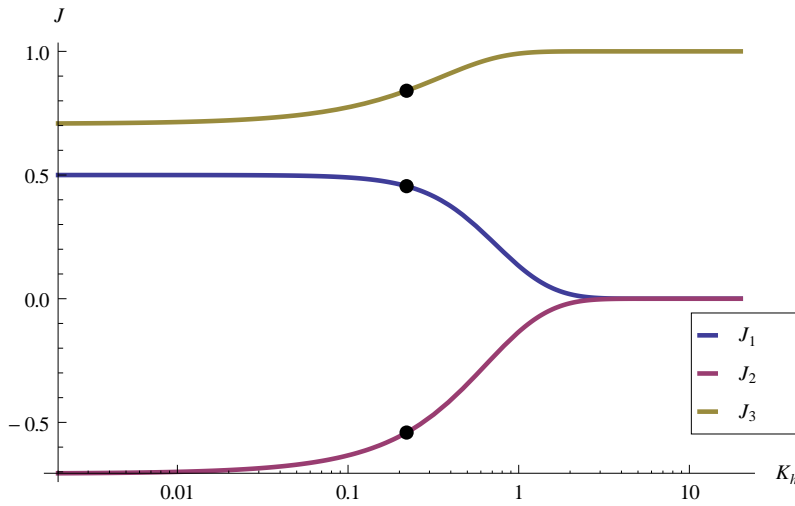


Figure 6.6: J_1, J_2 and J_3 couplings as function of K_h . The black dots corresponds to the value of the couplings at the critical $(K_h)_{crit} = \frac{\ln(1+\sqrt{2})}{4}$, where the correlations in the groundstate become long range. In the large K_h limit, the entanglement Hamiltonian is well approximated by the an Ising type Hamiltonian.

6.11 Discussion

2D VBS state

Given the structure of the VBS ground state, it is possible to define on any planar graph, without loops, a VBS state, where the local spin at site i is given by $z_i/2$, with z_i the coordination number at site i . Using the Schwinger

boson representation of the VBS ground state and the classical variable representation of this state, an expression for the partial density matrix ρ_A , which describe the physical subsystem A , obtained by partitioning the whole unique ground state, can be written. This expression for ρ_A decompose into a classical loop expansion of the $O(3)$ model in the gapped phase. Analyzing the different loop contributions, and assuming translation invariance, we have shown that the partial density matrix that describes a subsystem of the VBS ground state can be expressed as a sum over different rotation-invariant quantum operators, where the Heisenberg interaction between nearest neighbors gives the largest nontrivial contribution to the expansion. This quantum operators act on a spin 1/2 chain in the boundary of the partition. The translational invariance assures us that the different contributions along the boundary are equally weighted, so the boundary operator is given by the XXX Heisenberg Hamiltonian. Here we discuss the case of translation invariant lattices which can be embedded in a torus, but for other lattices with different topologies we expect similar results.

For non translational invariant lattices, the first nontrivial local interaction term is expected to be also of the type $\sigma_i \cdot \sigma_{i+1}$ but the Hamiltonian along the boundary will have different numerical prefactors for each local Heisenberg interactions, generating a non invariant Heisenberg Hamiltonian in the boundary.

In the continuous limit, we show that the entanglement Hamiltonian for this model is actually a local Hamiltonian, where the Hamiltonian density corresponds to a Heisenberg interaction of spin 1/2 particles.

The analysis shown in this chapter should be useful for studying other dimensions $d > 2$ or other two dimensional lattices with more than one bond between a pair of sites. In that case, the local dimension of the spin operators in the boundary Hamiltonian should increase, having then boundary chains with higher representations of $SU(2)$ per site, but still with $SU(2)$ invariant local interactions.

Ising Peps

Using the ideas presented in the VBS case is it possible to construct a state whose wavefunction correspond to the partition function of a classical model, the two dimensional Ising model in the square lattice. As is it well known, the classical Ising model in the square lattice has a phase transition from an order to a disorder phase at a critical temperature T_c . In one and two dimensions, quantum systems do not have a phase transition at finite non zero temperature, as the long range fluctuations (small momentum), destroy any possible order (this is known as the Mermin-Wagner theorem). The phase

transition in the classical side, translates then to a phase transition at zero temperature, where now the parameter that plays the role of the temperature in the classical model is a parameter that appears in the Hamiltonian, then driving in the quantum side a quantum phase transition at zero temperature. At zero temperature the system resides in its ground state, and the different phases correspond to different ground state properties. This is the natural scenario to study the change in the boundary Hamiltonian through a phase transition. We found that when the ground state is gapped, so the correlations functions decay exponentially, the boundary Hamiltonian is well approximated by a local spin 1/2 model at the boundary. This model remains short range in the gapped phase of the two dimensional ground state, but becomes long range at the critical point. At one side of the critical point ($\beta \gg 1$) the boundary Hamiltonian corresponds to the Ising model in transfer field, where the transfer field is a small perturbation to the Ising term. At the other side, ($\beta \ll 1$) the transfer field dominates. At intermediate values of β the situation is less clear at the moment, and more analysis has to be done.

Chapter 7

Conclusion

In this thesis we have explored some of the most recent ideas and applications related with entanglement in many body systems. We have concentrated in short range entangled states. This type of states have the characteristic that are entangled states which are in some sense close to a product state (which does not have entanglement). Here by close we mean that exist a quantum circuit, i.e. a set of unitary operations (gates) that can be applied locally to the state, that transform it to a product state. If we allow for any type of circuit, then we can more or less map anything into anything, so some restrictions on the depth of this circuit (how many layers of operations) is imposed. This construction is clear from the PEPS perspective, as it gives actually a prescription to construct the state from entangled pairs, which also can be created using two qubit gates acting on product states.

This short range entangled states follow an area law for the entanglement entropy of a subsystem. This entropy can be thought as the thermal entropy of an effective system of one dimension lower living on the edge of the partition. This correspondence is known as the Bulk-Edge correspondence. We have explored this correspondence in one and two dimensions for some analytically tractable MPS states. We found that for the AKLT case, although the model is described by spin $z/2$ particles (z is the coordination number of the graph), the boundary Hamiltonian corresponds to a spin $1/2$ (regardless of z), that inherits the rotational invariance of the original model. The model at the boundary is short ranged, and this short range interaction comes from the fact that is mediated through correlation functions in the bulk. This make the evident the question, what happens when the system undergoes a phase transition?. A naive answer would be that due to the vanishing mass gap at the transition, the boundary model becomes long ranged. We explore and confirmed this intuition studying a model with a quantum phase transition (of Landau type). This model is known as Ising PEPS and has a ground state

function given by the classical partition function of the Ising model in two dimensions. The transition in temperature in the classical model becomes a quantum phase transition, where the temperature enters as a parameter in the quantum Hamiltonian. This parameter controls the strength of an Ising type interaction relative to the transverse field.

Although in this work we have explored the case of Tensor networks states with the minimum bond dimension ($D = 2$), in one and two dimensions, this ideas can be applied to more general states, where we expect that the boundary Hamiltonians would be in general now Hamiltonians of higher symmetry groups, not just $SU(2)$ but in general could be decomposed in operators acting on irreducible subgroups of $GL(N)$, the general lineal group of dimension N , where N would be proportional to the bond dimension of the state construction.

Another interesting point to future analysis is the decomposition of bulk operators in terms of boundary operators. If such a decomposition exist and can be implemented efficiently, the bulk boundary description would be complete. The existence of this description is important from practical and philosophical points of view. In the practical side, such a description implies a drastic reduction in the effective Hilbert space for the description of bipartite entanglement as is is not necessary to simulate all degrees of freedom in the bulk, but just those living in the boundary. On the phylosphical point of view, it is interesting to think that the physics in the bulk can be encoded in a description at the boundary. This idea is not new in physics, in high energy physics appears as the Holographic principle [118]. Maybe, remembering Plato's *allegory of the cave*, we are in no better position than the prisoners obliged to stare at the white wall trying to make sense of the physical world.

Bibliography

- [1] E. Schrödinger. Die gegenwärtige Situation in der Quantenmechanik. *Naturwissenschaften*, 23:823–828, 1935.
- [2] M. A. Nielsen and I. Chuang. *Quantum Computation and Quantum Communication*. Cambridge University Press, Cambridge, 2000.
- [3] Luigi Amico, Rosario Fazio, Andreas Osterloh, and Vlatko Vedral. Entanglement in many-body systems. *Rev. Mod. Phys.*, 80:517–576, 2008.
- [4] J. Eisert, M. Cramer, and M. B. Plenio. Colloquium : Area laws for the entanglement entropy. *Rev. Mod. Phys.*, 82:277–306, 2010.
- [5] A. Einstein, B. Podolsky, and N. Rosen. Can Quantum-Mechanical Description of Physical Reality Be Considered Complete? *Phys. Rev.*, 47: 777–80, 1935.
- [6] J. S. Bell. On the Einstein Podolsky Rosen Paradox. *Physics*, 1(3): 195–200, (1964).
- [7] Emilio Santos. Bell’s theorem and the experiments: Increasing empirical support to local realism. *quant-ph/0410193*, 2004.
- [8] Charles H. Bennett, Gilles Brassard, Claude Crépeau, Richard Jozsa, Asher Peres, and William K. Wootters. Teleporting an unknown quantum state via dual classical and Einstein-Podolsky-Rosen channels. *Phys. Rev. Lett.*, 70:1895–99, 1993.
- [9] Charles H. Bennett and Stephen J. Wiesner. Communication via one- and two-particle operators on einstein-podolsky-rosen states. *Phys. Rev. Lett.*, 69:2881–2884, Nov 1992.
- [10] Artur K. Ekert. Quantum cryptography based on bell’s theorem. *Phys. Rev. Lett.*, 67:661–663, Aug 1991.

- [11] Ian Affleck, Tom Kennedy, Elliott H. Lieb, and Hal Tasaki. Rigorous results on valence-bond ground states in antiferromagnets. *Phys. Rev. Lett.*, 59:799, 1987.
- [12] F. D. M. Haldane. Nonlinear field theory of large-spin Heisenberg antiferromagnets: Semiclassically quantized solitons of the one-dimensional easy-axis Néel state. *Phys. Rev. Lett.*, 50:1153, 1983.
- [13] Tzu-Chieh Wei, Ian Affleck, and Robert Raussendorf. Affleck-Kennedy-Lieb-Tasaki state on a honeycomb lattice is a universal quantum computational resource. *Phys. Rev. Lett.*, 106:070501, 2011.
- [14] Hui Li and F. D. M. Haldane. Entanglement Spectrum as a Generalization of Entanglement Entropy: Identification of Topological Order in Non-Abelian Fractional Quantum Hall Effect States. *Phys. Rev. Lett.*, 101:010504, 2008.
- [15] Jie Lou, Shu Tanaka, Hosho Katsura, and Naoki Kawashima. Entanglement spectra of the two-dimensional Affleck-Kennedy-Lieb-Tasaki model: Correspondence between the valence-bond-solid state and conformal field theory. *Phys. Rev. B*, 84:245128, 2011.
- [16] J. Ignacio Cirac, Didier Poilblanc, Norbert Schuch, and Frank Verstraete. Entanglement spectrum and boundary theories with projected entangled-pair states. *Phys. Rev. B*, 83:245134, 2011.
- [17] F. Verstraete and J. I. Cirac. Renormalization algorithms for quantum-many body systems in two and higher dimensions. *arXiv:cond-mat/0407066*, 2004.
- [18] E. Schrödinger. Die gegenwärtige Situation in der Quantenmechanik. *Naturwissenschaften*, 23:823–8, 1935.
- [19] M. A Nielsen and I. L. Chuang. *Quantum Computation and Quantum Information*. Cambridge University Press, Cambridge, 2000.
- [20] G. Vidal. Entanglement monotones. *J. Mod. Opt.*, 47:355–76, 2000.
- [21] M. A. Nielsen. Continuity bounds for entanglement. *Phys. Rev. A*, 61:064301, Apr 2000.
- [22] Erhard Schmidt. Zur Theorie der linearen und nichtlinearen Integralgleichungen. *Math. Ann.*, 63:433–76, 1907.

- [23] Erhard Schmidt. Zur Theorie der linearen und nicht linearen Integralgleichungen Zweite Abhandlung. *Math. Ann.*, 64:161–74, 1907.
- [24] Artur Ekert and Peter L. Knight. Entangled quantum systems and the Schmidt decomposition. *Am. J. Phys.*, 63:415, 1995.
- [25] Hui Li and F. D. M. Haldane. Entanglement spectrum as a generalization of entanglement entropy: Identification of topological order in non-Abelian fractional quantum Hall effect states. *Phys. Rev. Lett.*, 101:010504, 2008.
- [26] Y. Xu, H. Katsura, T. Hirano, and V. E. Korepin. Entanglement and density matrix of a block of spins in AKLT model. *J. Stat. Phys.*, 133:347, 2008.
- [27] V. E. Korepin and Y. Xu. Entanglement in valence-bond-solid states. *Int. J. Mod. Phys. B*, 24:1361, 2010.
- [28] Ingo Peschel and Ming-Chiang Chung. On the relation between entanglement and subsystem Hamiltonians. *Europhys. Lett.*, 96:50006, 2011.
- [29] Ari M. Turner, Yi Zhang, and Ashvin Vishwanath. Entanglement and inversion symmetry in topological insulators. *Phys. Rev. B*, 82:241102, 2010.
- [30] Frank Pollmann, Ari M. Turner, Erez Berg, and Masaki Oshikawa. Entanglement spectrum of a topological phase in one dimension. *Phys. Rev. B*, 81:064439, 2010.
- [31] A Sterdyniak, B A Bernevig, N Regnault, and F D M Haldane. The hierarchical structure in the orbital entanglement spectrum of fractional quantum Hall systems. *New J. Phys.*, 13(10):105001, 2011.
- [32] Ronny Thomale, D. P. Arovas, and B. Andrei Bernevig. Nonlocal order in gapless systems: Entanglement spectrum in spin chains. *Phys. Rev. Lett.*, 105:116805, 2010.
- [33] S. Sachdev. *Quantum Phase Transitions*. Cambridge University Press, Cambridge, 1999.
- [34] Xiaolong Deng and Luis Santos. Entanglement spectrum of one-dimensional extended Bose-Hubbard models. *Phys. Rev. B*, 84:085138, 2011.

- [35] G. De Chiara, M. Lewenstein, and A. Sanpera. Bilinear-biquadratic spin-1 chain undergoing quadratic Zeeman effect. *Phys. Rev. B*, 84:054451, 2011.
- [36] Charles H. Bennett, Gilles Brassard, Sandu Popescu, Benjamin Schumacher, John A. Smolin, and William K. Wootters. Purification of Noisy Entanglement and Faithful Teleportation via Noisy Channels. *Phys. Rev. Lett.*, 76:722, 1996.
- [37] Charles H. Bennett, Herbert J. Bernstein, Sandu Popescu, and Benjamin Schumacher. Concentrating partial entanglement by local operations. *Phys. Rev. A*, 53:2046, 1996.
- [38] Charles H. Bennett, David P. DiVincenzo, John A. Smolin, and William K. Wootters. Mixed-state entanglement and quantum error correction. *Phys. Rev. A*, 54:3824, 1996.
- [39] V. Vedral, M. B. Plenio, M. A. Rippin, and P. L. Knight. Quantifying Entanglement. *Phys. Rev. Lett.*, 78:2275, 1997.
- [40] F. Franchini, A. R. Its, V. E. Korepin, and L. A. Takhtajan. Spectrum of the density matrix of a large block of spins of the XY model in one dimension. *Quantum Inf. Process.*, 10:325–41, 2011.
- [41] Pasquale Calabrese and John Cardy. Entanglement entropy and conformal field theory. *J. Phys. A: Math. Theor.*, 42(50):504005, 2009.
- [42] Alexei Kitaev and John Preskill. Topological Entanglement Entropy. *Phys. Rev. Lett.*, 96:110404, 2006.
- [43] Scott Hill and William K. Wootters. Entanglement of a Pair of Quantum Bits. *Phys. Rev. Lett.*, 78:5022–25, 1997.
- [44] William K. Wootters. Entanglement of Formation of an Arbitrary State of Two Qubits. *Phys. Rev. Lett.*, 80:2245–48, 1998.
- [45] Valerie Coffman, Joydip Kundu, and William K. Wootters. Distributed entanglement. *Phys. Rev. A*, 61:052306, Apr 2000.
- [46] Berry Groisman, Sandu Popescu, and Andreas Winter. Quantum, classical, and total amount of correlations in a quantum state. *Phys. Rev. A*, 72:032317, 2005.
- [47] Marcelo S. Sarandy, Thiago R. de Oliveira, and Luigi Amico. Quantum discord in the ground state of spin chains. *arXiv:1208.4817v1*, 2012.

- [48] Asher Peres. Separability Criterion for Density Matrices. *Phys. Rev. Lett.*, 77:1413–5, 1996.
- [49] G. Vidal and R. F. Werner. Computable measure of entanglement. *Phys. Rev. A*, 65:032314, 2002.
- [50] Tzu-Chieh Wei and Paul M. Goldbart. Geometric measure of entanglement and applications to bipartite and multipartite quantum states. *Phys. Rev. A*, 68:042307, 2003.
- [51] A. Shimony. Degree of Entanglement. *Ann. NY. Acad. Sci.*, 755:675–679, 1995.
- [52] H Barnum and N Linden. Monotones and invariants for multi-particle quantum states. *J. Phys. A: Math. Gen.*, 34:6787–805, 2001.
- [53] Reinhold A. Bertlmann and Philipp Krammer. Geometric entanglement witnesses and bound entanglement. *Phys. Rev. A*, 77:024303, 2008.
- [54] Román Orús. Universal Geometric Entanglement Close to Quantum Phase Transitions. *Phys. Rev. Lett.*, 100:130502, 2008.
- [55] Román Orús and Tzu-Chieh Wei. Geometric entanglement of one-dimensional systems: bounds and scalings in the thermodynamic limit. *Quant. Inf. Comput.*, 11:563–73, 2011.
- [56] F. Verstraete and J. I. Cirac. Matrix product states represent ground states faithfully. *Phys. Rev. B*, 73:094423, 2006.
- [57] Tobias J. Osborne. Efficient Approximation of the Dynamics of One-Dimensional Quantum Spin Systems. *Phys. Rev. Lett.*, 97:157202, 2006.
- [58] M. Fannes, B. Nachtergaele, and R. F. Werner. Exact Antiferromagnetic Ground States of Quantum Spin Chains. *Europhys. Lett.*, 10:633, 1989.
- [59] A. Klümper, A. Schadschneider, and J. Zittartz. Equivalence and solution of anisotropic spin-1 models and generalized t - J fermion models in one dimension. *J. Phys. A: Math. Gen.*, 24:L955, 1991.
- [60] M. Fannes, B. Nachtergaele, and R. Werner. Finitely correlated states on quantum spin chains. *Commun. Math. Phys.*, 144:443, 1992.
- [61] Ian Affleck, Tom Kennedy, Elliott H. Lieb, and Hal Tasaki. Valence bond ground states in isotropic quantum antiferromagnets. *Commun. Math. Phys.*, 115:477, 1988.

- [62] F. Verstraete, M. M. Wolf, D. Perez-Garcia, and J. I. Cirac. Criticality, the Area Law, and the Computational Power of Projected Entangled Pair States. *Phys. Rev. Lett.*, 96:220601, 2006.
- [63] M. B. Hastings. An area law for one-dimensional quantum systems. *J. Stat. Mech.: Theory Exp.*, 2007:P08024, 2007.
- [64] Heng Fan, Vladimir Korepin, and Vwani Roychowdhury. Entanglement in a valence-bond solid state. *Phys. Rev. Lett.*, 93:227203, 2004.
- [65] Daniel P. Arovas, Assa Auerbach, and F. D. M. Haldane. Extended heisenberg models of antiferromagnetism: Analogies to the fractional quantum hall effect. *Phys. Rev. Lett.*, 60:531–534, 1988.
- [66] Anatol N. Kirillov and Vladimir E. Korepin. The valence bond solid in quasicrystals. *Algebra and Analysis*, 1:47, 1989.
- [67] Paweł Horodecki. Separability criterion and inseparable mixed states with positive partial transposition. *Phys. Lett. A*, 232:333–9, 1997.
- [68] Karol Horodecki, Michał Horodecki, Paweł Horodecki, and Jonathan Oppenheim. Secure key from bound entanglement. *Phys. Rev. Lett.*, 94:160502, Apr 2005.
- [69] Paweł Horodecki, Michał Horodecki, and Ryszard Horodecki. Bound entanglement can be activated. *Phys. Rev. Lett.*, 82:1056–1059, Feb 1999.
- [70] Alessandro Ferraro, Daniel Cavalcanti, Artur García-Saez, and Antonio Acín. Thermal bound entanglement in macroscopic systems and area law. *Phys. Rev. Lett.*, 100:080502, Feb 2008.
- [71] D Patan, Rosario Fazio, and L Amico. Bound entanglement in the xy model. *New Journal of Physics*, 9(9):322.
- [72] S. Baghbanzadeh, S. Alipour, and A. T. Rezakhani. Bound entanglement in quantum phase transitions. *Phys. Rev. A*, 81:042302, Apr 2010.
- [73] M B Hastings. An area law for one-dimensional quantum systems. *Journal of Statistical Mechanics: Theory and Experiment*, 2007(08):P08024.
- [74] Berry Groisman, Sandu Popescu, and Andreas Winter. Quantum, classical, and total amount of correlations in a quantum state. *Phys. Rev. A*, 72:032317, Sep 2005.

- [75] Raul A. Santos, V. Korepin, and Sougato Bose. Negativity for two blocks in the one-dimensional spin-1 affleck-kennedy-lieb-tasaki model. *Phys. Rev. A*, 84:062307, Dec 2011.
- [76] Gavin K. Brennen and Akimasa Miyake. Measurement-based quantum computer in the gapped ground state of a two-body Hamiltonian. *Phys. Rev. Lett.*, 101:010502, 2008.
- [77] Michio Jimbo. A q -difference analogue of $U(\mathfrak{g})$ and the Yang-Baxter equation. *Lett. Math. Phys.*, 10:63–69, 1985.
- [78] V. G. Drinfeld. Hopf algebras and the quantum Yang-Baxter equation. *Doklady Akademii Nauk SSSR*, 5:1060–1064, 1985.
- [79] R. A. Santos, F. N. C. Paraan, V. E. Korepin, and A. Klümper. Entanglement spectra of the q -deformed affleck-kennedy-lieb-tasaki model and matrix product states. *Europhys. Lett.*, 98(3):37005, .
- [80] F. Verstraete, M. A. Martín-Delgado, and J. I. Cirac. Diverging Entanglement Length in Gapped Quantum Spin Systems. *Phys. Rev. Lett.*, 92:087201, 2004.
- [81] Yan Chen, Paolo Zanardi, Z D Wang, and F C Zhang. Sublattice entanglement and quantum phase transitions in antiferromagnetic spin chains. *New J. Phys.*, 8(6):97, 2006.
- [82] Scott D Geraedts and Erik S Sørensen. Exact results for the bipartite entanglement entropy of the AKLT spin-1 chain. *J. Phys. A: Math. Theor.*, 43:185304, 2010.
- [83] Hosho Katsura, Takaaki Hirano, and Yasuhiro Hatsugai. Exact analysis of entanglement in gapped quantum spin chains. *Phys. Rev. B*, 76:012401, 2007.
- [84] Martin Greiter and Stephan Rachel. Valence bond solids for $SU(n)$ spin chains: Exact models, spinon confinement, and the Haldane gap. *Phys. Rev. B*, 75:184441, 2007.
- [85] Hosho Katsura, Takaaki Hirano, and Vladimir E Korepin. Entanglement in an $SU(n)$ valence-bond-solid state. *J. Phys. A: Math. Theor.*, 41:135304, 2008.
- [86] Román Orús and Hong-Hao Tu. Entanglement and $SU(n)$ symmetry in one-dimensional valence-bond solid states. *Phys. Rev. B*, 83:201101, 2011.

- [87] M T Batchelor, L Mezincescu, R I Nepomechie, and V Rittenberg. q -deformations of the $O(3)$ symmetric spin-1 Heisenberg chain. *J. Phys. A: Math. Gen.*, 23:L141, 1990.
- [88] A. Klümper, A. Schadschneider, and J. Zittartz. Groundstate properties of a generalized VBS-model. *Z. Phys. B*, 87:281, 1992.
- [89] F. Verstraete, V. Murg, and J. I. Cirac. Matrix product states, projected entangled pair states, and variational renormalization group methods for quantum spin systems. *Adv. Phys.*, 57:143–224, 2008.
- [90] Raul A. Santos, V. Korepin, and Sougato Bose. Negativity for two blocks in the one-dimensional spin-1 Affleck-Kennedy-Lieb-Tasaki model. *Phys. Rev. A*, 84:062307, 2011.
- [91] Kohei Motegi. The matrix product representation for the q -vbs state of one-dimensional higher integer spin model.
- [92] Chikashi Arita and Kohei Motegi. Spin-spin correlation functions of the q -valence-bond-solid state of an integer spin model. *Journal of Mathematical Physics*, 52(6):063303, 2011.
- [93] Luigi Amico, Rosario Fazio, Andreas Osterloh, and Vlatko Vedral. Entanglement in many-body systems. *Rev. Mod. Phys.*, 80:517, 2008.
- [94] Hosho Katsura, Naoki Kawashima, Anatol N Kirillov, Vladimir E Korepin, and Shu Tanaka. Entanglement in valence-bond-solid states on symmetric graphs. *J. Phys. A.*, 43(25):255303, 2010.
- [95] L.C. Biedenharn and M.A. Lohe. *Quantum Group Symmetry and q -Tensor Algebras*. World Scientific, Singapore, 1995.
- [96] Andreas Fledderjohann, Andreas Klümper, and Karl-Heinz Mütter. Diagrammatics for $SU(2)$ invariant matrix product states. *J. Phys. A: Math. Theor.*, 44:475302, 2011.
- [97] Raul A Santos, Francis N C Paraan, Vladimir E Korepin, and Andreas Klümper. Entanglement spectra of q -deformed higher spin vbs states. *J. Phys. A*, 45(17):175303, .
- [98] Hosho Katsura and Yasuyuki Hatsuda. Entanglement entropy in the Calogero-Sutherland model. *J. Phys. A: Math. Theor.*, 40:13931, 2007.

- [99] A. Klümper, A. Schadschneider, and J. Zittartz. Matrix Product Ground States for One-Dimensional Spin-1 Quantum Antiferromagnets. *Europhys. Lett.*, 24:293, 1993.
- [100] E. Bartel, A. Schadschneider, and J. Zittartz. Excitations of anisotropic spin-1 chains with matrix product ground state. *Eur. Phys. J. B*, 31:209, 2003.
- [101] I. Affleck, T. Kennedy, E. H. Lieb, and H. Tasaki. Rigorous results on valence-bond ground states in antiferromagnets. *Phys. Rev. Lett.*, 59:799–802, 1987.
- [102] Vladimir E. Korepin and Ying Xu. Entanglement in Valence-Bond-Solid States. *IJMPB*, 24:1361–1440, 2010.
- [103] Hosho Katsura, Naoki Kawashima, Anatol N Kirillov, Vladimir E Korepin, and Shu Tanaka. Entanglement in valence-bond-solid states on symmetric graphs. *J. Phys. A: Math. Theor.*, 43:255303, 2010.
- [104] B. Nienhuis. Two-dimensional critical phenomena and the Coulomb Gas. In C. Domb and J. Lebowitz, editors, *Phase Transitions and Critical Phenomena*, volume 11. Academic Press, London, 1987.
- [105] Bernard Nienhuis. Exact Critical Point and Critical Exponents of $O(n)$ Models in Two Dimensions. *Phys. Rev. Lett.*, 49:1062–1065, 1982.
- [106] Wenan Guo, Henk W. J. Blöte, and F. Y. Wu. Phase Transition in the $n > 2$ Honeycomb $O(n)$ Model. *Phys. Rev. Lett.*, 85:3874–3877, 2000.
- [107] William A. Bardeen, Benjamin W. Lee, and Robert E. Shrock. Phase transition in the nonlinear σ model in a $(2 + \epsilon)$ -dimensional continuum. *Phys. Rev. D*, 14:985–1005, 1976.
- [108] E. Brézin, J. Zinn-Justin, and J. C. Le Guillou. Renormalization of the nonlinear σ model in $2 + \epsilon$ dimensions. *Phys. Rev. D*, 14:2615–2621, 1976.
- [109] Michael Edward Peskin and Daniel V. Schroeder. *An Introduction to Quantum Field Theory*. Westview Press, 1995. USA: Addison-Wesley (1995).
- [110] Alexander B. Zamolodchikov and Alexey B. Zamolodchikov. Factorized s-matrices in two dimensions as the exact solutions of certain relativistic quantum field theory. *Ann. of Phys.*, 120:253, 1979.

- [111] Taku Matsui. A link between quantum and classical Potts models. *Journal of Statistical Physics*, 59:781–798, 1990. ISSN 0022-4715.
- [112] F. Verstraete and J. I. Cirac. Matrix product states represent ground states faithfully. *Phys. Rev. B*, 73:094423, 2006.
- [113] Raul A. Santos. Bulk-edge correspondence of entanglement spectrum in two-dimensional spin ground states. *Phys. Rev. B*, 87:035141, 2013.
- [114] L.D. Faddeev. How Algebraic Bethe Ansatz works for integrable model. *arXiv:hep-th/9605187*, 1996.
- [115] T. D. Schultz, D. C. Mattis, and E. H. Lieb. Two-Dimensional Ising Model as a Soluble Problem of Many Fermions. *Rev. Mod. Phys.*, 36: 856–871, 1964.
- [116] Masuo Suzuki. Relationship among Exactly Soluble Models of Critical Phenomena. I. *Progress of Theoretical Physics*, 46(5):1337–1359, 1971.
- [117] Elliott Lieb, Theodore Schultz, and Daniel Mattis. Two soluble models of an antiferromagnetic chain. *Annals of Physics*, 16(3):407 – 466, 1961. ISSN 0003-4916.
- [118] Leonard Susskind. The world as a hologram. *Journal of Mathematical Physics*, 36(11):6377–6396, 1995.

Appendix A

Distance between states, Purification and Fidelity

A.0.1 Hilbert-Schmidt inner product

We denote the vector space $L_{\mathcal{H}}$ as the set of linear operators acting on a Hilbert space \mathcal{H} . Given the linear operators $A, B \in L_{\mathcal{H}}$, the Hilbert-Schmidt inner product is defined as the bilinear functional $(\cdot, \cdot) \in L_{\mathcal{H}} \times L_{\mathcal{H}}$

$$(A, B) = \text{tr}(A^\dagger B). \quad (\text{A.1})$$

A.0.2 Purifications

Purification is a procedure in which we can construct a state whose partial trace over some auxiliary system is equal to a desired density operator.

Let's start with the quantum system A , described by the density matrix ρ_A . This density matrix has a Schmidt decomposition

$$\rho_A = \sum_i \lambda_i |i\rangle\langle i|, \quad (\text{A.2})$$

where the states $|i\rangle$ form an orthonormal basis. We can construct a pure state $|\psi\rangle$ (hence the name purification), whose partial trace gives rise to ρ_A , simply by writing

$$|\psi\rangle = \sum_{i,j} \sqrt{\lambda_i} |i_A, i_B\rangle. \quad (\text{A.3})$$

We see trivially (using orthogonality of the basis $|i_B\rangle$) that $\text{tr}_B |\psi\rangle\langle\psi| = \rho_A$.

A.0.3 Fidelity

When we talk about two create a state which is similar to other with great fidelity, What do we mean?. We can actually define a distance between quantum states which is called *fidelity*.

The fidelity of states ρ and σ is defined to be

$$F(\rho, \sigma) = \text{tr} \sqrt{\rho^{1/2} \sigma \rho^{1/2}}. \quad (\text{A.4})$$

The fidelity F has the following properties [2]

Symmetry

$$F(\rho, \sigma) = F(\sigma, \rho), \quad (\text{A.5})$$

Invariance under unitary transformations

Given an unitary transformation U , we have

$$F(U\rho U^\dagger, U\sigma U^\dagger) = F(\rho, \sigma), \quad (\text{A.6})$$

which follows from the fact that $\sqrt{U A U^\dagger} = U \sqrt{A} U^\dagger$.

Uhlmann's theorem

Suppose ρ and σ are states of a quantum systems S_1 . Then

$$F(\rho, \sigma) = \max_{|\varphi\rangle, |\phi\rangle} |\langle \phi | \varphi \rangle|, \quad (\text{A.7})$$

where the maximization is done over the purifications (see A.0.2) $|\varphi\rangle$ of ρ and $|\phi\rangle$ of σ into $S_1 \cup S_1$.

Appendix B

More results on Negativity

B.0.4 Classical Variable representation

A known representation of the boson algebra introduced in the first section is given by $a_i^\dagger = u_i$, $a_i = \frac{\partial}{\partial u_i}$, $b_i^\dagger = v_i$, $b_i = \frac{\partial}{\partial v_i}$. In this representation the spin operators read

$$S_i^+ = u_i \frac{\partial}{\partial v_i}, \quad S_i^- = v_i \frac{\partial}{\partial u_i}, \quad S_i^z = \frac{1}{2} \left(u_i \frac{\partial}{\partial u_i} - v_i \frac{\partial}{\partial v_i} \right) \quad (\text{B.1})$$

Due to the rotational invariance of the AKLT model, it's useful to choose [\[65\]](#)

$$u_i = e^{i\phi_i/2} \cos \frac{\theta_i}{2}, \quad v_i = e^{-i\phi_i/2} \sin \frac{\theta_i}{2}, \quad (\text{B.2})$$

where θ and ϕ parametrize the unit sphere, with $\theta \in [0, \pi]$ $\theta = 0$ being the positive z axis and $\phi \in [0, 2\pi]$.

The condition $a_i^\dagger a_i + b_i^\dagger b_i = 2S$ imposes a restriction on the functions allowed to form spin states, namely

$$\frac{1}{2} \left(u_i \frac{\partial}{\partial u_i} + v_i \frac{\partial}{\partial v_i} \right) f(u_i, v_i) = S f(u_i, v_i) \quad (\text{B.3})$$

The solution to (B.3) is $f(u, v) = \sum_k f_k u^k v^{2S-k}$, a polynomial of degree $2S$ in u and v , with a_k an arbitrary constant. The inner product becomes $\langle g|f \rangle = \int \frac{d\Omega}{2\pi} \bar{g}(u, v) f(u, v)$ where Ω is the solid angle over the sphere, \bar{g} is the complex conjugate of g . In the subspace of degree $2S$ polynomials the matrix elements for S^+ are

$$\begin{aligned}
\langle g(u, v) | S^+ f(u, v) \rangle &\equiv \langle g(u, v) | u \frac{\partial}{\partial v} f(u, v) \rangle \\
&= \sum_{j,k} \bar{a}_j a_k \int \frac{d\Omega}{4\pi} \bar{u}^j \bar{v}^{2S-j} u \frac{\partial}{\partial v} u^k v^{2S-k} \\
&= \sum_{j,k} \bar{a}_j a_k \delta_{k+1,j} B(k+2, 2S-k)(2S-k).
\end{aligned} \tag{B.4}$$

with $B(x, y)$ the beta function. Following [65], we introduce the classical variable representation of S^+ as $S_{cl}^+ = 2(S+1)u\bar{v}$. The matrix elements for this operator are

$$\langle g(u, v) | S_{cl}^+ f(u, v) \rangle \equiv \langle g(u, v) | 2(S+1)u\bar{v} f(u, v) \rangle \tag{B.5}$$

$$\begin{aligned}
&= \sum_{j,k} 2(S+1) \bar{a}_j a_k \int \frac{d\Omega}{4\pi} \bar{u}^j \bar{v}^{2S-j+1} u^{k+1} v^{2S-k} \\
&= \sum_{j,k} \bar{a}_j a_k \delta_{k+1,j} B(k+2, 2S-k+1)(2S+2).
\end{aligned} \tag{B.6}$$

Now, writing the beta function in terms of the gamma function, and using $\Gamma(z+1) = z\Gamma(z)$, we have

$$B(k+2, 2S-k+1) = \frac{\Gamma(k+2)\Gamma(2S-k+1)}{\Gamma(2S+3)} = \frac{(2S-k)}{2S+2} B(k+2, 2S-k).$$

then $\langle g(u, v) | S_{cl}^+ f(u, v) \rangle = \langle g(u, v) | S^+ f(u, v) \rangle$. The classical representation of the spin operators is $S_{cl}^+ = (2S+2)u\bar{v}$, $S_{cl}^- = (2S+2)v\bar{u}$, and $S_{cl}^z = (S+1)(u\bar{u} - v\bar{v})$. These expressions provide the same matrix elements as the operators (B.1), as can be shown easily from the definitions.

Now using the relations $a = u = e^{i\phi/2} \cos \frac{\theta}{2}$, $a^\dagger = \bar{u} = e^{-i\phi/2} \cos \frac{\theta}{2}$ and $b = v = e^{-i\phi/2} \sin \frac{\theta}{2}$, $b^\dagger = \bar{v} = e^{i\phi/2} \sin \frac{\theta}{2}$, we can also prove that a similar relation holds for the overlap between states satisfying (B.3)

$$\frac{\langle g(a, b) | f(a, b) \rangle}{\sqrt{\langle g | g \rangle \langle f | f \rangle}} = \frac{\int \frac{d\Omega}{2\pi} \bar{g}(u, v) f(u, v)}{\sqrt{\int \frac{d\Omega}{2\pi} |g(u, v)|^2 \int \frac{d\Omega}{2\pi} |f(u, v)|^2}} \tag{B.7}$$

The state $|i^{i+L-1}\rangle$ containing L sites fulfills the condition (B.3) at every lattice point, except at the boundary sites i and $i+L-1$. The ground states $|A_\alpha^S\rangle$ of the bulk Hamiltonian defined by $|A_\mu\rangle = T_\mu^\dagger(i, j+1) |i^{j+1}\rangle$, introduced in (4.8), satisfy the relation (B.3) at each lattice site.

The norm of the VBS state (4.3) is in this language

$$\begin{aligned}\langle \text{VBS} | \text{VBS} \rangle &= \int \left[\prod_{i=0}^{N+1} \frac{d\Omega_i}{4\pi} \right] \prod_{i=0}^N (1 - \hat{\Omega}_i \cdot \hat{\Omega}_{i+1}) \\ &= 1.\end{aligned}\tag{B.8}$$

with $\hat{\Omega}_i$ being the radial vector on the unit sphere

$$\hat{\Omega}_i = (\sin \theta_i \cos \phi_i, \sin \theta_i \sin \phi_i, \cos \theta_i).\tag{B.9}$$

The norm of the states $|A_\mu\rangle = T_\mu^\dagger(i, i + L - 1) |i^{i+L-1}\rangle$ composed by L sites is then

$$\begin{aligned}\langle A_\mu | A_\nu \rangle &= \int \prod_{i=1}^L \frac{d\Omega_i}{4\pi} (1 - \hat{\Omega}_i \cdot \hat{\Omega}_{i+1}) \mathcal{T}_\mu^*(1, L) \mathcal{T}_\nu(1, L) \\ &= \frac{1}{4} \left(1 + s_\mu \left(-\frac{1}{3} \right)^L \right) \delta_{\mu\nu},\end{aligned}\tag{B.10}$$

with $s_\mu = (-1, -1, 3, -1)$. Here we have introduced \mathcal{T}_μ , the classical analog to the operators T_μ , defined as

$$\mathcal{T}_\mu(i, j) = \varphi_i^a (\sigma_\mu)_{ab} \varphi_j^b, \text{ with } \varphi_i^1 = u_i, \varphi_i^2 = v_i.\tag{B.11}$$

B.0.5 Identities

All the identities that we have use in this work can be obtained from the basic identity, (repeated indices are summed)

$$\psi_i^{a\dagger} \psi_k^{b\dagger} = -\frac{1}{2} (-1)^\mu T_\mu^\dagger(i, k) (\sigma_\mu)_{ab},\tag{B.12}$$

which can be checked directly by inspection, and makes use of the fact that the matrices σ_μ form a basis of the $GL(2, \mathbb{C})$ group. Then for two boundary operators (these operators appear naturally in the boundary between two different blocks in the bulk) $\hat{\partial}_i^\dagger = T_2^\dagger(i, i + 1)$ and $\hat{\partial}_j^\dagger = T_2^\dagger(j, j + 1)$, we have

$$\hat{\partial}_i^\dagger \hat{\partial}_j^\dagger = \psi_i^{a\dagger} (\sigma_2)_{ab} \psi_{i+1}^{b\dagger} \psi_j^{c\dagger} (\sigma_2)_{cd} \psi_{j+1}^{d\dagger}$$

now applying the identity (B.12) twice and using the fact that $(\sigma_\nu)_{ad} = (\sigma_\nu^T)_{da}$ which is also equal to $-(-1)^\nu g^{\nu\nu'} (\sigma_{\nu'})_{da}$, we get

$$\hat{\partial}_i^\dagger \hat{\partial}_j^\dagger = \frac{1}{4} (-1)^\mu g^{\nu\nu'} T_\mu^\dagger(i+1, j) T_\nu^\dagger(i, j+1) \text{Tr}(\sigma_2 \sigma_\mu \sigma_2 \sigma_{\nu'}).$$

The last term in the above expression is the trace of 4 matrices. To compute it we can use that $\sigma_2 \sigma_\mu \sigma_2 = (-1)^\mu \sigma_\mu$ and that $\text{Tr}(\sigma_\mu \sigma_\nu) = 2g^{\mu\nu}$ obtaining

$$\hat{\partial}_i^\dagger \hat{\partial}_j^\dagger = -\frac{1}{2} T_\mu^\dagger(i+1, j) T_\mu^\dagger(i, j+1) \quad (\text{B.13})$$

Using this identities it is possible to generate all the identities for any number of boundary operators $\hat{\partial}$. In this work, we used the identity for three and four $\hat{\partial}$ operators

$$\begin{aligned} \hat{\partial}_i^\dagger \hat{\partial}_j^\dagger \hat{\partial}_k^\dagger &= -\frac{1}{8} (-1)^\nu g^{\nu\nu'} T_\mu^\dagger(i+1, j) T_\nu^\dagger(j+1, k) T_\lambda^\dagger(i, k+1) \\ &\times \text{Tr}(\sigma_\mu \bar{\sigma}_\nu \sigma_2 \bar{\sigma}_\lambda), \end{aligned} \quad (\text{B.14})$$

$$\begin{aligned} \hat{\partial}_i^\dagger \hat{\partial}_j^\dagger \hat{\partial}_k^\dagger \hat{\partial}_l^\dagger &= \frac{(-1)^\nu}{16} g^{\nu\nu'} T_\mu^\dagger(i+1, j) T_\nu^\dagger(j+1, k) T_\rho^\dagger(k+1, l) T_\lambda^\dagger(i, l+1) \\ &\times \text{Tr}(\sigma_\mu \bar{\sigma}_\nu \sigma_\rho \bar{\sigma}_\lambda). \end{aligned} \quad (\text{B.15})$$

here $\sigma_\mu = (i, \sigma_1, \sigma_2, \sigma_3)$ where σ_k are the three Pauli matrices. We also define $\bar{\sigma}_\mu = (-i, \sigma_1, \sigma_2, \sigma_3)$. To compute the traces of the Pauli Matrices, we use the following tricks.

$$\sigma_\mu \bar{\sigma}_\nu + \sigma_\nu \bar{\sigma}_\mu = 2\delta_{\mu\nu}, \quad \frac{\sigma_\mu \bar{\sigma}_\nu - \sigma_\nu \bar{\sigma}_\mu}{2} \equiv \sigma_{\mu\nu}, \quad \sigma_\mu \bar{\sigma}_\nu = \delta_{\mu\nu} + \sigma_{\mu\nu}$$

The $\sigma_{\mu\nu}$ object is a generator of the Lorentz transformations in Euclidean space, so it satisfies the Euclidean Lorentz algebra

$$[\sigma_{\mu\nu}, \sigma_{\alpha\beta}] = 2(\delta_{\nu\alpha} \sigma_{\mu\beta} - \delta_{\nu\beta} \sigma_{\mu\alpha} + \delta_{\mu\beta} \sigma_{\nu\alpha} - \delta_{\mu\alpha} \sigma_{\nu\beta}). \quad (\text{B.16})$$

Further identities can be derived using the Dirac matrices technology, namely, in Euclidean space we have

$$\gamma_\mu = \begin{pmatrix} 0 & -i\sigma_\mu \\ i\bar{\sigma}_\mu & 0 \end{pmatrix} \quad \gamma_5 = \begin{pmatrix} I & 0 \\ 0 & -I \end{pmatrix} \quad (\text{B.17})$$

then we can compute the trace of four Pauli matrices using the identities for Dirac matrices [109], and projecting out the lower block with the chiral projector $(1 - \gamma_5)/2$. We have for example

$$\text{Tr}(\sigma_\mu \bar{\sigma}_\nu \sigma_\rho \bar{\sigma}_\lambda) = \frac{1}{2} \text{Tr}(\gamma_\mu \gamma_\nu \gamma_\rho \gamma_\lambda (1 - \gamma^5)) = 2(\delta_{\mu\nu} \delta_{\rho\lambda} + \delta_{\mu\lambda} \delta_{\rho\nu} - \delta_{\mu\rho} \delta_{\nu\lambda} + \epsilon_{\mu\nu\rho\lambda})$$

B.0.6 General Results

Block separation $L \geq 1$

In section 4.3 we found an explicit expression for the density matrix of two blocks of length L_A and L_B separated by L sites. In that section we presented the asymptotic results for the eigenvalues of ρ_{AB} . The result for any $L_A, L_B \geq 1$ is given in terms of the following quantities

$$\lambda_0(L) = \frac{1}{4} \left(1 + 3 \left(-\frac{1}{3} \right)^L \right), \quad \lambda_1(L) = \frac{1}{4} \left(1 - \left(-\frac{1}{3} \right)^L \right).$$

From those quantities we define $\lambda_{00} = \lambda_0(L_A) \lambda_0(L_B)$, $\lambda_{11} = \lambda_1(L_A) \lambda_1(L_B)$ and $\lambda_{10} = \lambda_0(L_A) \lambda_1(L_B) + \lambda_0(L_B) \lambda_1(L_A)$.

The characteristic polynomial associated to the density matrix ρ_{AB} , $p(Y) = \det(\rho_{AB} - Y)$ is $p(Y) = p_1(Y)^5 p_2(Y) p_3(Y)^3$, where $p_k(Y)$ is a polynomial of degree k on Y , given by ($z = (-3)^{-L}$)

$$\begin{aligned} p_1(Y) &= Y - (1 - z) \lambda_{11}, \\ p_2(Y) &= Y^2 - (\lambda_{00} + (1 + 2z) \lambda_{11}) Y + (1 - z) (1 + 3z) \lambda_{00} \lambda_{11}, \\ p_3(Y) &= Y^3 - (\lambda_{10} + \lambda_{11} (1 + z)) Y^2 + [(1 + z) \lambda_{00} + (1 + 2z) \lambda_{10}] (1 - z) \lambda_{11} Y \\ &\quad - (1 - z)^2 (1 + 3z) \lambda_{00} \lambda_{11}^2 = Y^3 + bY^2 + cY + d. \end{aligned} \tag{B.18}$$

We define $q \equiv \frac{1}{27}(2b^3 - 9bc + 27d)$, $p \equiv \frac{1}{3}(3c - b^2)$. The eigenvalues of ρ_{AB} are the solutions to $P(y) = 0$. They are

$$y = (1 - z)\lambda_{11} \quad \text{five-fold degeneracy,} \quad (\text{B.19})$$

$$y = \frac{1}{2} \left(a_1 \pm \sqrt{a_1^2 - 4a_2} \right), \quad (\text{B.20})$$

$$a_1 = (\lambda_{00} + (1 + 2z)\lambda_{11}), \quad a_2 = 4(1 - z)(1 + 3z)\lambda_{00}\lambda_{11}.$$

$$y = 2\sqrt{-\frac{p}{3}} \cos \left(\frac{1}{3} \arccos \left(\frac{3q}{2p} \sqrt{-\frac{3}{p}} \right) + \frac{2\pi k}{3} \right) - \frac{b}{3}, \quad (k = 0, 1, 2) \quad (\text{B.21})$$

triple deg.

Adjacent blocks

In section 4.3, we computed the transposed density matrix of a system consisting of two blocks inside the VBS state, A and B , of length L_A and L_B respectively. The spins which do not belong to $A \cup B$ have been traced away. In the general case when the blocks are separated by L sites we could prove that the negativity vanishes for $L \geq 1$, being the only nontrivial case when $L = 0$. In that case, the negativity in the asymptotic limit $L_A \rightarrow \infty, L_B \rightarrow \infty$ is given by

$$\mathcal{N}_{L_A, L_B \rightarrow \infty} = \frac{1}{2} - \frac{3}{4} \left(\left(-\frac{1}{3} \right)^{2L_A} + \left(-\frac{1}{3} \right)^{2L_B} \right). \quad (\text{B.22})$$

The decay in the thermodynamic limit is twice as fast compared to the usual decay of the spin correlations, a feature that is already seen in the case of the negativity of the pure system studied before.

The logarithmic negativity also show this behavior, for $L_A, L_B \gg 1$

$$E_{\mathcal{N}} = 1 - \frac{3}{4 \ln(2)} \left(\left(-\frac{1}{3} \right)^{2L_A} + \left(-\frac{1}{3} \right)^{2L_B} \right). \quad (\text{B.23})$$

In the case of adjacent blocks, for any $L_A, L_B \geq 1$, the characteristic polynomial associated to the transposed density matrix $\rho_{AB}^{T_A}$, $p(y) = \det(\rho_{AB}^{T_A} - Iy)$ is $\bar{p}(y) = \bar{p}_1(y)^5 \bar{p}_2(y) \bar{p}_3(y)^3$, where $\bar{p}_k(y)$ is a polynomial of degree k on y , given by (defined in terms of $\lambda_{00}, \lambda_{10}, \lambda_{11}$)

$$\begin{aligned} \bar{p}_1(y) &= y - 2\lambda_{11}, \\ \bar{p}_2(y) &= y^2 - y(\lambda_{00} - \lambda_{11}) - 4\lambda_{00}\lambda_{11}, \\ \bar{p}_3(y) &= y^3 - \lambda_{10}y^2 - 2\lambda_{10}\lambda_{11}y + 8\lambda_{00}\lambda_{11}^2 \equiv y^3 + by^2 + cy + d, \end{aligned} \quad (\text{B.24})$$

this polynomials are related with the polynomials of previous section by taking $z = -1$ in eq. (B.18). Out of the 16 eigenvalues (y_n), 4 are negative, with y_1 (no degeneracy) given by the expression

$$y_1 = \frac{1}{2} \left(\lambda_{00} - \lambda_{11} - \sqrt{\lambda_{00}^2 + 14\lambda_{00}\lambda_{11} + \lambda_{11}^2} \right), \quad (\text{B.25})$$

and y_2 (triple degeneracy) given by (using again $q \equiv \frac{1}{27}(2b^3 - 9bc + 27d)$, $p \equiv \frac{1}{3}(3c - b^2)$).

$$y_2 = -2\sqrt{-\frac{p}{3}} \sin \left(\frac{1}{3} \arccos \left(\frac{3q}{2p} \sqrt{-\frac{3}{p}} \right) + \frac{\pi}{6} \right) - \frac{b}{3}. \quad (\text{B.26})$$

The negativity of the system is then $\mathcal{N} = -(y_1 + 3y_2)$, while the logarithmic negativity is given by $E_{\mathcal{N}} = \log_2(1 - 2(y_1 + 3y_2))$. In the special case when $L_A = L_B = l$, the negativity simplifies to (using $x = (-3)^{-l}$)

$$\begin{aligned} \mathcal{N}(l) &= \frac{1}{8} \sqrt{1 + 4x + 2x^2 - 4x^3 + 13x^4} - \frac{x+x^2}{4} + \frac{3}{16} \sqrt{(1+3x)(1-x)^3}, \\ &\simeq \frac{1}{2} - \frac{3}{2}(x^2 - x^3), \quad \text{for } x \ll 1. \end{aligned} \quad (\text{B.27})$$

The logarithmic negativity is given by $E_{\mathcal{N}}(\rho_{AB}) \simeq 1 - \frac{3}{2\ln(2)}(x^2 - x^3)$.

Appendix C

Representation theory of $SU_q(2)$

C.1 Identities for q -CG coefficients

Among the key properties of the q -CG coefficients that we use above are the orthogonality relations

$$\sum_{Jm} \begin{bmatrix} j_1 & j_2 & J \\ m_1 & m_2 & m \end{bmatrix}_q \begin{bmatrix} j_1 & j_2 & J \\ m'_1 & m'_2 & m \end{bmatrix}_q = \delta_{m_1 m'_1} \delta_{m_2 m'_2}, \quad (\text{columns}), \quad (\text{C.1})$$

$$\sum_{m_1 m_2} \begin{bmatrix} j_1 & j_2 & J \\ m_1 & m_2 & m \end{bmatrix}_q \begin{bmatrix} j_1 & j_2 & J' \\ m_1 & m_2 & m' \end{bmatrix}_q = \delta_{JJ'} \delta_{mm'}, \quad (\text{rows}). \quad (\text{C.2})$$

We also make much use of the following identities involving column transpositions:

$$\begin{bmatrix} j_1 & j_2 & J \\ m_1 & m_2 & m \end{bmatrix}_q = (-1)^{j_1 - J + m_2} q^{-m_2/2} \sqrt{\frac{[2J+1]}{[2j_1+1]}} \begin{bmatrix} J & j_2 & j_1 \\ m & -m_2 & m_1 \end{bmatrix}_q, \quad (\text{C.3})$$

$$\begin{bmatrix} j_1 & j_2 & J \\ m_1 & m_2 & m \end{bmatrix}_q = \begin{bmatrix} j_2 & j_1 & J \\ -m_2 & -m_1 & -m \end{bmatrix}_q, \quad (\text{C.4})$$

$$\begin{bmatrix} j_1 & j_2 & J \\ m_1 & m_2 & m \end{bmatrix}_q = (-1)^{J - j_2 - m_1} q^{m_1/2} \sqrt{\frac{[2J+1]}{[2j_2+1]}} \begin{bmatrix} j_1 & J & j_2 \\ -m_1 & m & m_2 \end{bmatrix}_q. \quad (\text{C.5})$$

C.2 q -deformed F-matrix and $6j$ symbols

The equation for the lower diagram given in (5.4) reads

$$\begin{aligned} & \sum_{abcdk} \begin{bmatrix} A & B & D \\ a & b & d \end{bmatrix}_q \begin{bmatrix} D & K & J \\ d & k & j \end{bmatrix}_q \begin{bmatrix} B & C & K \\ b & c & k \end{bmatrix}_q |A, a\rangle \otimes |C, c\rangle = \\ & \sum_N \sum_{abcdn} F_q[DBJC; NK] \begin{bmatrix} A & B & D \\ a & b & d \end{bmatrix}_q \begin{bmatrix} D & B & N \\ d & b & n \end{bmatrix}_q \begin{bmatrix} N & C & J \\ n & c & j \end{bmatrix}_q |A, a\rangle \otimes |C, c\rangle. \end{aligned} \quad (\text{C.6})$$

Using the identity (C.3) in the righthand side of (C.6) and applying the orthogonality condition (C.2) to evaluate the sum gives

$$\begin{aligned} & l \sum_{bdk} \begin{bmatrix} A & B & D \\ a & b & d \end{bmatrix}_q \begin{bmatrix} B & C & K \\ -b & c & k \end{bmatrix}_q \begin{bmatrix} D & K & J \\ d & k & j \end{bmatrix}_q (-1)^{-b} q^{b/2} \\ & = (-1)^{A-D} \sqrt{\frac{[2D+1]}{[2A+1]}} F_q[DBJC; AK] \begin{bmatrix} A & C & J \\ a & c & j \end{bmatrix}_q, \end{aligned} \quad (\text{C.7})$$

$$= (-1)^{A+B+C+J} \sqrt{[2D+1][2K+1]} \left\{ \begin{matrix} D & B & A \\ C & J & K \end{matrix} \right\}_q \begin{bmatrix} A & C & J \\ a & c & j \end{bmatrix}_q. \quad (\text{C.8})$$

Here $\left\{ \begin{matrix} D & B & A \\ C & J & K \end{matrix} \right\}_q$ is the q -deformed $6j$ symbol. It is related to the elements of the q -deformed F -matrix by [95]

$$F_q[DBJC; AK] = (-1)^{D+B+J+C} \sqrt{[2K+1][2A+1]} \left\{ \begin{matrix} D & B & A \\ C & J & K \end{matrix} \right\}_q. \quad (\text{C.9})$$